ASSESSMENT OF THE NONLINEAR BEHAVIOR OF RC MOMENT RESISTING FRAMED BUILDINGS MADE OF STRUCTURAL LIGHTWEIGHT CONCRETE

A THESIS SUBMITTED TO
THE GRADUATE SCHOOL OF NATURAL AND APPLIED SCIENCES
OF
MIDDLE EAST TECHNICAL UNIVERSITY

BY

MEHMET ALİ ŞENEL

IN PARTIAL FULFILLMENT OF THE REQUIREMENTS
FOR
THE DEGREE OF MASTER OF SCIENCE
IN
CIVIL ENGINEERING

JUNE 2015

Approval of the thesis:

ASSESSMENT OF THE NONLINEAR BEHAVIOR OF RC MOMENT RESISTING FRAMED BUILDINGS MADE OF STRUCTURAL LIGHTWEIGHT CONCRETE

Submitted by **MEHMET ALİ ŞENEL** in partial fulfillment of the requirements for the degree of **Master of Science in Civil Engineering Department, Middle East Technical University** by,

Prof. Dr. Gülbin Dural Ünver ____________________
Dean, Graduate School of **Natural and Applied Sciences**

Prof. Dr. Ahmet Cevdet Yalçıner ____________________
Head of Department, **Civil Engineering**

Assoc. Prof. Dr. Afşin Sarıtaş ____________________
Supervisor, **Civil Engineering Dept., METU**

Assoc. Prof. Dr. Lutfullah Turanlı ____________________
Co-Supervisor, **Civil Engineering Dept., METU**

Examining Committee Members:

Asst. Prof. Dr. Çağla Meral ____________________
Civil Engineering Dept., METU

Assoc. Prof. Dr. Afşin Sarıtaş ____________________
Civil Engineering Dept., METU

Assoc. Prof. Dr. Lutfullah Turanlı ____________________
Civil Engineering Dept., METU

Assoc. Prof. Dr. Eray Baran ____________________
Civil Engineering Dept., METU

Assoc. Prof. Dr. Mehmet Baran ____________________
Civil Engineering Dept., Yıldırım Beyazıt University

Date: 17.06.2015

I hereby declare that all information in this document has been obtained and presented in accordance with academic rules and ethical conduct. I also declare that, as required by these rules and conduct, I have fully cited and referenced all material and results that are not original to this work.

Name, Last Name : Mehmet Ali Şenel

Signature :

ABSTRACT

ASSESSMENT OF THE NONLINEAR BEHAVIOR OF RC MOMENT RESISTING FRAMED BUILDINGS MADE OF STRUCTURAL LIGHTWEIGHT CONCRETE

Şenel, Mehmet Ali

M.S., Department of Civil Engineering

Supervisor: Assoc. Prof. Dr. Afşin Sarıtaş

Co-Supervisor: Assoc. Prof. Dr. Lutfullah Turanlı

June 2015, 85 pages

Lightweight concrete does differ from normal weight concrete with the aggregate type used in the composition. Use of lightweight concrete reduces the dead weights of structures. On the contrary to general idea in Turkey, lightweight concrete has adequate performance to be used for structural purposes. The drawback of the use of lightweight concrete for structural purposes is the lack of reliable studies as performed for normal weight concrete.

In the scope of this study, confinement effect of lightweight concrete has been investigated with experimentation and compared with reliable confined concrete models. The data from experimentation is used for the comparison of structural lightweight concrete and normal weight concrete buildings through the use of structural analysis program Perform-3D. The method chosen for the analysis is the nonlinear static analysis or push-over analysis. Widely accepted building codes are used in the design phase and in carrying out the chosen method of analysis, and these are ACI 318-08, ASCE 7-05, ASCE 7-10, FEMA 356 and FEMA P695. Through the use of the building codes and structural analysis program, ordinary 5 story buildings made of normal weight and lightweight concrete are analyzed and compared in 2-D modelling with pushover analysis.

The outcomes obtained from study demonstrate sufficient structural performance from lightweight concrete specimens and RC framed structures, and these results are expected to ease and widen the use of lightweight concrete for structural purposes.

Keywords: Structural Lightweight Concrete, Natural Perlite Aggregate, Confined Concrete Behavior, Nonlinear Structural Analysis, Pushover Analysis

ÖZ

YAPISAL HAFİF BETONLU MOMENT AKTARAN BETONARME ÇERÇEVELİ BİNALARIN DOĞRUSAL OLMAYAN DAVRANIŞININ DEĞERLENDİRİLMESİ

Şenel, Mehmet Ali

Yüksek Lisans, İnşaat Mühendisliği Bölümü

Tez Yöneticisi: Doç. Dr. Afşin Sarıtaş

Ortak Tez Yöneticisi: Doç. Dr. Lutfullah Turanlı

Haziran 2015, 85 sayfa

Hafif beton, içerdiği agrega tipi ile normal betondan ayrılır. Hafif beton kulanımı, yapılarda ölü yüklerin azaltılabilmesine olanak sağlar. Türkiye'deki genel kanının aksine, hafif beton yapısal kullanım için yeterli performansa sahiptir. Hafif betonun taşıyıcı malzeme olarak kullanılmasındaki engel, normal betonda olduğu kadar güvenilir çalışmaların bulunmamasıdır.

Bu çalışma kapsamında, hafif betondaki sargı etkisi deneysel olarak irdelenmiş ve güvenilir sargılı beton modelleriyle karşılaştırılmıştır. Deneysel çalışma sonucu elde edilen bilgi, hafif beton ve normal betonlu yapıların, yapısal analiz programı Perform-3D kullanılarak karşılaştırılmasında dikkate alnmıştır. Analiz metodu olarak doğrusal olmayan statik analiz, ya da elastik ötesi itme analizi seçilmiştir. Tasarım aşamasında ve seçilen analiz metodunda geniş kabul görmüş yapım kodları kullanılmıştır ki bunlar ACI 318-08, ASCE 7-05, ASCE 7-10 FEMA 356 ve FEMA P695'dir. Yapım kodları ve yapısal analiz programının kullanılmasıyla 5 katlı normal beton ve hafif betondan yapılmış binalar, 2 boyutlu olarak modellenerek elastik ötesi itme analiz metodu ile analiz edilmiş ve karşılaştırılmıştır.

Bu çalışmada hafif beton numuneleri ve çerçeve sistemlerinden elde edilen sonuçlara göre hafif betonun yapısal davranışının yeterli düzeyde olduğu tespit edilmiştir ve bu çalışma sonuçlarına göre bu malzemenin yapılarda kullanımının kolaylaşması ve yaygınlaşması beklenmektedir.

Anahtar Kelimeler: Yapısal Hafif Beton, Doğal Perlit Agregası, Sargılı Beton Davranışı, Doğrusal Olmayan Yapısal Analiz, Elastik Ötesi İtme Analizi

ACKNOWLEDGEMENTS

I would like to express my deepest gratitude to my supervisor and co-supervisor Dr. Afşin Sarıtaş and Lutfullah Turanlı for their encouragement and endless support.

Also, I am appreciated for Burhan Alam and Materials of Construction Laboratory staff.

Additionally, I would like to offer my thanks for my father, mother and sister for their patience.

TABLE OF CONTENTS

LIST OF TABLES

TABLES

LIST OF FIGURES

FIGURES

LIST OF SYMBOLS AND ABBREVIATONS

2D	Two Dimensional
3D	Three Dimensional
ACI	American Concrete Institute
ASCE	American Society of Civil Engineers
ASTM	American Society for Testing and Materials
ATC	Applied Technology Council
CP	Collapse Prevention
E	Modulus of Elasticity
f_c	Compressive Strength of Concrete
FEMA	Federal Emergency Management Agency
I_{cr}	Moment of Inertia of Cracked Concrete Section
I_g	Moment of Inertia of Gross Concrete Section
IO	Immediate Occupancy
LPDT	Linear Potentiometric Displacement Transducer
LS	Life Safety
LWC	Lightweight Concrete
MLWC	Modified Lightweight Concrete
NWC	Normal Weight Concrete
RC	Reinforced Concrete
A_0	Cross Sectional Area of Confinement Reinforcement
l_s	Total Length of Confinement Reinforcement in Cross Section
w_c	Unit Weight of Concrete

f_c	Unconfined Concrete Strength
f_{cc}	Confined Concrete Strength
ε_{c0}	Strain of Unconfined Concrete at Ultimate Stress
ε_{c20}	Confined Concrete Strain at Stress Value of 20% of f_{cc}
ε_{c0c}	Strain at Ultimate Confined Concrete Strength
ρ_s	Volumetric Ratio of Confinement Reinforcement
s	Confinement Spacing
Δ_U	Deformation at Ultimate Point
Δ_Y	Deformation at Yield Point
μ	Ductility Index

CHAPTER 1

INTRODUCTION

The use of lightweight concrete in load carrying structural members has received less attention in practice and research studies in Turkey as well as in the world compared to normal weight concrete. This thesis provides a comparative study on the use of lightweight concrete in reinforced concrete (RC) framed structures with respect to the use of normal weight concrete. An experimental study is also undertaken so that nonlinear behavior of unconfined and confined lightweight concrete can be accurately modelled in the numerical analyses.

This chapter will first provide general information and history on lightweight concrete. The use of structural lightweight concrete in structural codes is presented next. Advantages and disadvantages of using lightweight concrete with respect to normal weight concrete is elaborated, where the cause of difference stems from the use of lightweight aggregates. Lastly, the scopes and objectives of this thesis are presented.

1.1. General Information on Lightweight Concrete

The use of lightweight concrete has spread out into various aspects of construction industry. In the earlier times, lightweight concrete has been used for isolation and nonstructural purposes, and then the use of lightweight concrete has also been observed in structural application. The main difference between lightweight concrete and normal weight concrete is due to the aggregate type used for production, where thereby the weight of the end product is affected.

The air-dried density of lightweight concrete is defined by ACI-213R-87 (1987) to be between 1440 to 1850 kg/m^3. Furthermore, in order for lightweight concrete to be used in structural load carrying members and named as structural lightweight concrete, it should have at least 17 MPa compressive strength at the end of 28 days. The aggregate used for lightweight concrete could be obtained after several chemical and physical processes or in some cases the lightweight aggregates could be found in nature and used without being processed. In this regards, Turkey has a great potential of raw materials to be used as lightweight aggregate due to its geomorphologic structure; however the Turkish Specification TS-500 does not allow the use of lightweight concrete in structural load carrying members.

1.1.1. History of Lightweight Concrete

The use of Grecian and Italian pumice as binding material to produce mortar/concrete is known dating back to the Roman Empire. The effort on the invention/production of modern concrete is credited to an English bricklayer, Joseph Aspdin, who mixed pulverized raw limestone and siliceous materials in different percentages in order to obtain an optimum mixture as a binding material in early 19th Century. He patented the outcome product from his studies as Portland Cement. Invention of cement from that time on gained greater importance and started the Age of Concrete.

The reason behind the start of use of lightweight concrete as opposed to normal weight concrete was due to its reduced weight, and first application was observed in the military field. In World War I, U.S. government started to look for any material to be used for ship construction other than steel, due to scarcity of high-grade steel. At that point, lightweight concrete had come into mind, while in those days, lightweight concrete had already been in use for construction of ships in Scandinavian countries. Evaluating the current technologies and availabilities, the first lightweight concrete ship, Selma had found a place in history in this regards. Although not able to service for long years, Selma performed great performance for three years for transportation of crude oil and was the pioneer reason for building up confidence towards the use of lightweight concrete in United States. With regards to structural applications, the first lightweight concrete building was a gymnasium of a high school in Kansas City USA in 1922 according to ESCSI (1971). First use of lightweight concrete in high-rise buildings was in later 1930's in St. Louis USA, where the lightweight concrete was used in both frame and floor systems. From that time on lightweight concrete has come to an industry and made possible the construction of greater structures with greater performance.

1.1.2. Lightweight Concrete in Codes

In 1963 in United States, the use of structural lightweight concrete has been permitted with the release of ACI 318-63 (1963). In the study, conducted with the support of National Science Foundation in U.S. in 1982, the columns made of structural lightweight concrete had been proven to have lateral strength as much as columns made of normal weight concrete. The use of lightweight concrete was encouraged in the light of the studies with the release of ACI 318-83 (1983) in 1983. In ASTM 330/330M-14 (2014), all lightweight aggregate concretes have been classified as having 28 day compressive strength varying between 18-28 MPa with density of 1600-1760 kg/m^3 successively. The elasticity modulus of concrete is defined as $E_c = w_c^{1.5} 0.043\sqrt{f_c'}$, for concretes having densities between 1440-2560 kg/m^3 in ACI 318-08 (2008). Moreover, the use of a modification factor, λ is noted to be used for all equations as a multiplier of $\sqrt{f_c'}$, not limited to elasticity modulus, for all equations. The modification factor is stated as λ =0.85 for sand-lightweight concrete and λ =0.75 for all-lightweight concrete. Additionally, a linear interpolation is permitted between the values according to concrete's volumetric fractions. Furthermore, minimum depth for non-prestressed beams and one-way slabs is advised to be multiplied with a factor of (1.65-0.0003w_c), not greater than 1.09 for lightweight concrete having densities between 1440 and 1840 kg/m^3.

1.1.3. Advantages and Disadvantages

The structural lightweight concrete has certain advantages on the normal weight concrete as well as disadvantages. The most remarkable advantage is its reduced weight compared to normal weight concrete. The dimensions of structural elements, particularly foundations and columns, can be made smaller due to reduced dead weight of structure. Especially in infrastructure projects such as bridges, these reductions could provide savings in terms of structural safety, economy and ease of construction. The proposed equation for structural lightweight concrete's modulus of elasticity has been mentioned above, and generally yields lower values compared to normal weight concrete. The lower values of elasticity modulus can lead to lower shrinkage stresses, lower differential settlements especially in bridge beams. Additionally, lower permeability and comparatively high freeze-thaw resistance are taken into account as advantages of structural lightweight concrete.

On the other hand, structural lightweight concrete has some drawbacks over normal weight concrete. One of the most important ones is the higher temperature rise due to higher rate of heat of hydration. Furthermore, the strength of lightweight aggregates in mostly smaller than that observed by normal weight aggregates, where this requires a careful study with regards to the final performance of the concrete used in structural applications.

1.1.4. Lightweight Aggregate Types

Structural lightweight aggregate types can be classified into two groups according to ACI 213R-87 (1987), namely naturally occurring and unprocessed aggregates, and processed aggregates, where the naturally occurring and unprocessed aggregates are more favorable type among them. The materials classified in the former group can be used after pulverization processes. The main types used as naturally occurring and unprocessed aggregates are perlite, pumice and tuff.

The expanded lightweight aggregates may be less advantageous when compared to the naturally occurring and unprocessed aggregates. The processed lightweight aggregates are obtained after several operations, such as expansion, pelletization and sinterization. The main types used for processed aggregates are clay, shale, blast-furnace slag and slate. These materials are bloated at high temperatures in rotary kilns, and a very popular lightweight aggregate called as haydite is obtained. Haydite has been popularly used in the production of lightweight concrete around the world, but feasibility of using haydite has always been possible due to the special needs of a project (such as reducing the dead weight of a structure or improve fire ratings). Other than special needs, the use of normal weight aggregates mostly becomes more economical in most structural applications, since normal weight aggregates can be used with none or few processes in the production of concrete.

1.2. Motivation, Objective and Scope

Turkish Specification TS-500 does not allow the use of lightweight concrete in load carrying members of structures. If any lightweight aggregate is especially available for use in its natural form, then limitation of its use should be abandoned while its use has already been allowed by ACI 318 even in earthquake prone regions. The main motivation to carry out this research study was the vast availability of naturally occurring lightweight aggregate perlite in Turkey to be used towards the production of lightweight concrete. Actually, 75% of total worldwide perlite reserves are in Turkey. The aggregate to be used in the scope of this thesis, perlite, is found in raw form in Mollaköy, Erzincan, which is an earthquake prone region in Turkey. Mollaköy perlite has been shown by Aşık (2006) and Eser (2014) to be used as lightweight concrete after a few physical processes.

The use of lightweight concrete in RC framed structures should be tested by carrying out experimental studies on RC members. Few documented studies are available in this regards, where the reason for this is the fact that lightweight concrete in the world is especially not popular compared to normal weight concrete. Furthermore, assessment of the constitutive behavior of lightweight concrete material also needs to be studied with regards to its ductility under both unconfined and confined stress conditions as present in load carrying members of structures.

This thesis in this regards firstly aims to determine the stress-strain behavior of structural lightweight concrete. Although there are several studies on the confinement effects on normal weight concrete, there is lack of reliable information about the confinement behavior attained by structural lightweight concrete by spiral or stirrup reinforcement. In order to evaluate the performances of structural lightweight concrete and normal weight concrete in a reliable manner, an experimental study is conducted in Construction Materials Laboratory in Middle East Technical University. Through the experimental study on cylinder specimens that are unconfined and confined in different percentages by spiral reinforcement, the elastic and inelastic, namely post-peak behavior of structural lightweight concrete is recorded and plotted with displacement-controlled testing machines.

In the second phase of study, the results obtained from the experimental study are evaluated in order to find a reliable concrete model for confined structural lightweight concrete similar to the model suggested in Kent and Park Model (1971). The confined concrete model obtained from experimental studies and Kent and Park model are used in order to verify the experimental study of an RC beam conducted in the literature. After this verification study, in order to demonstrate that RC framed structures that employ lightweight load carrying members can actually serve under seismic loadings, nonlinear structural analysis is carried out for a 5 story RC building. The data obtained from the experimental study is used in order to properly define the nonlinear behavior of the beams and columns of the building. Results obtained from this 5 story building that is designed both as normal weight and light weight are then compared. The results indicate that structural lightweight concrete use in RC buildings can provide a reliable nonlinear structural response under seismic loadings.

CHAPTER 2

REVIEW OF PREVIOUS STUDIES

In recent years, there have been few studies performed on determination of the behavior of structural members with lightweight concrete and no studies to the knowledge of the author of this thesis on the nonlinear response estimation of reinforced concrete moment resisting framed structures. The studies on lightweight concrete member response determination are categorized under experimental as well as analytical, where the study of Almousawi (2011) is one of the most notable of them.

Almousawi has mainly focused on the high performance high strength lightweight concrete by conducting both experimental and analytical studies. The main aim of his study is to strengthen the analytical studies with verification of experimental studies. In experimental studies, the aggregate type chosen for lightening of concrete is expanded shale. After several tests performed on micro-silica fume, expanded shale, gravel, granite and sand; Almousawi has decided to proceed with expanded shale. In the light of experiments, among those expanded shale has been chosen as the most appropriate material with a dry density of nearly 400 kg/m^3. Experiments have been performed in two sets, Flexure LWC Beams and Shear LWC Beams. In order to keep the relevancy, only first set of experiments has been reviewed in this chapter.

In flexure LWC Beams test, the flexural behavior of lightweight concrete has been investigated with a simply supported beam of 3600 mm length including 150 mm cantilever parts at the ends. In first part, lightweight concrete beams having compressive strengths of 68.5, 58.3 and 50.9 MPa have been loaded with constant reinforcement ratio. In the second part of the experiments, the first scheme has been applied with a lightweight concrete of 43.56 MPa for varying reinforcement ratios. In the light of experiments, researcher has been concluded with findings whereas some of them listed below:

- Increase in compressive strength ends up with an increase in the number of flexural cracks
- Increase in compressive strength ends up with a decrease in ultimate displacement
- Increase in tension reinforcement ends up with a capacity increase of ultimate load
- Decrease in tensile steel reinforcement ends up with an increase in ultimate compressive strain
- Lightweight concrete beams perform larger strains than normal weight concrete beams

In the analytic part of the study, Almousawi has performed several analyses in a finite element analysis program, ANSYS. He has performed more than 1,400 analyses with different shear span to depth ratios, shear reinforcement spacing, longitudinal steel reinforcement ratio and various concrete models with different compressive strengths. In addition to verification of experimental outcomes, analytical results conclude that ultimate flexure capacity of lightweight concrete beams increases with increasing compression steel ratios. Furthermore, he has stated that ACI 318-08 (2008) formulas underestimates the maximum deflection of reinforced lightweight concrete beams at ultimate load and ultimate moment capacity compared with nonlinear finite element analysis program results whereas cracking moment capacity is proven to be well estimated by ACI 318-08 (2008).

In a similar manner, Ahmad, Xie and Yu (1995) have performed series of experiments focused on shear ductility of reinforced lightweight concrete beams in North Caroline State University. In the scope of study, 15 reinforced concrete beams with and without shear reinforcement have been investigated. In the production phase of reinforced concrete beams, expanded shale, not being greater than 12.5 mm, has been used. The test specimens have been prepared according to various concrete strength varying between 30.5-89.3 MPa, span to depth ration varying between 1-4 and shear reinforcement ratio between 0-0.784%. The dimensions of beams, used in study, are 127x254 mm with tension reinforcement of 2ϕ13 to 4ϕ19 for varying specimen types. The existence of shear reinforcement is expected to make the flexural behavior to act in a gradual or a ductile way of failure rather than a brittle failure. The issue is further proven by the authors that load versus deflection curve become milder as the shear reinforcement ratio increases. Additionally, the ultimate load capacity increases as the shear reinforcement ratio increases. Actually, the behavior of shear ductility is measured a parameter named shear ductility index which is calculated by the ratio of the area under the load versus deflection curve up to a strain of three times the ultimate load strain to area under the load versus deflection curve up to ultimate load strain. It is stated that shear ductility index tend to increase with an increase in the shear reinforcement. Moreover, shear ductility index increases by 25% for the reinforcement increase from 0.51% to 0.65% whereas further increase does not have an impact on shear ductility index. Furthermore, the shear ductility index decreases with increasing concrete strength.

In the study of Zandi (2012), structural performance of lightweight concrete has been investigated with help of several experimental studies by comparing the lightweight concrete with normal weight concrete. Zandi has performed experiments including slump test, cylindrical concrete compression test, cylindrical splitting test, pull-out test, flexural beam test and axial column test. In the production phase of lightweight concrete, sand, natural and expanded perlite, fly ash, microsilis and pumice are used. Initially, he has tested 21 different samples in order to investigate their compressive stresses varying between 5-30 MPa by differentiating their ingredients. Being experienced on different mixes, an additional three different samples are also produced in order to have lightweight concretes having compressive strength greater than 25 MPa.

In the flexural analysis phase of the experiments, the lightweight concrete named SLC19, which has a compressive strength of 29.08 MPa at the end of 28 days, is used. The test specimen is a 1250 mm length beam with 95 mm cantilever parts. The dimensions of beam are 250 mm depth and 200 mm wide with reinforcement of 2ϕ12 at the top and 3ϕ12 at the bottom. The same procedure is applied for a normal weight concrete with a compressive strength of 33.15 MPa at the end of the 28 days. The beam is started loading on its mid-span until the ultimate.

Furthermore, the study of Okuyucu, Turanlı, Uzal and Tankut (2011) is one of the remarkable studies performed on fiber reinforced semi-lightweight concrete properties. In their studies, the steel fibers and polypropylene fiber are used as reinforcement in precast lightweight concrete panel production.

They have tested the unreinforced, steel fiber reinforced and polypropylene fiber reinforced semi-lightweight cylindrical and precast panel specimens at various ages of concrete. It is stated that existence of unexpanded perlite powder is resulted in remarkable increase in 28^{th} day compressive strength of specimens. On the other hand, perlite powder replacement instead of cement has resulted in a decrease in the tensile strength and modulus of elasticity of the tested samples.

With regards to the nonlinear analysis of reinforced concrete framed structures by using finite element programs, there are no studies to the knowledge of the author of this thesis that considered the nonlinear behavior of lightweight concrete framed structures. For this purpose, general studies on nonlinear static and/or dynamic analysis procedures will be discussed here.

In the study of Kalkan and Kunnath (2007), nonlinear time-history analysis is stated to conclude better results than nonlinear static procedure. However, nonlinear static procedure has a wider use in engineering practice due to greater computational effort required for nonlinear time-history analysis. On the other hand, it is stated that procedures in ATC-40 (1996) and FEMA 356 (2000) regarding nonlinear static procedures, are found to be inadequate when higher modes are more effective rather than first modes. Therefore, the need for a modification is needed in order to terminate the computational inefficiency. In FEMA 356, two sets of lateral load distribution are proposed. In first set, pseudo lateral load pattern (applicable if $T1<0.5$ s), elastic first mode shape and story shear distribution obtained with response spectrum analysis are listed. In the second set, distribution of lateral load according to mass at each level and adaptive load distribution method are proposed. However, as Kalkan and Kunnath stated there is no detailed information on the adaptive procedures mentioned in FEMA 356. Since FEMA 356 recommends the evaluating the seismic demand by using one load pattern from both of the two sets, authors have taken into account both load pattern sets. In the Modified Modal Pushover Analysis Method (MMPA), suggested by Chopra and Goel (2001) the inelastic response obtained from first mode nonlinear static procedure is combined with elastic response of higher modes with a modal combination rule. The Adaptive Modal Combination Procedure (AMC) has found a place in the study of the authors, which combines the direct adaptive method by Gupta and Kunnath (2000), capacity spectrum method in ATC-40 and pushover analysis method advanced by Chopra and Goel. The authors stated that “The AMC procedure combines the response of individual modal pushover analysis to account for the influence of higher modes and incorporates the effects of changing modal properties during inelastic response through its adaptive feature.” Namely, the target displacement is recalculated step by step in an adaptive scheme during the analysis through the combination of, as authors stated “energy based modal capacity curves with the inelastic response spectra”. Consequently, the need for the estimation of the target displacement is terminated.

In the modelling phase of the study, steel frame buildings of 6 and 13 story, and reinforced concrete buildings of 7 and 20 stories are used. Two dimensional models are used in order to demonstrate the seismic behavior of the structures in a finite element analysis program, named OpenSees. The frame elements are modelled with nonlinear column beam analogy using fiber elements. The Kent-Park concrete model is used while steel material model is bilinear with 2% post-yield response. Furthermore, masses are assigned according to their tributary areas of floors. In order to perform the time history analysis, thirty sets of ground motions have been applied, whereas ten near-fault ground motions with forward directivity, ten near-fault ground motions with fling and ten far-fault ground motions. These are scaled to perform a roof drift of 1.5% for steel buildings and 7 story reinforced concrete building whereas 1% for reinforced concrete buildings.

In the evaluation of roof drift ratio analysis for both steel framed and reinforced concrete framed buildings, results are investigated in terms of FEMA 356, MMPA, UBPA and AMC requirements. It is concluded that FEMA 356 procedure overestimates the peak story displacements in the intermediate story levels whereas UBPA underestimates the related displacements when compared to nonlinear time-history analysis. The MMPA and AMC methods are performed similar results and these are thought to be referenced for the other models. In the inter-story drift ratio profile analysis, FEMA 356 procedures generally perform an underestimation for upper stories and an overestimation for lower stories. On the other hand, UBPA has been concluded with an underestimation for lower levels and an overestimation for upper levels. Although MMPA performs better results than FEMA 356, it generally ends up with underestimation for upper levels. Among the other methods, AMC is proven to have closer results when compared the nonlinear time-history analysis.

Furthermore, AMC and MMPA procedures are compared with nonlinear time-history analysis in terms of plastic rotations for 6 story steel and 7 story reinforced concrete buildings. MMPA procedures are concluded with far from results of plastic rotation values of columns at 5th story of 6 story steel building when compared with AMC and nonlinear time-history procedures although it results with close values at 1st story. Similarly, it yields good results for 4th story of 7 story RC building whereas the values of those at other levels are seen to stay poor. On the other hand, AMC procedures are concluded with more preferable results at 1st and 5th levels of 6 story steel building. Additionally, AMC procedures have resulted in a far close performance for determination of plastic rotation capacities for 7 stories RC building when compared with nonlinear time-history analysis.

In the end of the analysis, the authors conclude the results listed below:

- The FEMA 356 procedures perform less accurate results when the contribution of higher modes dominates for the determination of drift ratios and column plastic rotation capacities
- UBPA procedures are found to have a very low performance among the other procedures by underestimating the drift ratios for lower levels and overestimating the drift ratios for upper levels of drift ratios and plastic rotation capacities of columns
- Although MMPA procedures are concluded with closer results to nonlinear time-history analysis, it performs inadequate performance for determination of plastic rotation of columns in upper stories

CHAPTER 3

INVESTIGATION OF CONFINEMENT EFFECT BY EXPERIMENTATION FOR NORMAL WEIGHT CONCRETE, LIGHTWEIGHT CONCRETE AND MODIFIED LIGHTWEIGHT CONCRETE

The investigation of previous studies lead to the conclusion that there are few studies on the issue of determination of confinement effects on lightweight concrete material. Although there are widely accepted confined concrete models for normal weight concrete, researchers did not pay so much attention as they did for normal weight concrete. The study of Hlaing, Huan, and Thangayah (2010) is one of the remarkable ones investigating confinement effect of lightweight concrete. In their study, they have also noted that there are almost no studies that they can record on the determination of the response of lightweight concrete material's stress-strain response. In their study, different lightweight concrete samples varying between 38 MPa and 58 Mpa are tested with different spiral reinforcements those having tensile stress of 1245, 1457 and 1675 MPa. Although they have performed great effort, since sample spiral spacing is comparatively low and using spiral reinforcement with comparatively high tensile capacity, minimum 1245 MPa as mentioned, they have not been able to conclude with a fair post peak responses, i.e. the post-peak response of the stress-strain plots from the experiments yielded significant hardening response, which is actually not the most characteristic response that would be studied for concrete material.

While not related to lightweight concrete, the study of Leung and Burgoyne (2001) can be cited as one of the remarkable studies on the determination of confinement effects on concrete. Different from their counterparts, they studied the confinement effects attained by aramid fibers. In first set of experiments, aramid fibers are placed as single spirals with a spiral spacing of 10, 20, 35 and 50 mm, those having elasticity module of 90.1 GPa. In the second set, in order to visualize the confinement effect of non-circular elements, two different spirals are placed to be interlocked. The concrete has been molded with design strength of 40 MPa.

In the light of experiments, they have concluded the following:

- The load versus displacement of the specimens are merely differed before reaching the peak load, for unconfined and confined ones
- The ultimate strain is 4 times greater for spirals those 50 mm spaced, and 7.5 times greater for spirals those 10 mm spaced, than the unconfined specimens
- When the overlapping distance becomes smaller, the ductility becomes greater, and ductility increases with increasing overlapping

In order to visualize the success of the aim of the study in this thesis, the author of this thesis performed a trial testing on unconfined and confined lightweight concrete at Materials of Construction Laboratory of Middle East Technical University (Figure 3.1).

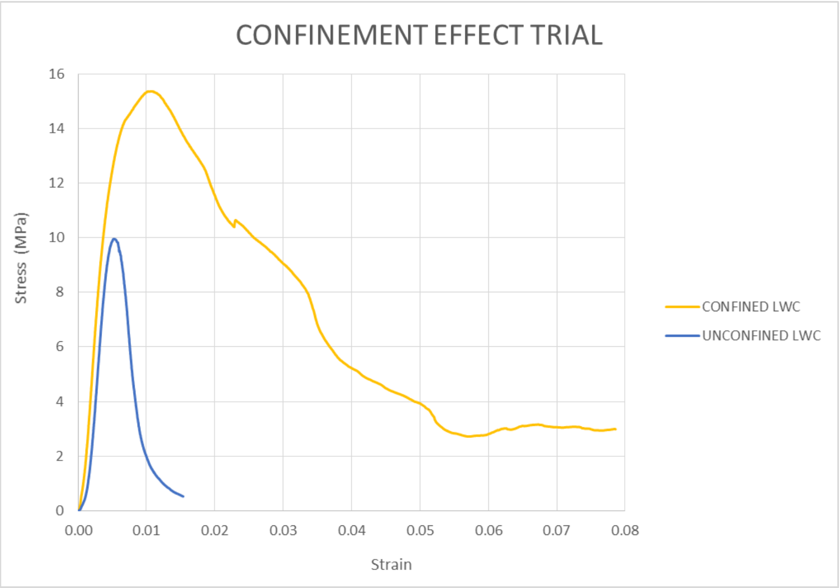

Figure 3.1 Early Trials on Confined LWC

In Figure 3.1, a schematic graph of confined and unconfined lightweight concrete is presented. As seen confinement has a great effect on both maximum compressive stress and ultimate strain. Furthermore, the balance between the concrete and spiral reinforcement is proven to be successful to give a softening post-peak responses, which is the typical response that would be present in RC beams and columns.

3.1. Materials

In the experimentation, three different concrete types are considered. These are normal weight concrete, lightweight concrete and modified lightweight concrete. The concrete types differed from each other in some respects. The crushed stone is used as aggregate in normal weight concrete whereas natural perlite aggregate is used in lightweight concrete. In the modified lightweight concrete, the natural perlite aggregate is used; different from lightweight concrete, the amount of cement is replaced with perlite powder by 50% in order to visualize the effect of perlite powder as a binder. The properties of natural perlite aggregate used in this thesis is the same as that obtained from the studies of Eser (2014) and perlite powder; obtained from the studies of Aşık (2006), and these are presented in Table 3.1 and Table 3.2.

Table 3.1 Physical Properties of Perlite Aggregate

Aggregate Size (mm)	0-3	8-12
Dry-Loose Unit Weight (kg/m^3)	1288	1002
Oven Dry Specific Gravity	2.06	1.93
Saturated-Surface Dry Specific Gravity	2.18	2.04
Water Absorption Capacity (%) – 72 hr	5.64	5.59
No.200 Sieve % Passing	11.64	-
Los Angeles Abrasion (%)	-	49.7

Table 3.2 Chemical and Physical Properties of Perlite Powder

Chemical Composition of Perlite Powder	
SiO_2	70.96
Al_2O_3	13.40
Fe_2O_3	1.16
MgO	0.28
CaO	1.72
Na_2O	3.20
K_2O	4.65
Loss on ignition	3.27
Physical Properties of Perlite Powder	
Specific Gravity	2.38
Fineness	
Passing 45-µm (%)	80
Specific Surface, Blaine (m^2/kg)	413
Median Particle Size (µm)	19.1
Strength Activity Index (%) *	
7 Days	78
28 Days	80

* In accordance with ASTM C311 Standards

Additionally, the physical properties of limestone aggregate, used in normal weight concrete is cited below in Table 3.3.

Table 3.3 Physical Properties of Limestone Aggregate

Aggregate Type	0-4 mm	4-12 mm	12-25 mm
Saturated-Surface Dry Specific Gravity	2.62	2.71	2.71
Oven Dry Specific Gravity	2.59	2.70	2.70
Water Absorption Capacity (%)	1.4	0.29	0.22

In the experiments, the Portland cement, type of CEM I 42.5 R is used. The chemical properties and physical properties, provided by quality control department of Bolu Çimento, is cited below in Table 3.4.

Table 3.4 Chemical and Physical Properties of Portland Cement

CEM I 42.5 R	
Chemical Composition, %	
CaO	62.54
SiO_2	19.32
Al_2O_3	4.76
Fe_2O_3	4.36
MgO	2.04
SO_3	3.49
K_2O	0.67
Na_2O	0.21
Cl-	0.0219
LOI	2.26
IR	0.63
Physical Properties	
Specific Gravity	3.17
Blaine Fineness, cm^2/g	4534
Initial Set, min	115
Final Set, min	160

Furthermore, BASF Gilenium 51, is used as superplasticizer in a ratio of 1% by mass. The properties of superplasticizer are cited in Table 3.5.

Table 3.5 Properties of Superplasticizer

Structure of Material	Polycarboxylic ether based
Density	1.082 - 1.142 kg/lt
Chlorine Content (%)	< 0.1
Alkaline Content (%)	< 3

The reinforcing steel, used as confining reinforcement is tested in universal testing machine, and the stress-strain performance is presented in Figure 3.2. The tension test of reinforcing steel resulted in a yield strength of 226 MPa and ultimate strength of 351 MPa. The diameter of the confinement reinforcement is chosen as 4mm in order to demonstrate the confinement properties properly.

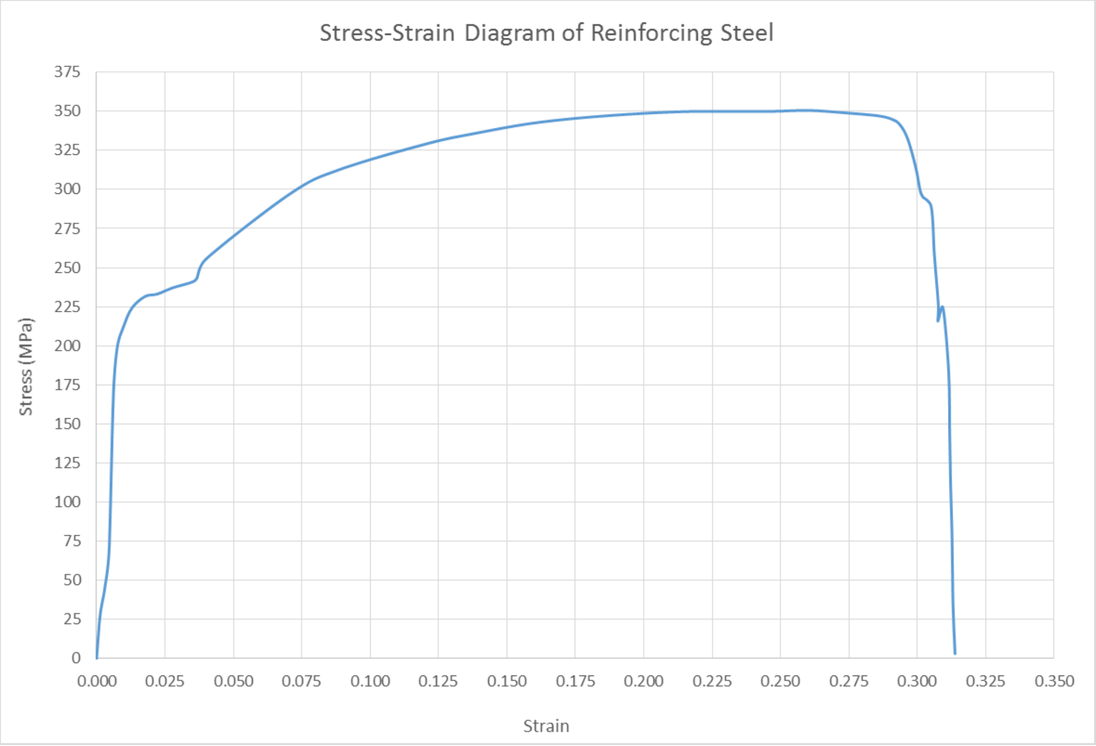

Figure 3.2 Stress-Strain Diagram of Reinforcing Steel

In the preparation phase of concrete samples, concrete is molded into 10x20 cm cylindrical specimens. When the unconfined concrete samples' compressive strength is close to 20 MPa, confined concrete samples are expected to be tested due to limitations of the MTS testing machine at Materials of Construction Lab. Each of the concrete types is prepared as they will be tested for 3 specimens in each group in order to reduce the experimentation errors, where the results are evaluated as an average of these three tests. In a similar manner, confined concrete samples are molded as they will be tested for 3 specimens, as well. On the other hand, two different levels of confinement are used for each of the concrete types. In the first set of samples, the specimens are confined with 30 mm spaced spiral reinforcing steel, which has a volumetric reinforcement ratio of approximately 1.5%. In the second set, they are confined with 50 mm spaced spiral confining steel, which has a volumetric reinforcement ratio close to 0.9% (Figure 3.3).

Figure 3.3 Spiral Reinforcement for Confinement

The reinforcing spiral presented in Figure 3.3 is prepared under a controlled setup in order not violate the clear cover of specimens. In all reinforcing samples, the clear cover is provided as 1 cm with the help of wooden sticks.

3.2. Concrete Mixture Composition

The composition of concrete samples are presented in Table 3.6. The idea behind the mixed design is to obtain 20 MPa compressive strength at the time of testing. In order to monitor the progress in a successful manner, the specimens are tested in seven days intervals. For the unconfined concrete samples that reach a compressive strength close to 20 MPa, their successor spirally confined ones are started to be tested.

Table 3.6 Mixture Proportions of Concretes

Mix Proportions (kg/m^3)			
Concrete Type	Normal Weight Concrete	Lightweight Concrete	Modified Lightweight Concrete
Cement	250	250	125
Perlite Powder	0	0	125
Water	133	202	202
0-3 mm Perlite Aggregate	0	883	883
8-12 mm Perlite Aggregate	0	657	657
0-4 mm Limestone Aggregate	1111	0	0
4-12 mm Limestone Aggregate	421	0	0
12-25 mm Limestone Aggregate	526	0	0
Superplasticizer	2.5	2.5	2.5

3.3. Fresh Concrete Tests

After preparing the concrete mixture, various fresh concrete tests have been performed. The purpose of these tests is to measure and evaluate workability, durability and the integrity of mixtures of the fresh concrete. The results obtained from the fresh concrete samples are presented in Table 3.7. In the light of results obtained from fresh concrete samples, the time for removal of plastic mould cases are decided. The removal time of cases of normal weight concrete is 24 hours after pouring of concrete. The removal time of cases of lightweight concrete and modified lightweight concrete is 48 hours after the moulding. In order to prevent the dehydration of fresh concrete, humid blankets are used. The concrete samples, after removal process, left for the curing in the curing pool with a temperature of 21 °C in the Construction Materials Laboratory.

Table 3.7 Properties of Fresh Concrete

CONCRETE TYPE	W/C	SLUMP (mm)	AIR-CONTENT (%)	DENSITY (kg/m^3)
NWC	55	85	2	2410
LWC	80	100	2.5	1913
MLWC	80	90	2.2	1910

3.4. Experimentation Setup

In the experimentation, the most obvious difference is the use of displacement controlled testing machine. Through the help of machine, the stress-strain diagrams are allowed to appear even after the ultimate load capacity is reached. Before starting the tests, the specimens are covered with caps in order to conclude with a more uniform loading surface.

In the loading case, after being placed the specimens in a symmetric form as much as achieved, the loading is started with a rate of 1 mm per minute as suggested in ASTM C469/C469M-14 (2014).

3.5. Experimentation Results

Throughout the experiments, the relevance between the scope and work done is tried to be kept in line. In this respect, the concrete types, unconfined samples of those reached about 20 MPa regardless of their curing time, are taken into consideration in order to perform the confined concrete tests. The test results and the procedure for all the concrete types, normal weight concrete, lightweight concrete and modified lightweight concrete is explained in remaining sections of this chapter.

The results obtained from the experiments are compared with a widely accepted confined concrete model, named Kent and Park Model (1971). The response curves of Modified Kent and Park Model is presented in Figure 3.4 as available in Ersoy and Özcebe (2001).

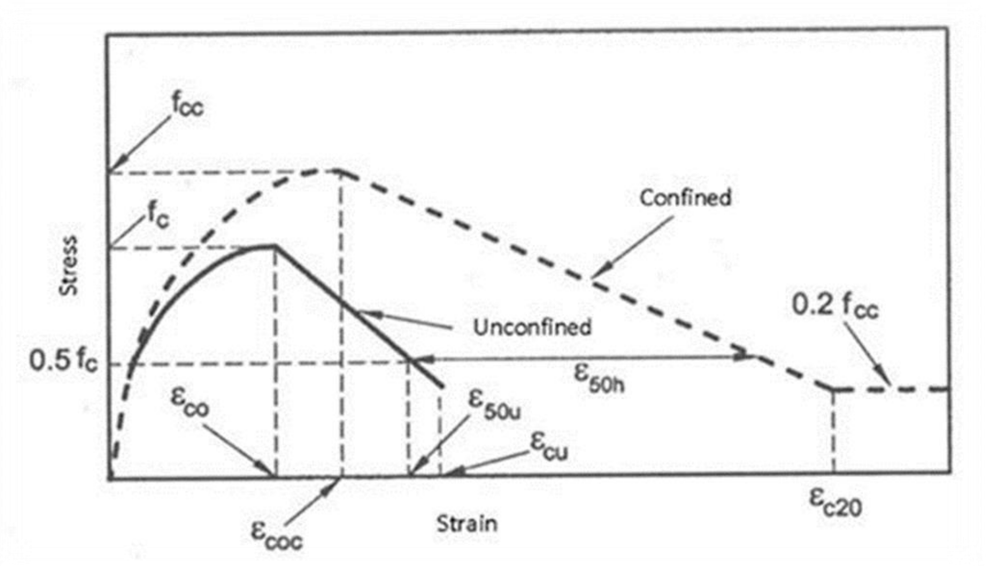

Figure 3.4 Modified Kent and Park Model in Ersoy and Özcebe (2001)

In comparison studies in this thesis, confined concrete strength, f_{cc}, strain at the ultimate confined concrete strength, ε_{coc}, and confined concrete strain at the stress value of 20% of f_{cc}, ε_{c20} are used. In the calculation of this parameters, level and effect of confinement are taken into account with a coefficient, K, and f_{cc}, ε_{coc}, and ε_{c20} values are calculated according to formulations defined below.

$$K = 1 + \frac{\rho_s f_{ywk}}{f_c}$$

$$f_{cc} = K f_c$$

$$\varepsilon_{coc} = K \varepsilon_{c0}$$

$$\rho_s = \frac{A_0 \; x \; l_s}{s \; x \; b_k \; x \; h_k}$$

3.5.1. Normal Weight Concrete Experiment & Results

In the experimentation of normal weight concrete specimens, the concrete has gained early strengths in a couple of days as expected due to confidence from the previous trials before the experimentation. The unconfined specimens are started to be tested at 3rd day and the confined specimens are tested at 4th day after unconfined specimens are tested. The loading rate is, as mentioned 1mm/min, in the experimentation.

The peak strength, observed in unconfined samples is about 16 MPa, and due to time limitations of the author of thesis this value was considered to be an acceptable level of peak strength gain, where the strain at peak strength is observed as 0.0038.

The 30 mm spiral spaced concrete samples are tested after unconfined ones are tested. The maximum observed strength is recorded as 17.7 MPa with a strain of 0.006. The energy absorbed at the ultimate strain is calculated as 1709 kN.mm.

Lastly, 50 mm spiral spaced normal weight concrete samples are tested. Maximum stress is recorded as 16.7 MPa with a strain of 0.0055 regarding at this point. The energy absorbed at the ultimate strain, ε_{c20}, is recorded as 802 kN.mm. The stress-strain diagrams, regarding the average of three samples, for unconfined and confined with 30 mm and 50 mm spiral spaced concrete samples are presented in Figure 3.5.

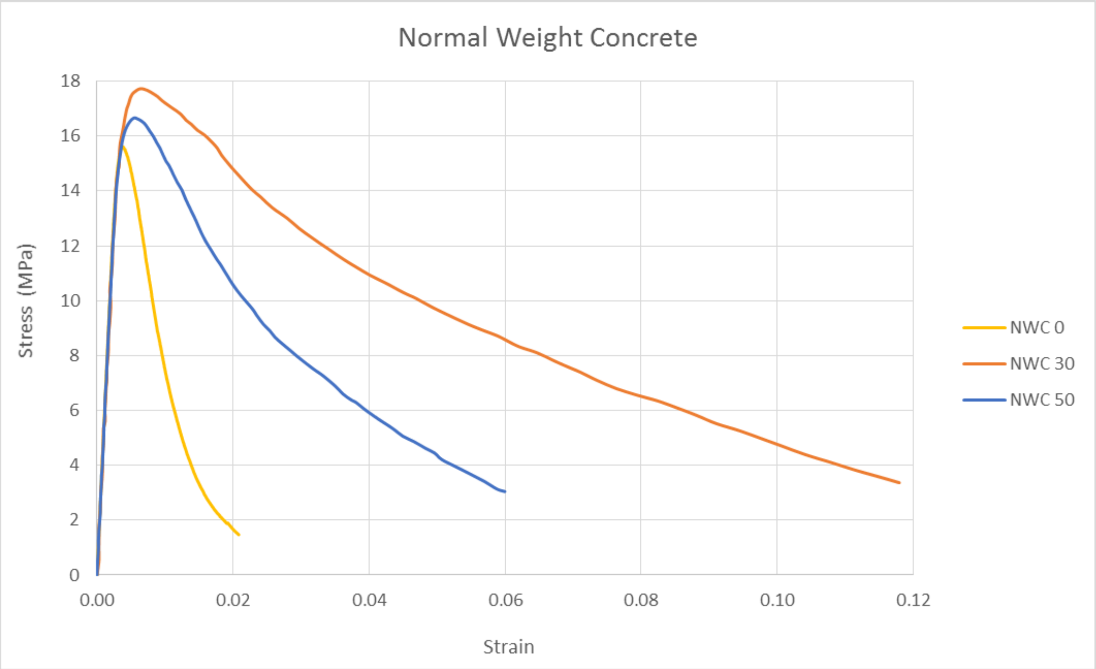

Figure 3.5 Stress-Strain diagram of Normal Weight Concrete

The results obtained from the series of experiments are compared with the theoretical calculations, those obtained in the light of Kent and Park Model (1971). The theoretical and experimental results differed from each other in some respects. In the experimentation of 30 mm spiral spaced concrete, maximum stress is 6% smaller from the theoretical results, whereas the strain at the ultimate stress is 30% greater than the theoretical calculations. Similarly, the maximum stress for the 50 mm spiral spaced concrete is 5% smaller than the theoretical calculations, with a 28% smaller strain at the point of maximum stress.

3.5.2. Lightweight Concrete Experiment & Results

In the case of lightweight concrete, the concrete specimens are tested starting from 7th days to reach the expected results. The maximum load carrying capacity is recorded as 133.5 kN and 17 MPa with a strain of 0.0042. The strain and stress experienced are in line with the predicted results.

As unconfined samples reach the 19 MPa, confined samples are started to be tested. In Figure 3.7, relevant stress-strain diagrams are presented for unconfined and confined concrete with spiral spacing of 30 mm and 50 mm spacing. The test set up and experimentation is presented in Figure 3.6.

Figure 3.6 Test Set up and Experimentation

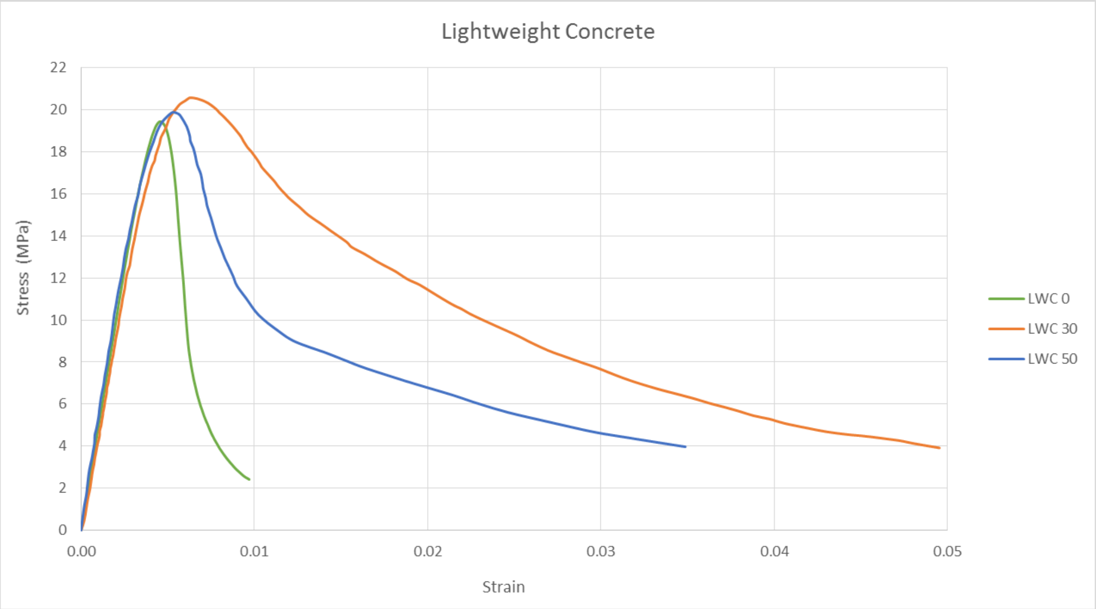

Figure 3.7 Stress-Strain diagram of Lightweight Concrete, 11 Days

The maximum stress of unconfined lightweight concrete samples is recorded as 19 MPa with a strain of 0.0046. Successively, the confined concrete samples are being tested under compressive loading with a loading rate of 1 mm/min.

The maximum stress observed in the test of 30 mm spiral spaced samples are recorded as 20.6 MPa with a strain of 0.006. The energy absorbed at the ultimate strain is recorded as 776 kN.mm.

Following the 30 mm spiral spaced samples, 50 mm spiral spaced concrete samples are tested. The maximum stress is recorded as 19.88 MPa with a strain of 0.0054. The energy absorbed, according to the results mentioned, is observed as 498 kN.mm.

The results obtained from the experimentation is compared with the theoretical calculations based on Kent and Park Model (1971). The ultimate stress experienced is 9% smaller than the theoretic calculations, whereas the strain at ultimate load is 20 % greater than the theoretic calculations.

The results observed for 50 mm spacing do differ from the results of 30 mm spiral spaced samples. The ultimate stress is 6 % smaller than the theoretical calculations. On the other hand, the strain at the ultimate load for 50 mm spiral spaced is 8% greater than the theoretical calculations (1971).

3.5.3. Modified Lightweight Concrete Experiment & Results

The compressive strength of modified lightweight concrete has been tested in several days. These experiments are conducted on 7^{th}, 14^{th}, 21^{st}, 28^{th} and 42^{nd} days. Being close to the results expected, the final tests are conducted on 42^{nd} day.

The compressive strength of modified lightweight concrete has increased day by day after moulding. As seen in the Figure 3.8, the compressive strength has increased from 7 MPa to 15 MPa between 7^{th} and 42^{nd} days. Also, the elasticity modulus of it has increased in a similar manner, approximately it doubled itself between 7^{th} day and 42^{nd} day.

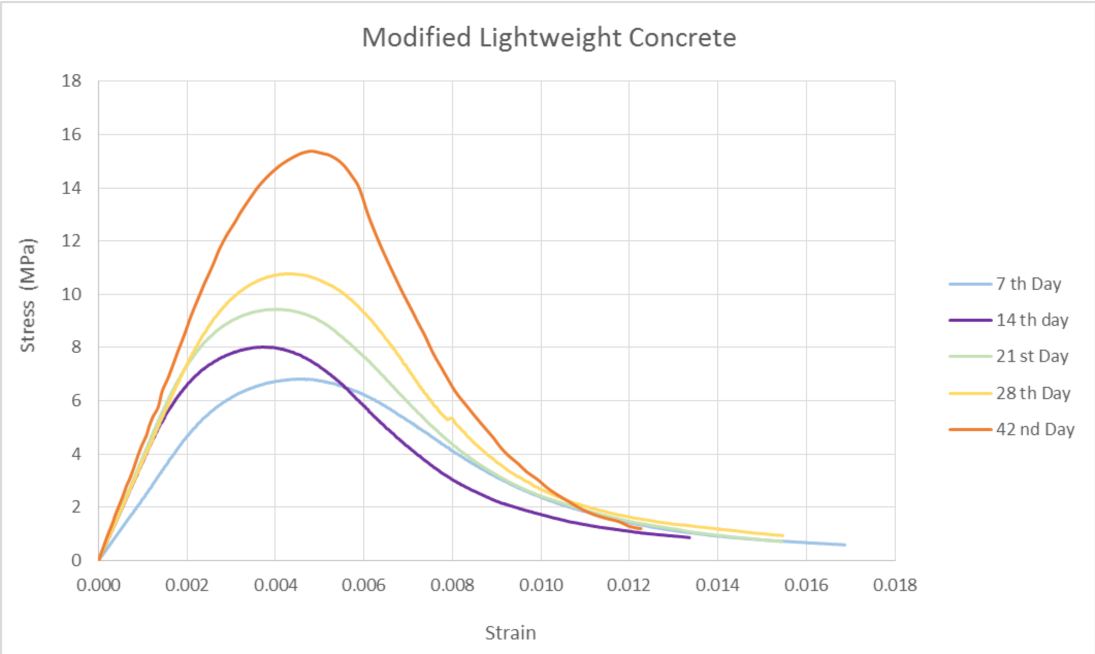

Figure 3.8 Stress-Strain diagram of Unconfined Modified Lightweight Concrete

As seen in the Figure 3.8, the unconfined sample of modified lightweight concrete has reached a compressive strength of 15.37 MPa with a strain of 0.005 relatively. The amount of strain at the ultimate strain demonstrates the great energy absorption capacity of modified lightweight concrete.

In the next step, confined samples of modified lightweight concrete is tested. Initially, the samples of confined with 30 mm spiral spacing is tested. The samples tested have reached an average value of 17.6 MPa with a strain of 0.008. The energy absorption capacity of the sample is recorded as 1159.55 kN.mm.

Finally, the confined sample of 50 mm spiral spacing is tested. The sample has an average compressive strength of 16.23 MPa with a strain of 0.006. Also, the energy absorption capacity is recorded as 499.93 kN.mm.

The overall results of tests performed on modified lightweight concrete is presented in Figure 3.9. The results of modified lightweight concrete are compared with the Kent and Park Model (1971), as well.

In the case of samples with 30 mm spiral spacing, the experienced ultimate stress is 6% smaller than the theoretical calculations. On the other hand, the samples experienced a strain of 26% greater than the theoretical calculations.

Similarly, the 50 mm spiral spaced specimens have a 6% smaller ultimate stress with 12% greater strain, when compared the theoretical calculations.

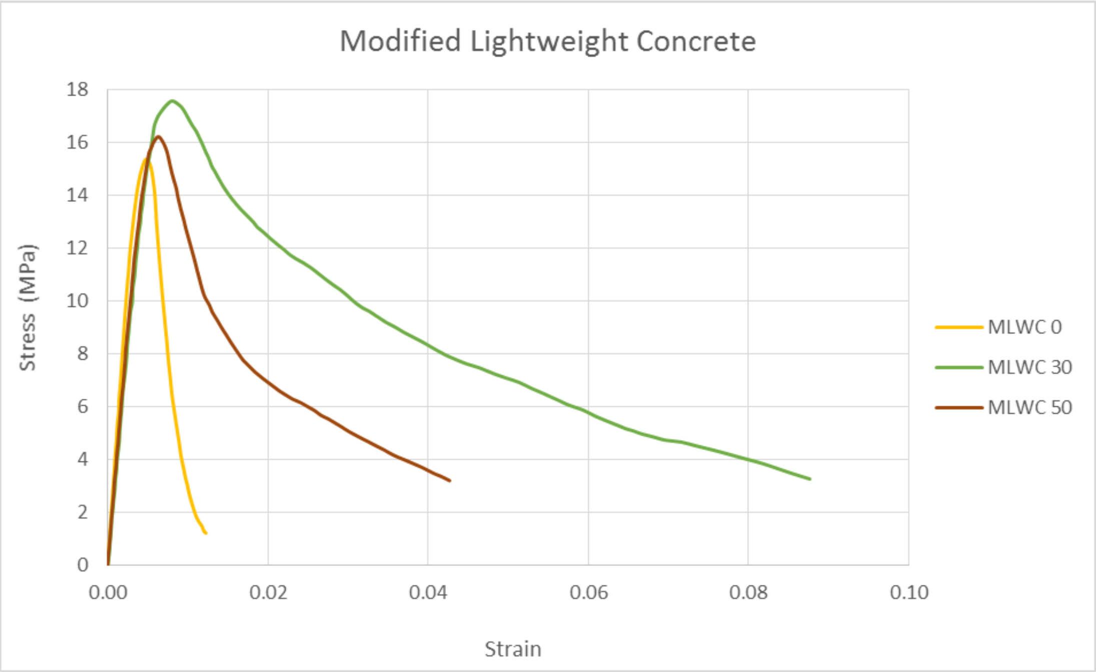

Figure 3.9 Stress-Strain diagram of Modified Lightweight Concrete

3.6. Comparison and Discussion of Results

Through the experimentations, performed in the scope of this thesis, observation of confinement effect of several concrete types has been possible.

In Table 3.8, the results obtained from the experimentation are presented and compared with the theoretical expressions, calculated according to the Kent and Park Model (1971).

Table 3.8 Results and Comparison of Experimentation Results

Type	Spiral Spacing (mm)	Experimental Maximum Stress (MPa)	Experimental Strain at Maximum Stress	Theoretical Maximum Stress (MPa)	Theoretical Strain at Maximum Stress
NWC	0	15.60	0.0038	-	-
	30	17.70	0.0060	18.91	0.0046
	50	16.70	0.0055	17.59	0.0043
LWC	0	19.00	0.0046	-	-
	30	20.60	0.0060	22.53	0.0053
	50	19.88	0.0054	21.20	0.0050
MLWC	0	15.37	0.0050	-	-
	30	17.60	0.0080	18.68	0.0060
	50	16.23	0.0060	17.35	0.0055

As seen in the Table 3.8, lightweight concrete and modified lightweight concrete have great performance when compared with the normal weight concrete. Also, the theoretical and experimental elasticity modulus of the three concrete types are presented in Table 3.9.

Table 3.9 Theoretical and Experimental Modulus of Elasticity Values

Type	Experimental Modulus of Elasticity (MPa)	Theoretical Modulus of Elasticity (MPa)
NWC	5123.2	18203.0
LWC	4706.1	13736.8
MLWC	3878.7	12186.6

The difference between experimental and theoretical values of elasticity moduli are caused from several reasons. Modulus of elasticity of normal weight concrete falls behind the theoretical values, since it has been tested at 4th day after moulding due time and testing machine capacity problems. Therefore, mechanical properties of normal weight concrete cannot be set completely. The reason behind for the lightweight and modified lightweight concrete is effect of pozzolanic activity. Since, the specimens are tested at early ages when the pozzolanic reactions continue even after than 28th day of concrete, the elasticity moduli of these type of concretes are undervalued.

Further studies that will be conducted on lightweight concrete and modified lightweight concrete, concerning about different testing methodologies, including real time beam and column testing; also the cyclic testing methods, will improve, strengthen and empower the use of lightweight and modified lightweight concrete as much as normal weight concrete.

CHAPTER 4

VERIFICATION OF AN EXPERIMENTAL STUDY IN PERFORM-3D

In the scope of this thesis, before embarking on nonlinear structural analysis of reinforced concrete framed lightweight structures, first the finite element program that will be used in those simulations will be presented. For this purpose, the lightweight RC beams tested by Zandi (2012) is taken into account, and these beams are modelled in Perform-3D in order to study the analytical modelling capabilities in the context of this thesis. In the determination phase of material properties and confined concrete behavior, the experimentation performed by the author of this thesis presented in the previous chapter is used as a guide in order to describe the post-peak responses of reinforced lightweight concrete material.

4.1. Review of Perform-3D

Perform-3D (2006) is a finite element analysis program which is specialized for nonlinear analysis of framed type structures. The most important task when using the program is Component Properties. The task is used for defining materials, sections and compounds. The reinforced concrete properties and structure are modelled with the procedures as described below:

- The material for concrete and reinforcing steel is defined. Perform-3D allows for different material models such as elastic perfectly plastic (E-P-P) or Trilinear, Cyclic Degradation and Strength Loss options.
- In next step, the cross sections are defined to be used as structure components and the materials defined in the previous step are available

to be used; such as forming reinforced concrete section by defining coordinates and quantity of concrete and reinforcing steel for inelastic fiber sections.

- The compounds are set in order to form a structural element composed of different cross sections with different lengths.

4.2. Material Properties for Lightweight Concrete and Normal Weight Concrete by Zandi

In the study of Zandi, cylindrical specimens are tested under compressive load with a displacement controlled compression test machine. Although compressive strength of concrete is thought to gain the most of the strength in 28 days in engineering practice, he has used the 42^{nd} day strength of concrete since it continues to gain strength rapidly even after 28 days up to 42 days.

The strength of lightweight concrete has reached a value of 32.63 MPa at the end of 42 days with a 0.0033 strain. The ultimate strain of the lightweight concrete is recorded as 0.0045. After examining the strength of concrete, the same mixture is prepared to be used in test beam. The test beam is 1250 mm long with 200x250 mm cross sectional dimensions. The supports are located at the 95 mm far from ends. The reinforcement is composed of 2ϕ12 bars at the top and 3ϕ12 bars at the bottom, with a confinement spacing of 100 mm at the mid span and 50 mm at the supports. The strength of normal weight concrete is recorded as 33.15 MPa at the end of 28 days.

In order to model the post peak responses of lightweight and normal weight concrete, Kent and Park Model (1971) is used to fit the behavior in Perform-3D in this thesis. In the case of normal weight concrete, the Kent and Park Model (1971) is used as it is. On the other hand, this model is modified in the light of experimental studies performed by author to account for lightweight concrete behavior in order to visualize the post-peak responses.

4.3. Modelling of Flexural Behavior in Perform-3D

After evaluating the material model for concrete and reinforcing steel, two different cross sections are formed for each of the two experiments. The beam is composed of two different sections; elastic part and inelastic part. In the real behavior of flexural element of simply supported beam, formation of plastic hinges is thought to be in the mid-span of the element. As used in engineering practice, the length of plastic hinge is taken as half of the cross sectional dimension in the direction of loading.

In the modelling phase of inelastic section, fiber elements are used which are composed of nonlinear concrete and steel material. The quantity and placement of reinforcing steel is simulated as in the experimental study of Zandi. In addition, reinforced concrete cross section is used for elastic part of the reinforced concrete beam. In order to perform a pushover analysis, the beam is modelled vertically and loading is simulated in the mid span of the beam as in the experimental study.

4.4. Interpretation of Results in Experimental and Analytical Study

In the experimental study, the lightweight concrete, used for casting of beam is named as SLC19 (2012). The natural unit weight of the concrete is specified as 1485 kg/m^3 whereas it weighs 1270 kg/m^3 after the oven drying process. The material, SLC19 has gained compressive strength of 18.56 MPa, 29.08 MPa, 32.63 MPa and 33.25 MPa at the end of the 7, 28, 42 and 90 days successively. In the mix of concrete, expanded perlite, natural perlite, fly ash, micro silica and pumice are used with the amounts specified below in Table 4.1.

In the light of compression tests, compressive strength of normal weight concrete has reached a value of 33.15 MPa at the end of the 28 days. The mix ratios regarding normal weight concrete are specified below in Table 4.2.

Table 4.1 Mixture Proportions of Lightweight Concrete by Zandi (2012)

Ingredient	**Quantity**
Cement	500 kg/m^3
Expanded Perlite	70 kg/m^3
Fly Ash	450 kg/m^3
Water	380 kg/m^3
Sand	200 kg/m^3
Micro Silica	70 kg/m^3
Calcium Silica	35 kg/m^3
Pumice	200 kg/m^3
Plasticizer	6.5 kg/m^3

Table 4.2 Mixture Proportions of Normal Weight Concrete by Zandi (2012)

Ingredient	**Quantity**
Cement	350 kg/m^3
Expanded Perlite	210 kg/m^3
Aggregate	1740 kg/m^3

In the experimentation, loading is applied gradually whereas displacements are recorded with LPDT devices. The beam, made of lightweight concrete, has performed a nearly linear behavior up to a mid-span displacement of 15 mm under 121.05 kN. After this point, the beam has started to act in an inelastic manner. The beam has continued to carry load up to 123.12 kN with a displacement of 31.45 mm at the ultimate stage (Figure 4.1). Moreover, the lightweight concrete beam performs a maximum strain of 0.012 at the end of the elastic stage and 0.02516 at ultimate stage.

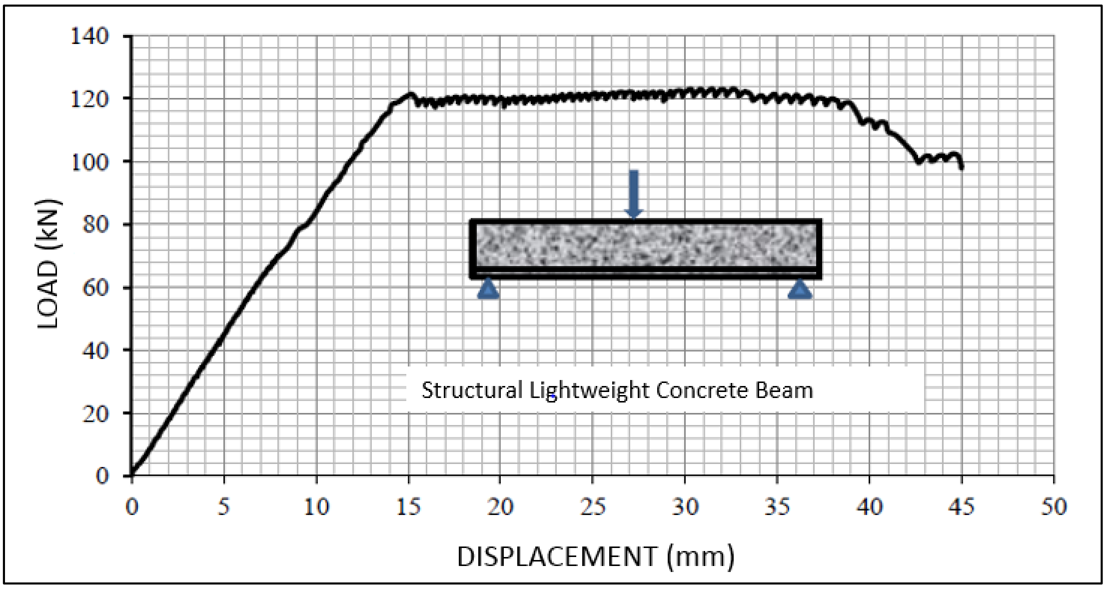

Figure 4.1 Load vs. Displacement Relation in Lightweight Concrete Beam by Zandi (2012)

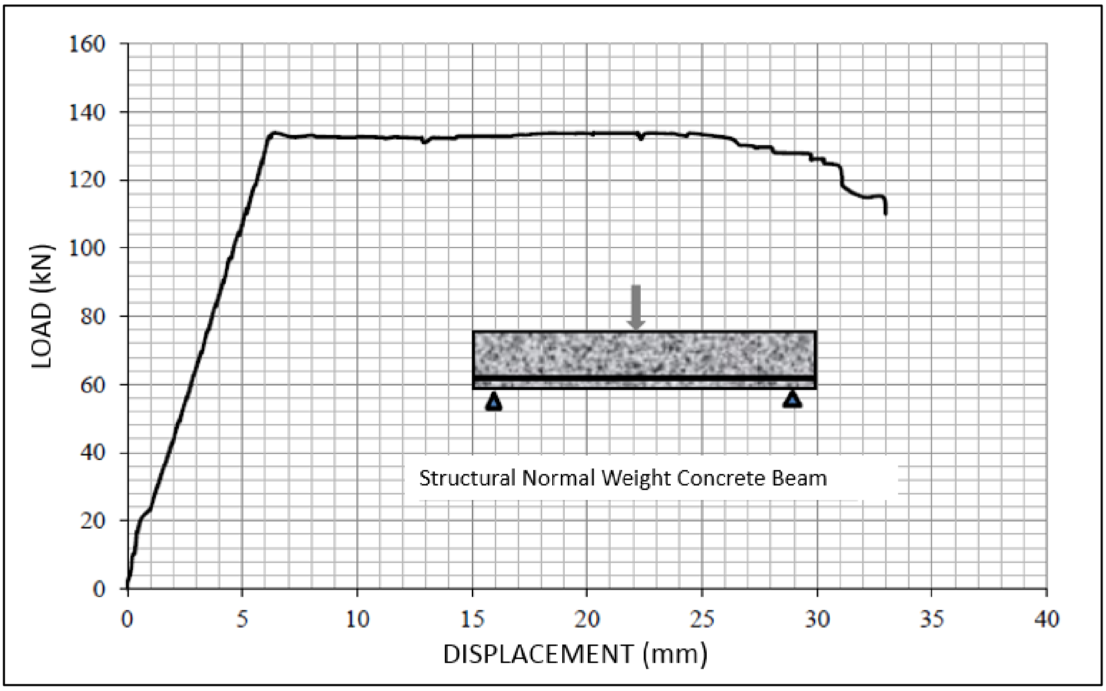

Figure 4.2 Load vs. Displacement Relation in Normal Weight Concrete Beam by Zandi (2012)

In the case of normal weight beam, the displacement has stayed in a more fair value when compared to the lightweight concrete beam. The beam made of normal weight concrete has deformed only 6.35 mm in the elastic range, under a load of 133.73 kN. In the inelastic range, the behavior does not differ that much, and it is deformed 22.17 mm under a load of 133.90 kN which leads to a more brittle behavior when compared to the lightweight concrete beam (Figure 4.2).

In the elastic range, the lightweight concrete has been deformed gradually with an energy absorption capacity of 1032 kN.mm when compared the energy absorption capacity of normal weight concrete, which is 429 kN.mm whereas the energy absorption capacity refers to the are beneath the load versus displacement curve. Although the energy absorption capacities perform in a similar manner in inelastic range, the beam made of lightweight concrete has been proven to have larger energy absorption capacity in the elastic range. In this respect, the lightweight concrete beam has an energy absorption capacity of 4592 kN.mm by overwhelming the capacity of normal weight concrete by 18%, whereas the energy absorption capacity of normal weight concrete is 2891 kN.mm.

The experimental study of Zandi (2012) has proved that the beam made of lightweight concrete has reached the ultimate capacity with a great energy absorption capacity. In the light of these experiments, the flexural behavior of normal weight and lightweight concrete beams are modelled in Perform-3D. According to the properties used in experimental study, the analytical study is started with defining the similar material properties in Perform-3D.

As seen in the Figure 4.3 and 4.4, the lightweight concrete model is defined as elastic-perfectly plastic, with no tension strength and strain capacities. On the other hand, the material is thought to lose strength after it reaches its ultimate strength. The post-peak responses of lightweight concrete are also calculated according to modified Kent and Park Model according to the experimental studies performed by the author of this thesis, and the overall behavior of lightweight concrete and normal weight concrete are compared with the experimental studies. Through the results obtained from the experimental studies concerning the confinement effect of lightweight concrete, several modifications have been performed. Regarding the parameters shown in Figure 4.3 and Figure 4.4, the value of FU, DL & DU, DR & DX are multiplied with 0.95, 1.25 and 2.4 respectively. The modulus of elasticity of lightweight is calculated according to formulation, $E_c = w_c^{1.5} 0.0043\sqrt{f_c'}$ stated in ACI 318-08

(2008). Since the lightweight concrete performs a more flexible behavior comparatively to the normal weight concrete, strain at ultimate load for unconfined concrete, ε_{c0} is taken as 0.003 whereas the number is used as 0.002 for normal weight concrete as stated in the study of Zandi (2012).

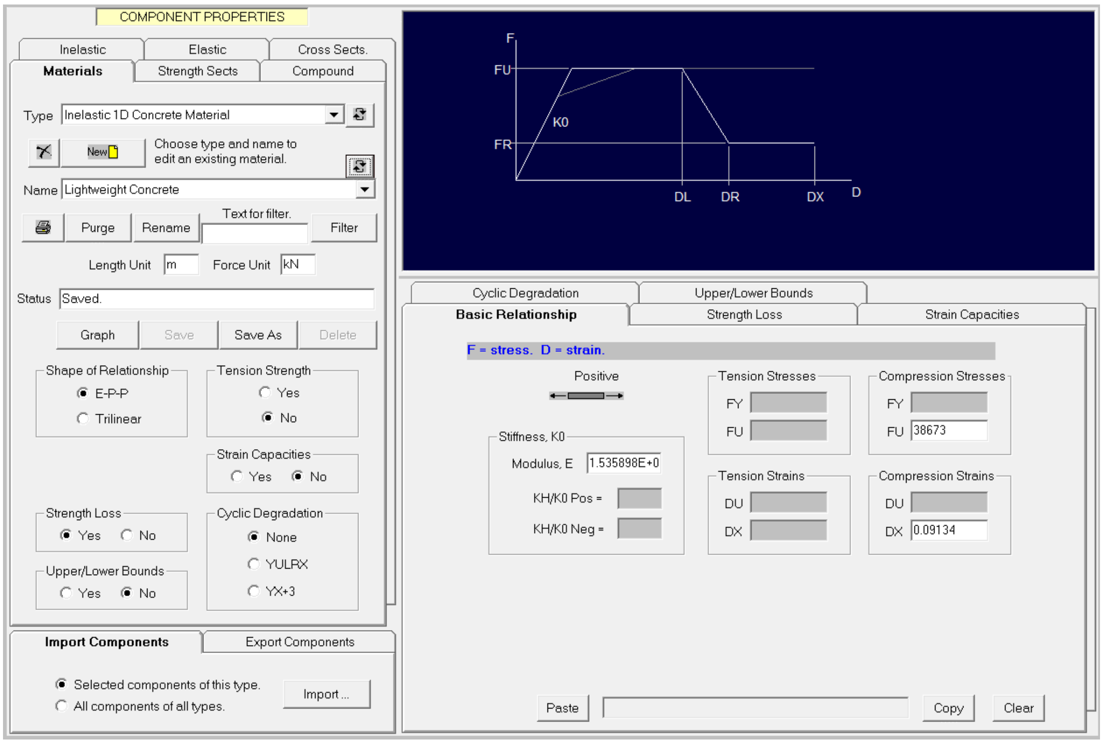

Figure 4.3 Material Properties of Lightweight Concrete Defined in Perform-3D, 1/2

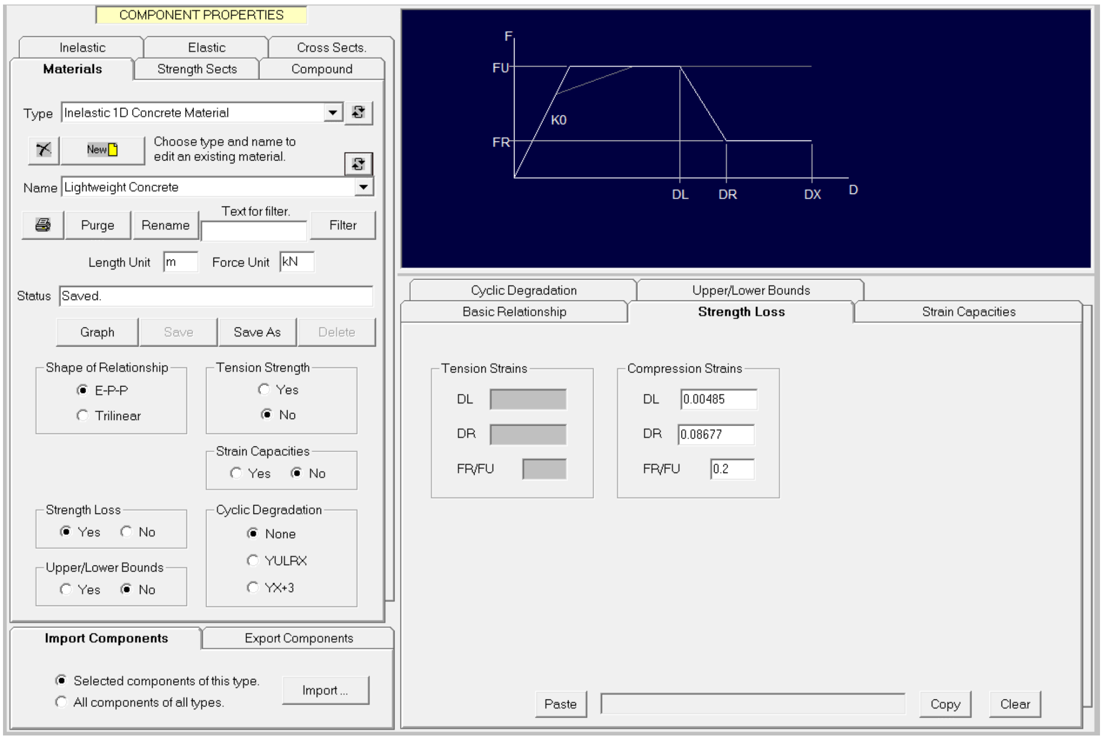

Figure 4.4 Material Properties of Lightweight Concrete Defined in Perform-3D, 2/2

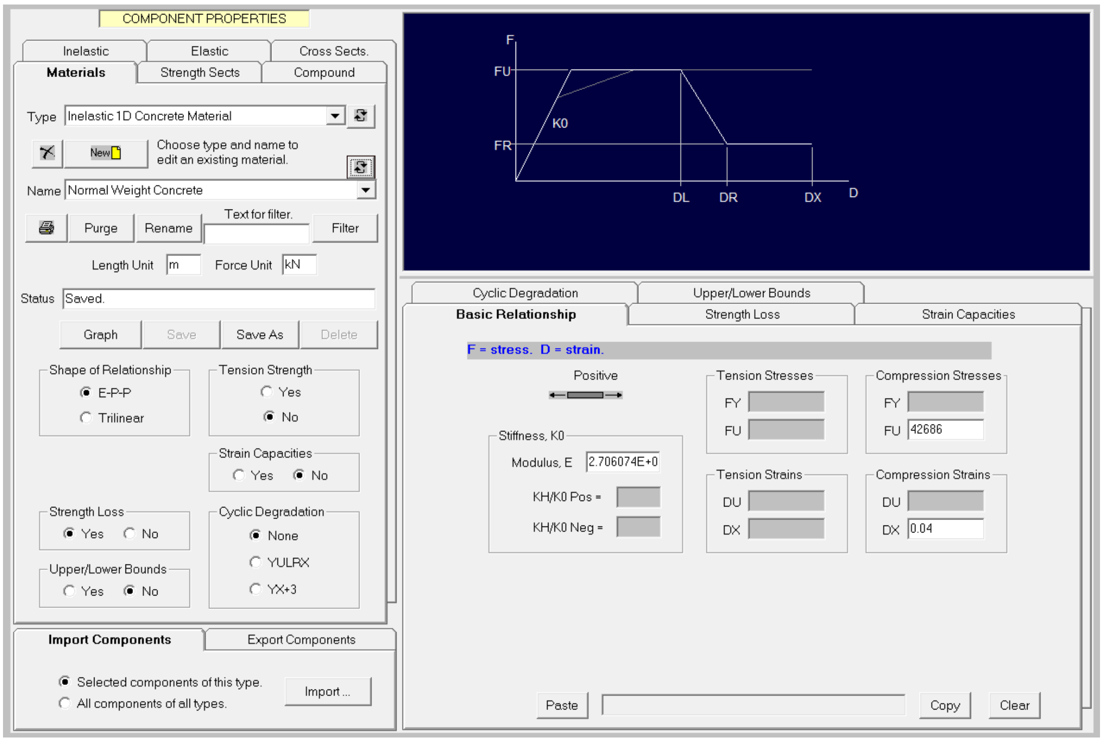

Figure 4.5 Material Properties of Normal Weight Concrete Defined in Perform-3D, 1/2

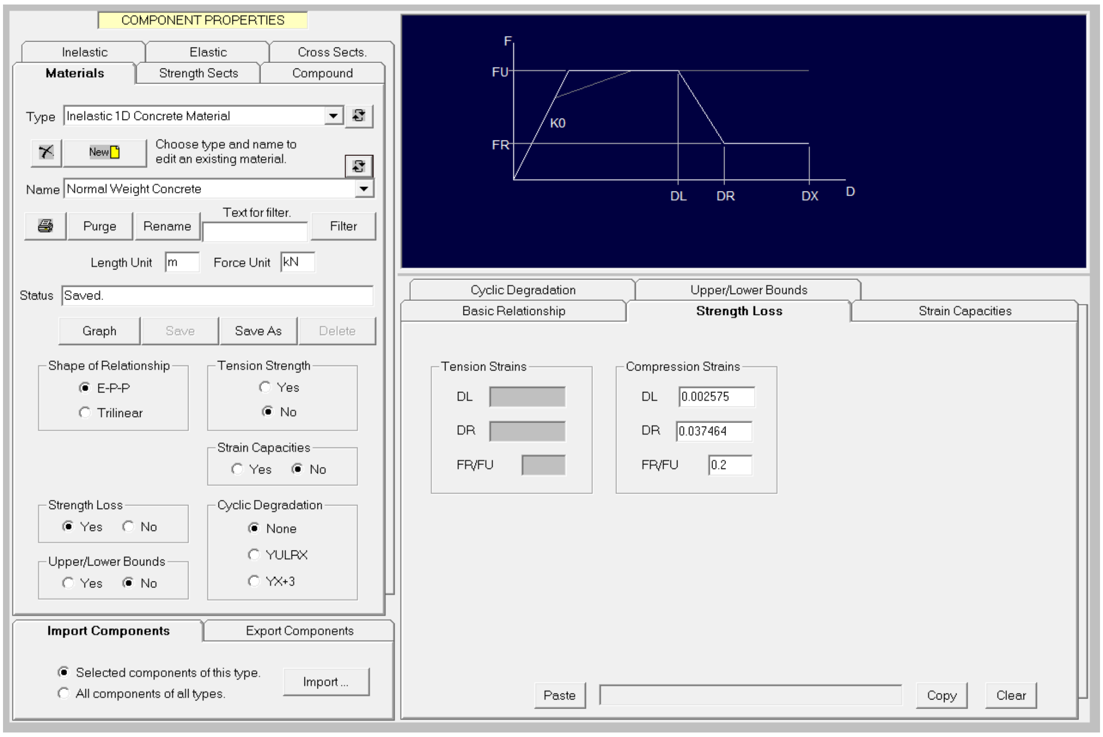

Figure 4.6 Material Properties of Normal Weight Concrete Defined in Perform-3D, 2/2

In a similar manner, the properties of normal weight concrete are defined according to Kent and Park Model (1971). In the case of normal weight concrete, the modulus of elasticity is calculated with a more widespread formulation, $E = 4700\sqrt{f_c'}$ stated in ACI 318-08 (2008). Additionally, ε_{c0} is also differed from lightweight concrete with a value of 0.002 as used in engineering practice. As seen in Figures 4.5 and 4.6, the normal weight concrete is also modelled with an elastic-perfectly plastic material model with no tension strength and strain capacities. On the other hand, strength loss is also calculated similar to lightweight concrete.

The reinforcing steel is also modelled according to the results of experimental studies (2012). In order to examine the mechanical properties, behavior of the reinforcing steel is observed with a universal tension test. The yield strength and ultimate strength of the reinforcing steel are observed as 495 MPa and 598 MPa successively with an ultimate strain of 0.24 for ϕ12 bar as seen in Figure 4.7.

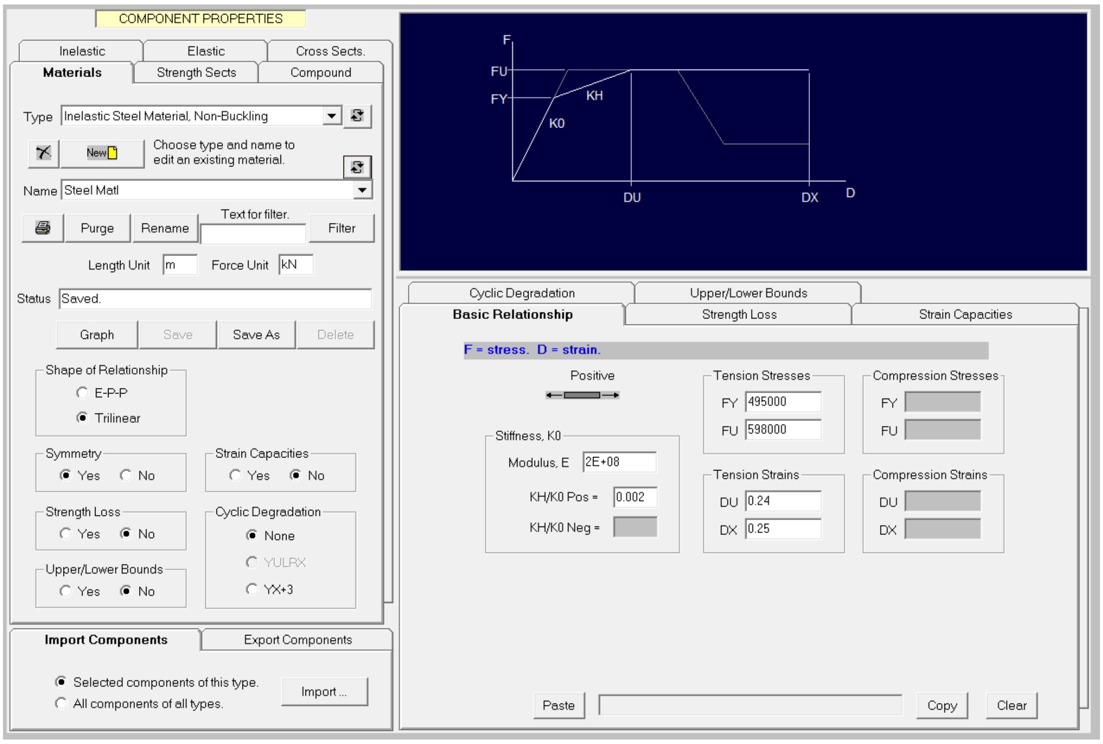

Figure 4.7 Material Properties of Reinforcing Steel Defined in Perform-3D

Furthermore, the elastic part of the elements is defined as reinforced concrete section. In the properties of the reinforced concrete section, the material is defined with the same modulus of elasticity (Figure 4.8). The inelastic parts of the beam are calculated to account for half of the beam dimension in the direction of loading. The remaining parts are thought to be elastic, reinforced concrete section. Combining these two cross sections, beam compounds are generated as seen in the Figure 4.9. The generated compounds are assigned as beam elements.

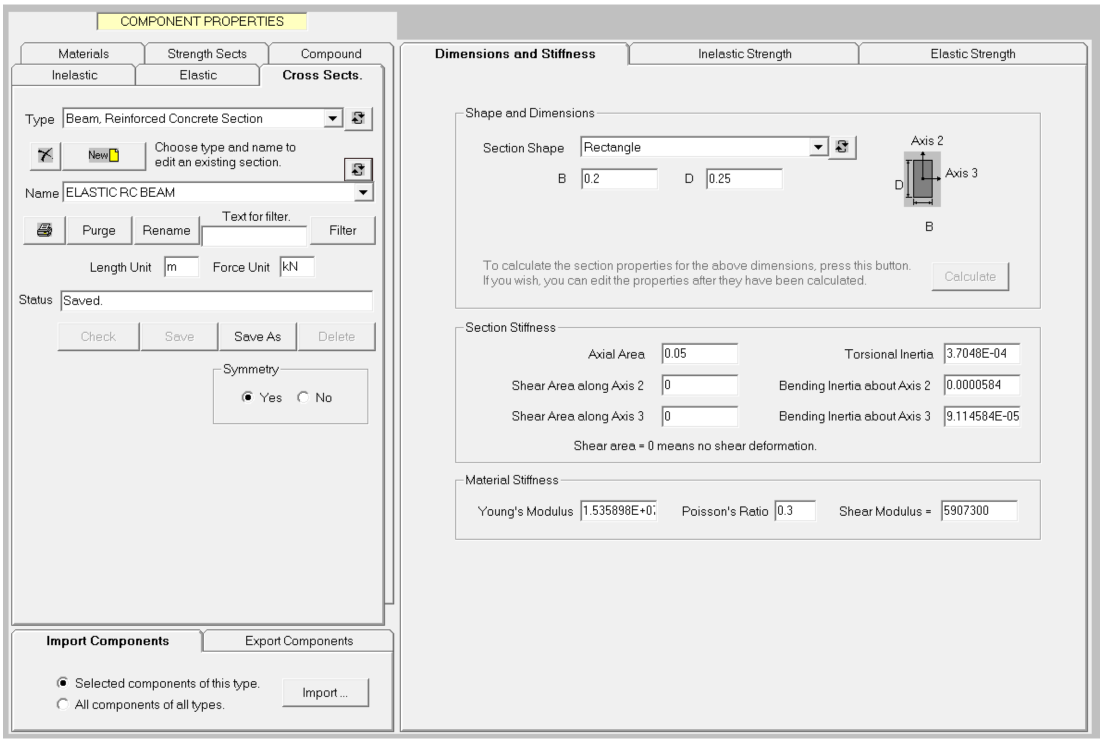

Figure 4.8 Elastic Lightweight Reinforced Concrete Section Defined in Perform-3D

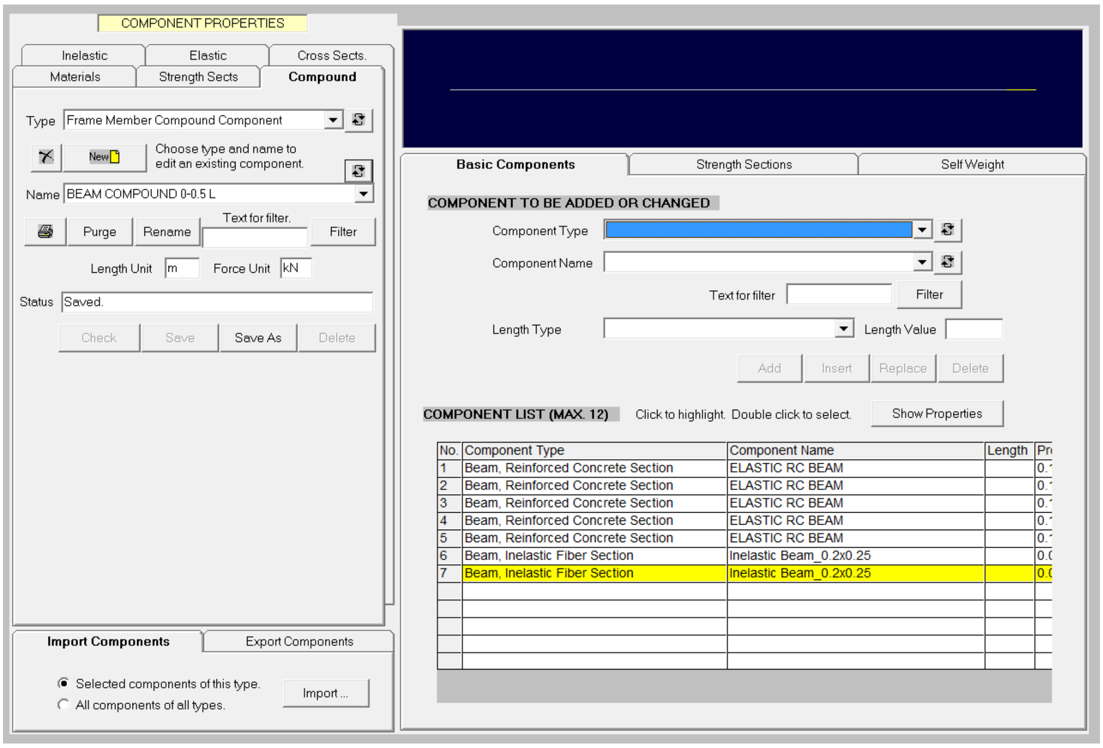

Figure 4.9 Compound Properties Defined in Perform-3D

Although the formation of plastic hinge zones generally occur at the support locations of moment resisting frames, the plastic hinge zones are accepted to occur at the mid-span of the simply supported beam.

The overall push-over behavior of the beam is controlled with the mid-span deflection. In order to make the beam to drift along the loading direction, the mid-span of the system is restrained to prevent the out of plane drift of the beam. Moreover, the non-linear geometric effects are not taken into consideration due to its minor effects. In the analysis case of the beam, the system is analyzed with static push-over loading with 200 number of load steps those perform 200 events maximum for each load step.

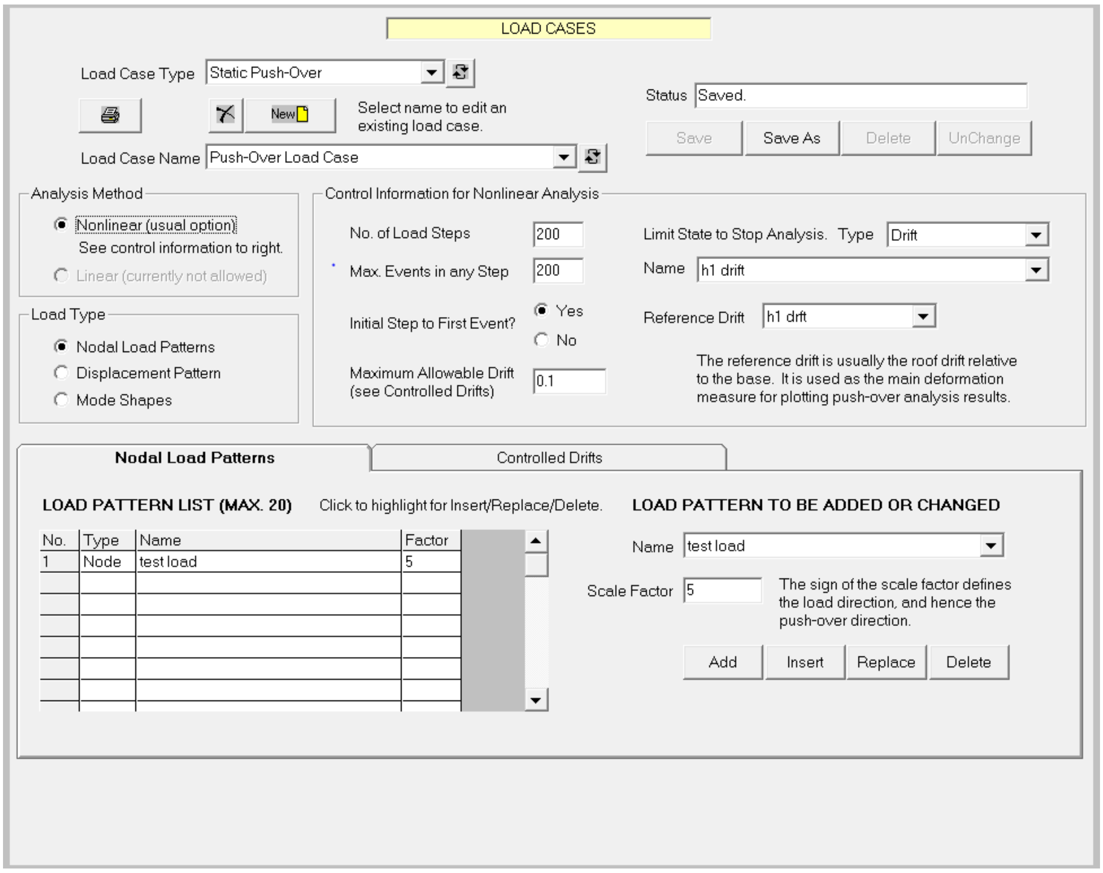

Figure 4.10 Push-Over Load Case Defined in Perform-3D

4.5. Evaluation of Results

According to material and modelling properties mentioned above, the flexural behavior is visualized in Perform-3D. The main goal of this part of study is the verification of material and modelling capabilities of the program. In the case of comparison of flexural behaviors, the energy absorption capacities of the system are compared for the ultimate displacement of the experimental study. In the study of Zandi, the normal weight concrete beam has failed with a 22.17 mm displacement and 3891 kN.mm energy absorption capacity. Furthermore, the beam carries 133.9 kN at maximum load capacity (2012). In the analytical study performed in Perform-3D, the beam, made of normal weight of concrete carries 136.36 kN at the ultimate stage. Although the ultimate load capacities behave in a similar fashion, the energy absorption capacity visualized in the analytical study differs from the experimental study by about 30%. The energy absorption capacity of the flexural beam in the analytical case is recorded as 2740 kN.mm. The calculated error of the analytical study is thought to be tolerable due to expected errors faced during the experimental study as well as the numerical modelling of nonlinear behavior of the real situation. Moreover, the flexural experiment has been concluded with only a single experiment contrary to the accepted opinion which claims that the experimentation shall be performed at least two to three times in order to reduce the experimentation errors.

In the case of lightweight concrete beam, the experimentation performed by Zandi has been concluded with a 31.45 mm displacement at the ultimate stage with an energy absorption capacity of 4592 kN.mm. Also, the beam carries 123.12 kN at the maximum load capacity. In the analytical case, the flexural beam is concluded with an energy absorption capacity of 3948 kN.mm. The calculated error, 14% is more tolerable when compared with the case of normal weight concrete. The load versus displacement diagrams of analytical studies, for both normal weight and lightweight concrete beams are presented in Figure 4.11.

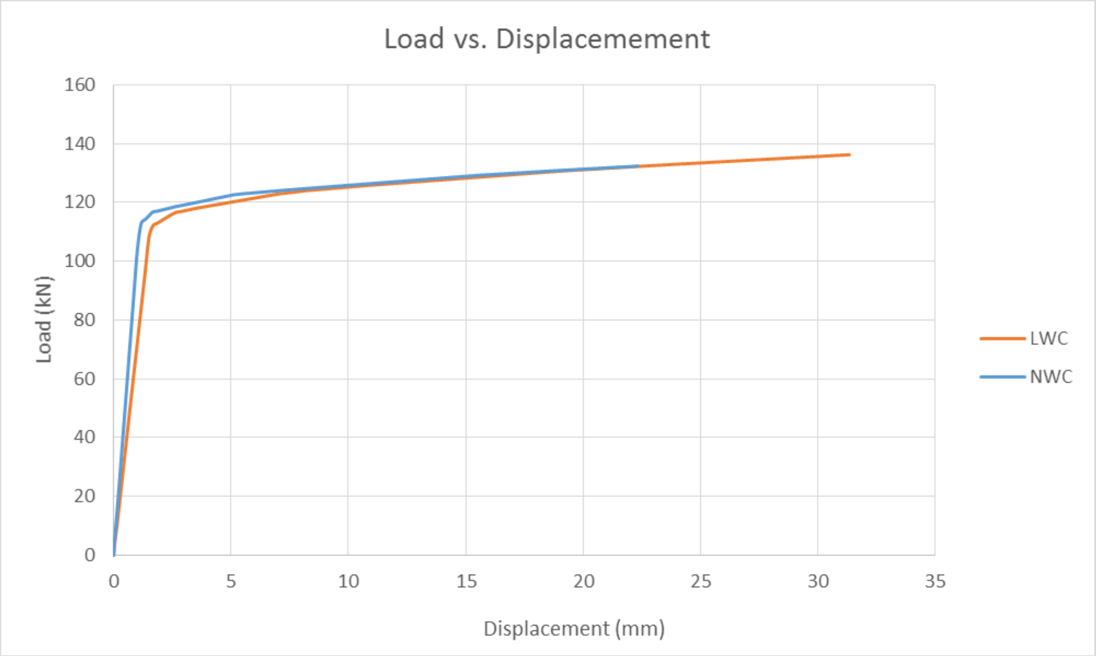

Figure 4.11 Load versus Displacement Diagram of Analyses of NWC and LWC Beams

According to the comparison discussed above, the analytical study of flexural behavior is thought to provide reasonable accuracy with respect to the experimental data. In this point of view, the 5 story moment resisting framed buildings, made of normal weight and lightweight concrete are compared and evaluated in the next chapter.

CHAPTER 5

EVALUATION OF NONLINEAR BEHAVIOR OF RC MOMENT RESISTING FRAMED BUILDINGS MADE OF NWC & LWC

5.1. General

In the light of results obtained from the experimental and analytical studies, seismic demands of a 5 story building, having 3 m story height, made of normal weight concrete and lightweight concrete are evaluated and compared (Figure 5.1). In the selection phase of the structural system, a more common type residential building is considered in order to conclude up with a comprehensive solution to be implemented for general purposes.

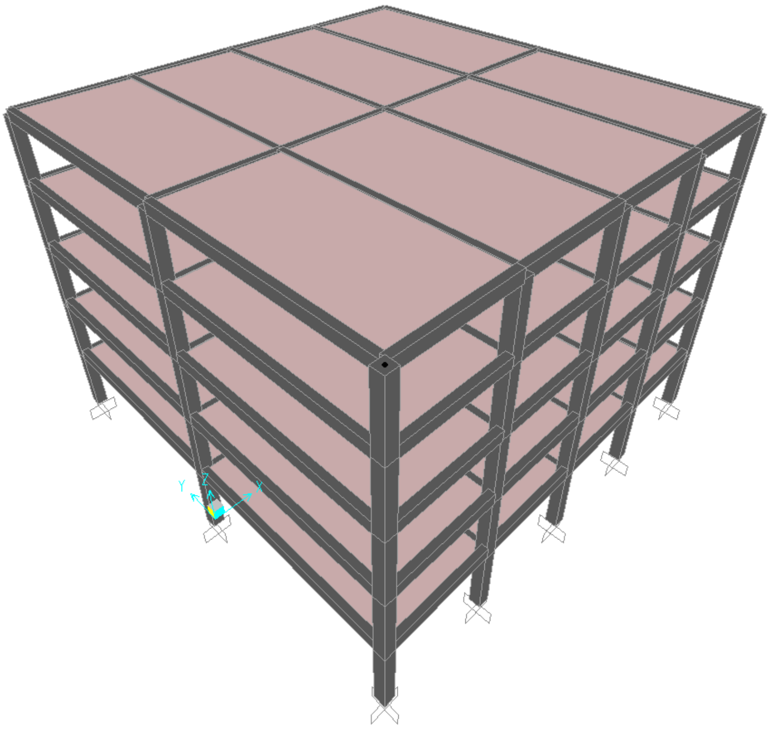

Figure 5.1 3D View of 5 Story Building Modelling

In order to visualize the behavior of structures under service and earthquake loads, several structural analysis approaches are being developed through the years. These approaches can be divided into two main groups and two sub-groups under them. Linear or elastic method of analysis is one of the analysis models. In this approach, the behavior of the structure is evaluated through the acceptation that the behavior of material will be kept in elastic range, or only the use of elastic capacity is permitted. Beyond the elastic capacity of material is disregarded. Since the post-peak response of the structure is not accounted, a response modification factor, R is used in order to reduce the forces instead of using inelastic capacities in most cods for the elastic capacity analysis. The linear method of analysis is divided into two groups; static linear analysis and dynamic linear analysis.

Non-linear or inelastic method of analysis is the second approach used for evaluation of the structures. In this approach, the behavior of material and/or structure is thought to be loaded up to its ultimate limit beyond its elastic limit. Non-linear method of analysis is thought to be closer to the real behavior of the structure since it allows capturing actual, post-peak behavior of structures. The non-linear procedures can be categorized in sub-groups, as well. Non-linear time history analysis is used in order to model the non-linear behavior of structure under dynamic loading. Although this method of analysis is proven to be successful for modelling the real time behavior of a structure, use of method of analysis is complicated by several limitations, such as ground motion characteristics, and very dependent on cyclic load-deformation properties; thus the use of this method is not practical as non-linear static or push-over methods.

The non-linear or inelastic static method of analysis, or also called as push-over analysis is known to be more practical when compared to time history analysis in engineering practice. In push-over analysis, the inelastic material model is created for concrete and reinforcement as also done in non-linear time history analysis. The lateral loads, distributed according to story masses, are applied after the dead and live loads are applied in push-over analysis. The most important output of the analysis is thought to be the force-displacement curve which provides estimation for the ductility and energy absorption capacity of the structure. In order to compare the seismic demands of the structures built with structural lightweight concrete and normal weight concrete, force-displacement curves are going to be produced in this chapter.

In the case of selected building type, higher mode effects are thought to be not significant due to low number of stories. As stated in FEMA 356 (2000), this acceptation is valid for short and regular buildings and static procedures are appropriate and sufficient for these types of buildings. In accordance with this statement, nonlinear static procedure is selected as analysis type in order to evaluate the seismic demands of the structures. In geometric modelling, 2D frame system is selected since the torsional irregularity does not have so much importance for the building type selected. According to the results obtained from the modal analysis performed in SAP2000, it is concluded that modal participating mass ratios are above the 90% for lower modes.

In geometric modelling, the dimensions are selected to visualize a ductile behavior and over dimensioning are avoided. The column dimensions are selected as 50x50 cm with reinforcement of 20ϕ18 longitudinal reinforcement, confined with a perimeter reinforcement of ϕ12 having a 15 cm spacing. The beam dimensions are selected as 30x50 cm with longitudinal reinforcement of 16ϕ18, confined with ϕ12 placed with a 15 cm spacing. The longitudinal reinforcements are selected to be ended up with a reinforcement ratio of $\rho = 2\%$ for both column and beam elements. The supports at the base level are fixed to ground whereas the movement of the structure is restricted in the out of plane direction. The 2D geometric model is thought to be 10 m wide in the 3rd dimension and dead and live loads are calculated according to this width.

The column and beam elements are modelled with composition of two different sections. Elements are composed of elastic and inelastic sections, where the fiber elements are used to account for spread of inelasticity through the depth of the section. In the calculation of inelastic section length, half of the section dimension in the way of loading is taken into account in order to model the plastic zone length. The column and beam elements accounted in fiber model are constructed with ten equal length segments with concrete material properties defined in the material section (Figure 5.2 & Figure 5.3). The reinforcement used in the elements is lumped at the top and bottom of the sections. In the elastic zone, reinforced concrete elements are modelled with elastic material properties. In the modelling phase of elastic sections, cracked moment of inertias is used as suggested in ACI 318-08 (2008). The cracked moment of inertia,

I_{cr} of column elements are taken as 0.70 I_g and cracked moment of inertia of beam elements are taken as 0.35 I_g (Figure 5.4 & Figure 5.5).

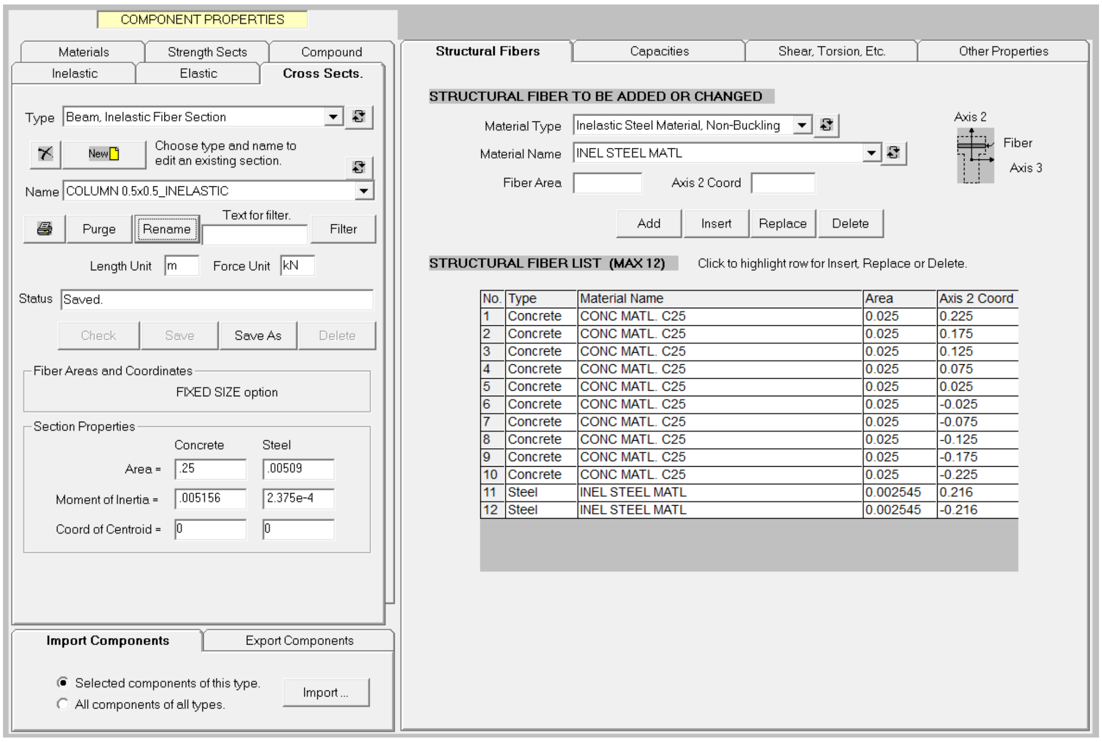

No.	Type	Material Name	Area	Axis 2 Coord
1	Concrete	CONC MATL. C25	0.025	0.225
2	Concrete	CONC MATL. C25	0.025	0.175
3	Concrete	CONC MATL. C25	0.025	0.125
4	Concrete	CONC MATL. C25	0.025	0.075
5	Concrete	CONC MATL. C25	0.025	0.025
6	Concrete	CONC MATL. C25	0.025	-0.025
7	Concrete	CONC MATL. C25	0.025	-0.075
8	Concrete	CONC MATL. C25	0.025	-0.125
9	Concrete	CONC MATL. C25	0.025	-0.175
10	Concrete	CONC MATL. C25	0.025	-0.225
11	Steel	INEL STEEL MATL	0.002545	0.216
12	Steel	INEL STEEL MATL	0.002545	-0.216

Figure 5.2 Inelastic Column Section Defined in Perform-3D

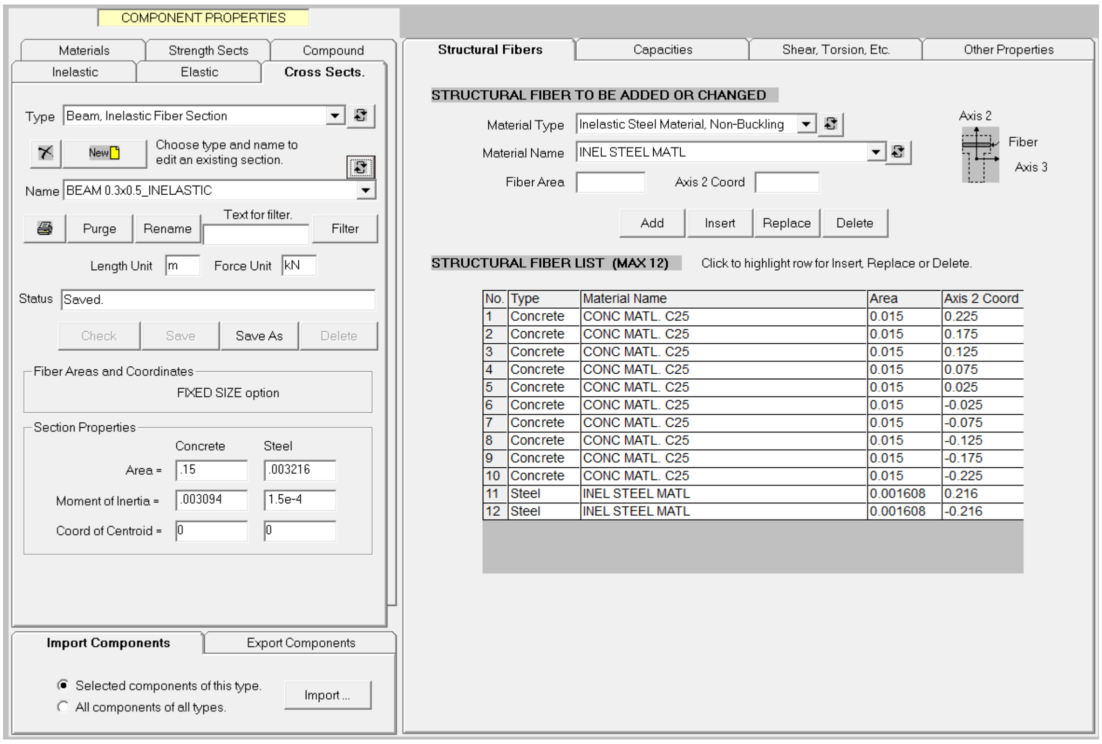

No.	Type	Material Name	Area	Axis 2 Coord
1	Concrete	CONC MATL. C25	0.015	0.225
2	Concrete	CONC MATL. C25	0.015	0.175
3	Concrete	CONC MATL. C25	0.015	0.125
4	Concrete	CONC MATL. C25	0.015	0.075
5	Concrete	CONC MATL. C25	0.015	0.025
6	Concrete	CONC MATL. C25	0.015	-0.025
7	Concrete	CONC MATL. C25	0.015	-0.075
8	Concrete	CONC MATL. C25	0.015	-0.125
9	Concrete	CONC MATL. C25	0.015	-0.175
10	Concrete	CONC MATL. C25	0.015	-0.225
11	Steel	INEL STEEL MATL	0.001608	0.216
12	Steel	INEL STEEL MATL	0.001608	-0.216

Figure 5.3 Inelastic Beam Section Defined in Perform-3D

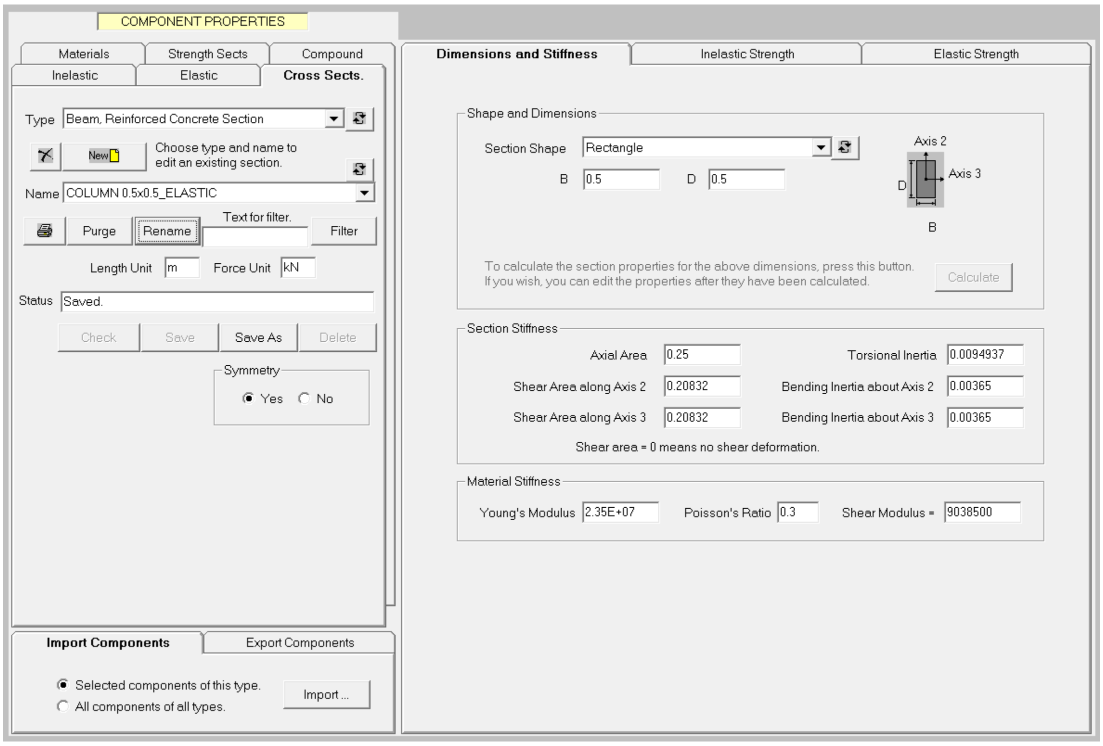

Figure 5.4 Elastic Column Section Defined in Perform-3D

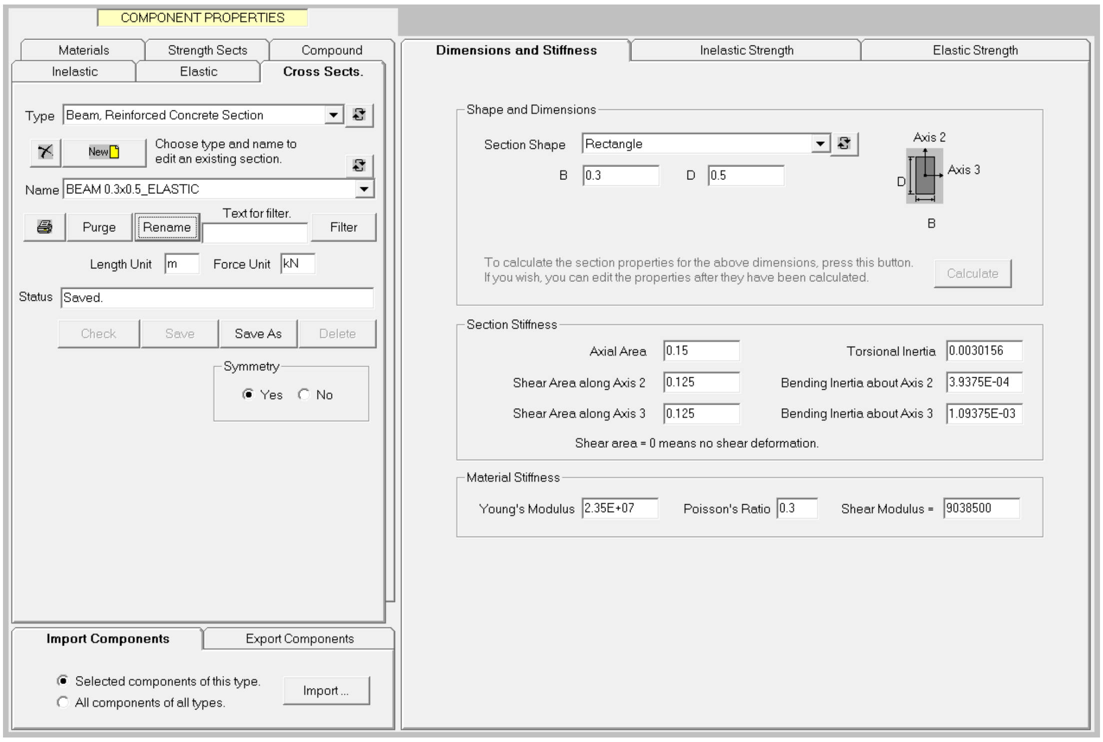

Figure 5.5 Elastic Beam Section Defined in Perform-3D

5.2. Properties of Normal Weight Concrete and Lightweight Concrete

In the decision of material selection, as intended in building type selection, an ordinary range of materials are tried to be decided. In case of normal weight concrete, 25 MPa concrete is selected whereas its inelastic properties are calculated according to Kent and Park Model (1971). The properties of the selected material and its elastic and inelastic properties are presented in Figure 5.8 and Figure 5.9.

On the other hand, as mentioned earlier, the literature is lacking reliable information for lightweight concrete to demonstrate its inelastic properties, namely a confined concrete model for lightweight concrete. In this respect, the experimental study undertaken as part of the research study in this thesis is considered for the description of inelastic behavior of lightweight concrete. In line with the model proposed by Kent and Park (1971), three important parameters are selected for lightweight concrete as presented in Table 5.1.

Table 5.1 Suggested Coefficients for Confined Lightweight Concrete

Parameter	Definition	Suggested Coefficient for LWC
f_{cc}	Confined Concrete Strength	0.92
ε_{coc}	Maximum Strain for Confined Concrete at Ultimate Strength	1.25
ε_{c20}	Confined Concrete Strain at 0.2 f_{cc}	2.40

Having modified the confined concrete properties of lightweight concrete, the material properties defined in the analytical studies are presented in Figure 5.6 and Figure 5.7 for lightweight concrete. Moreover, the properties of normal weight concrete, calculated according to Kent and Park Model (1971) are presented in Figure 5.8 and Figure 5.9.

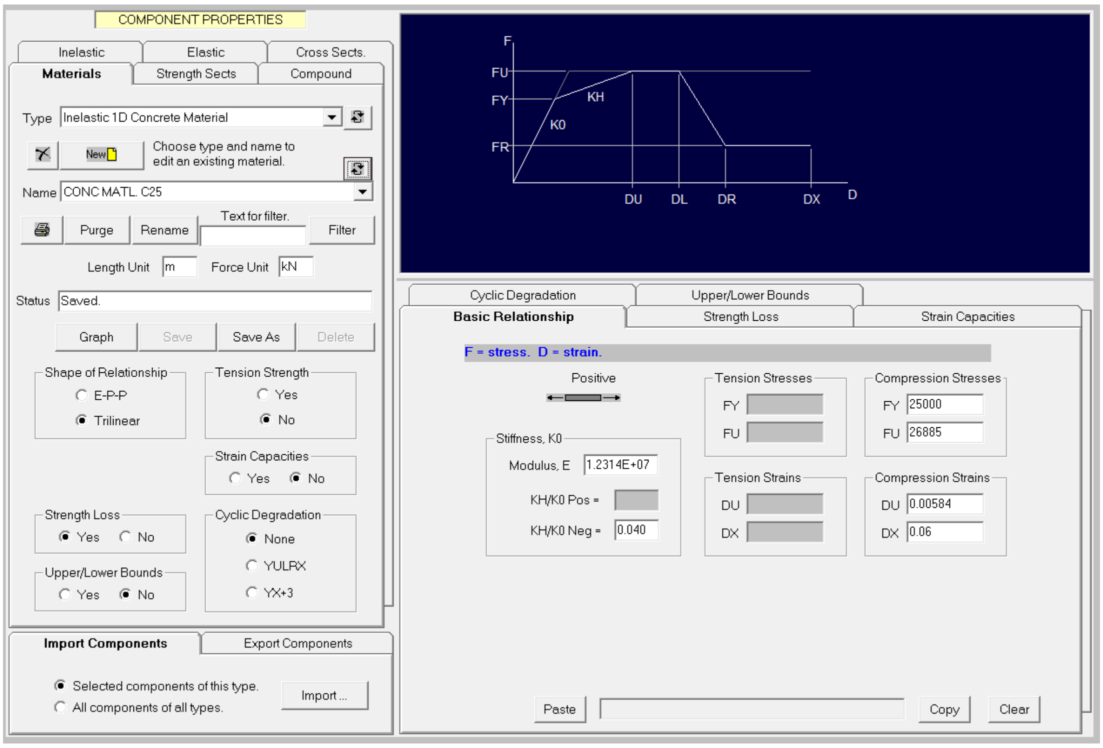

Figure 5.6 Material Properties of Lightweight Concrete Defined in Perform-3D, Basic Relationship

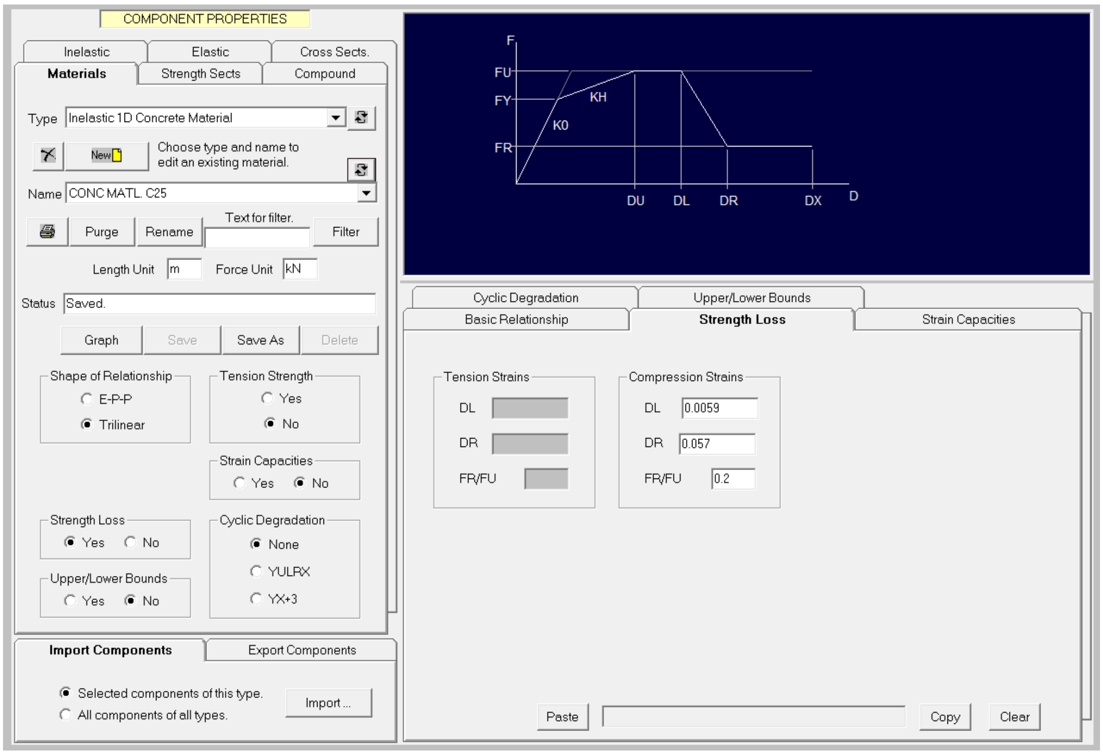

Figure 5.7 Material Properties of Lightweight Concrete Defined in Perform-3D, Strength Loss

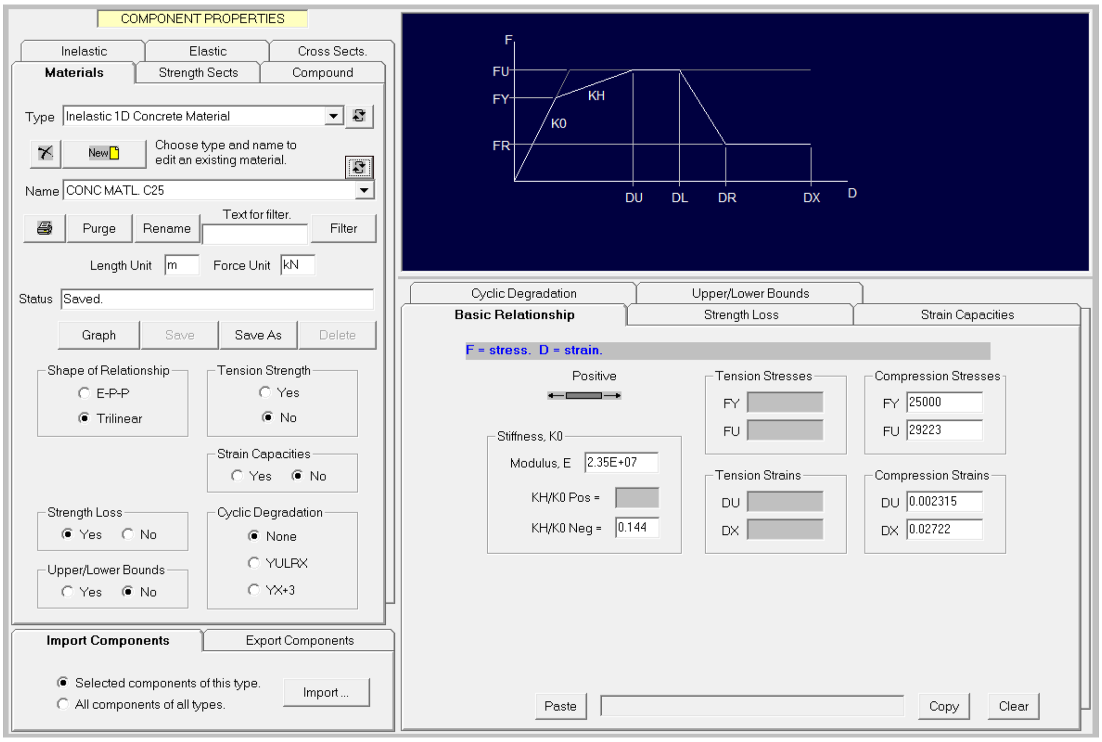

Figure 5.8 Material Properties of Normal Weight Concrete Defined in Perform-3D, Basic Relationship

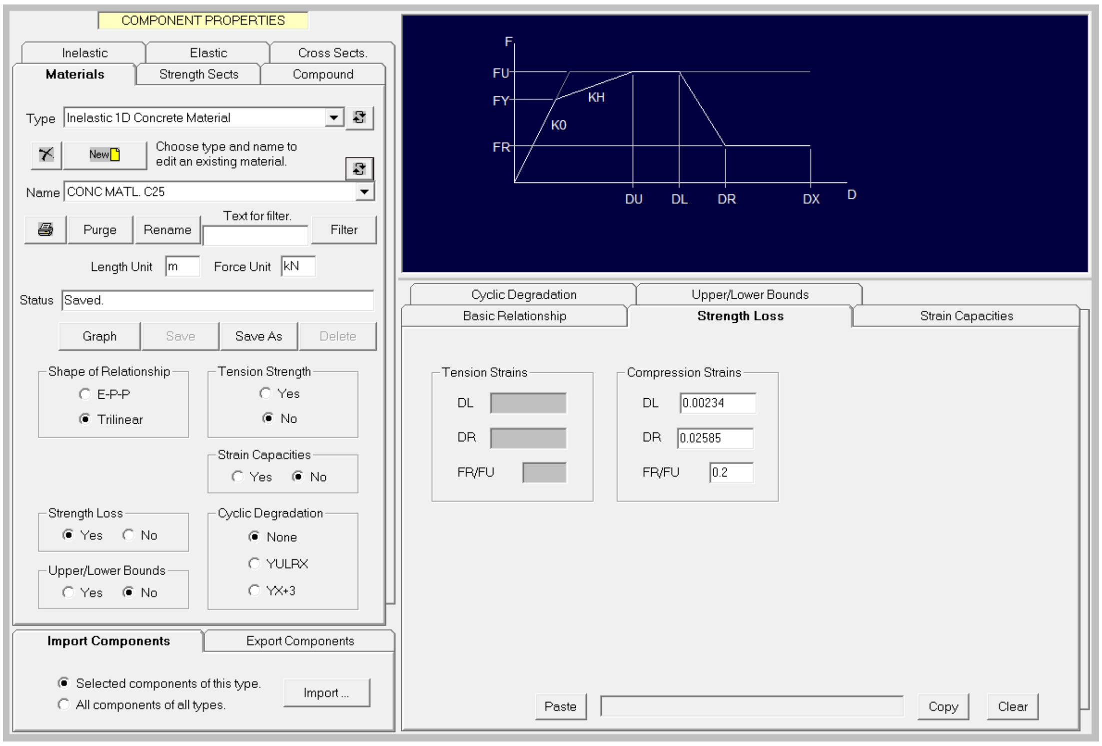

Figure 5.9 Material Properties of Normal Weight Concrete Defined in Perform-3D, Strength Loss

5.3. Loading Conditions

U.S. technical specifications are taken into account for the determination of the loads. The conditions and loading systems stated in ASCE 7-05 (2005), FEMA 356 (2000), ACI 318-08 (2008) are used for this purpose. In order to carry out nonlinear static analysis, the system is loaded with dead loads and live loads, and then seismic lateral loads are applied on the structure. According to ASCE 7-05 (2005), live loads are taken as 1.92 kN/m^2 and live load is calculated for 10 m wide tributary area lumped at the beams. In this respect, 19.2 kN/m^2/m is loaded on to the beams. In order to account for dead load, 25 kN/m^3 is taken for normal weight concrete and 20 kN/m^3 is taken for lightweight concrete. As applied for the live load case, the dead load is also calculated for 10 m wide tributary area. The slab depth is taken as 20 cm and its contribution is transferred on to the beams. The contribution of dead load and live load are accounted in a combination as advised in FEMA P695 (2009) as 1.05D+0.25L.

On the other hand, lateral seismic loading is applied according to the specifications stated in FEMA 356 (2000). In order to account for lateral loading, two modal load pattern are selected. Initially, a modal distribution, namely triangular distribution is applied as seen in the equation below:

$$C_{vx} = \frac{w_x h_x^k}{\sum_{i=1}^{n} w_i h_i^k}$$

C_{vx} = Vertical Distribution Factor

k = 2.0 for T≥2.5 seconds

= 1.0 for T≤0.5 seconds

w_i = Portion of the total weight of building assigned on floor i

w_x = Portion of the total weight of building assigned on floor x

h_i = Height from base level to floor i

h_x = Height from base level to floor x

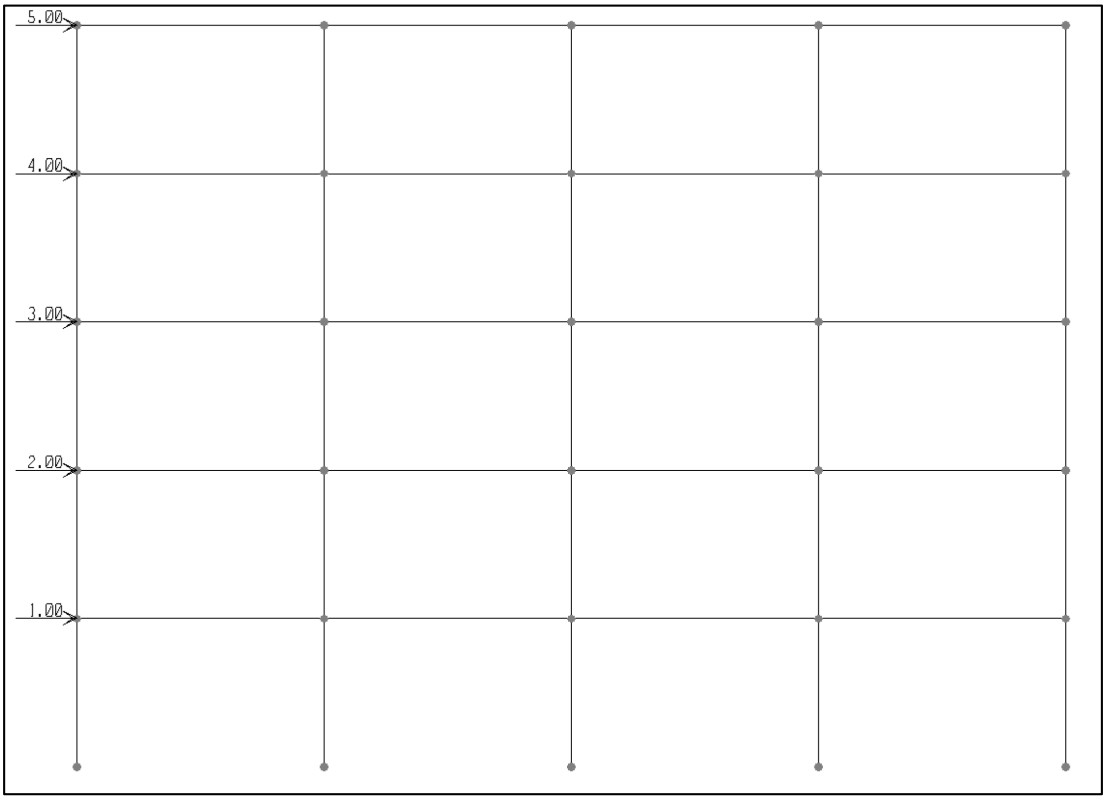

Figure 5.10 Triangular Load Distribution

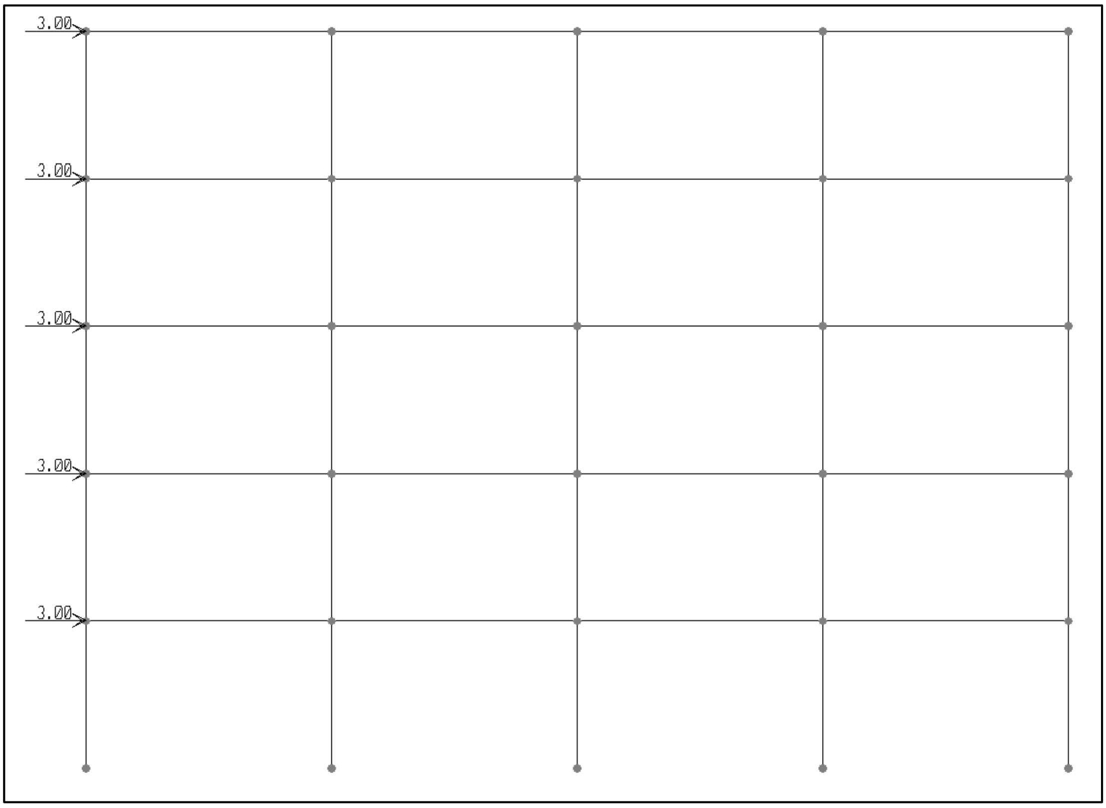

Figure 5.11 Uniform Load Distribution

In addition to triangular load distribution, a uniform load pattern is also applied on to the structure. The more critical outcomes are taken into account for the evaluation of seismic demands of the structures. The lateral load to be applied in the analysis is calculated according to the formulation in FEMA 356 (2000) as stated below:

$$V = C_1 C_2 C_3 C_m S_a W$$

C_1 = Modification factor to relate the expected maximum inelastic displacements to displacements calculated for linear elastic response

C_2 = Modification factor for hysteresis shape, stiffness degradation, strength deterioration

C_3 = Modification factor for increased displacements due to P-Δ effects

C_m = Effective mass factor for higher mode mass participation factor

S_a = Response spectrum acceleration

W = Effective seismic weight of the building

As seen in the Figure 5.10 and Figure 5.11, the system is loaded with unit loads. In the running phase of the structure, reference lateral load patterns are increased through a load factor in the push-over analysis.

5.4. Analysis of 5 Story Moment Resisting Framed Buildings

In the analysis case, the structures are loaded with lateral loads after having loaded with gravity loads, which contain live load and dead load. The overall behavior of structure is controlled by the story drifts. In order to visualize the general behavior, the structures are being allowed to drift by an amount of 10%. In the evaluation of the seismic demands, the story drifts, advised in FEMA 356 (2000) are used. The story drift limit states are stated as 1% for Life Safety, 2% for Immediate Occupancy and 4% for Collapse Prevention in FEMA 356 (2000).

Although it is stated in FEMA 356 (2000) that control node for displacement shall be at the center of the mass of the roof floor, the remaining story drifts are also taken into account in the scope of this study. On the other hand, the energy absorption capacities of the structures are evaluated according to the area between top level displacements versus base shear curves.

In the case of normal weight concrete structure, the base shear for the uniform loading condition is calculated as 1589 kN whereas the triangular load distribution is concluded with a value of 1346 kN. In this respect, uniform loading case is proven to be critical for the normal weight concrete case. Although the uniform load distribution is used for comparison of normal weight and lightweight concrete, the results those belong to triangular load distribution are also discussed.

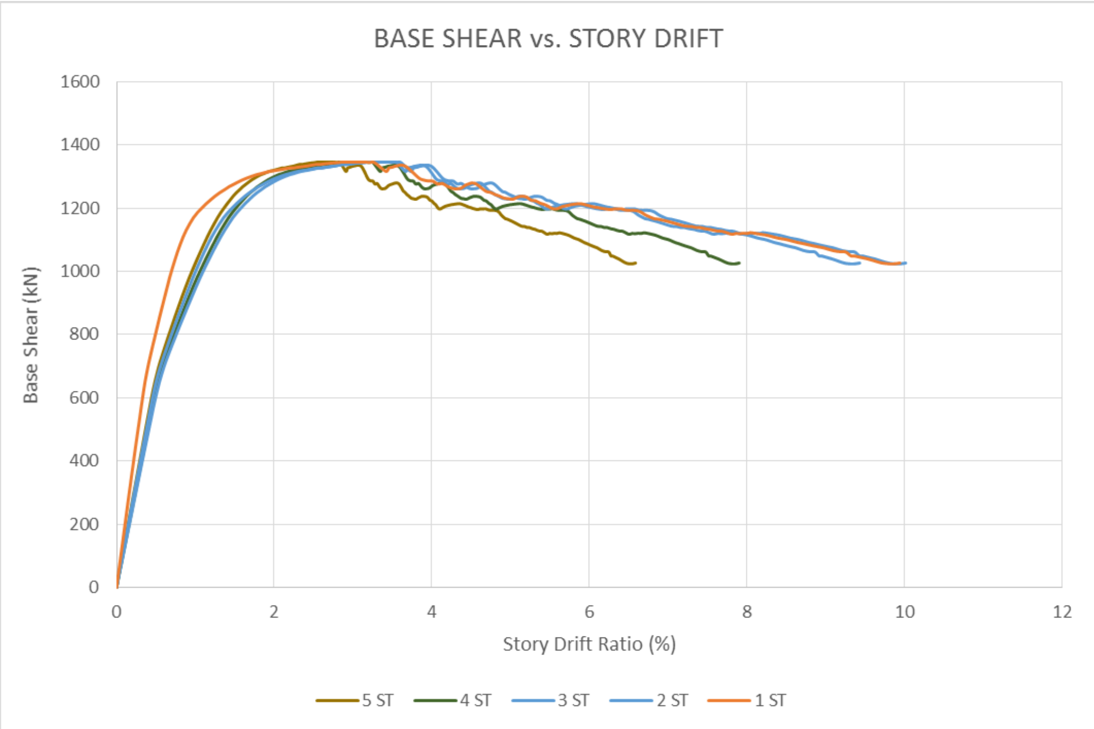

Figure 5.12 Base Shear vs. Story Drift Diagram of Triangular Load Distribution, NWC

As seen in Figure 5.12, 1st and 2nd stories appear to be the limit stories in terms of maximum story drift. Although the top story drift stays below 7% for 10% overall roof story drift, the first two stories are observed to drift in a greater manner. On the other hand, these trends are not valid for the allowable drift limit states.

In the case of Immediate Occupancy Limit, 3rd story has been seen to reach the limit drift state first. Furthermore, the Life Safety Limit State is also reached at this floor. On the other hand, Collapse Prevention Limit State is seen in the 2nd floor. As seen in Figures 5.13 and 5.14, general behavior of these two floors is very similar. Although the roof drift is thought to be important for the evaluation, 5th story has reached only 0.88%, 1.68% and 3.1% for the Immediate Occupancy, Life Safety and Collapse Prevention Limit States successively.

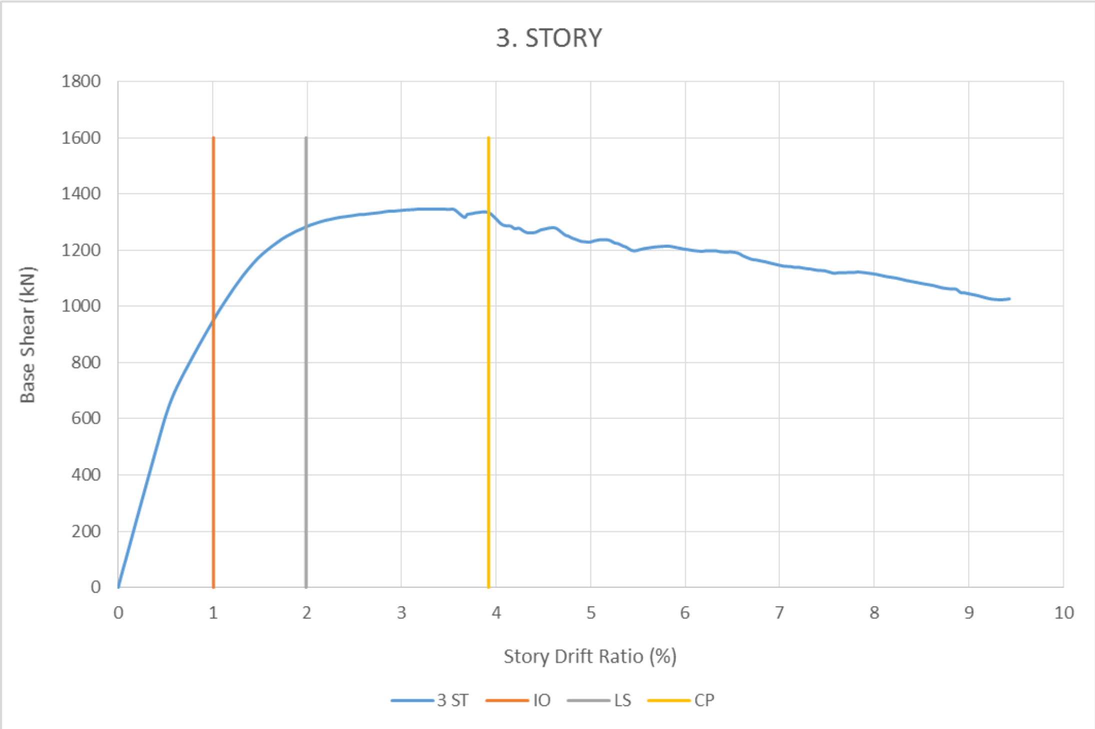

Figure 5.13 Base Shear vs. Story Drift Diagram of Triangular Load Distribution of 3rd Story, NWC

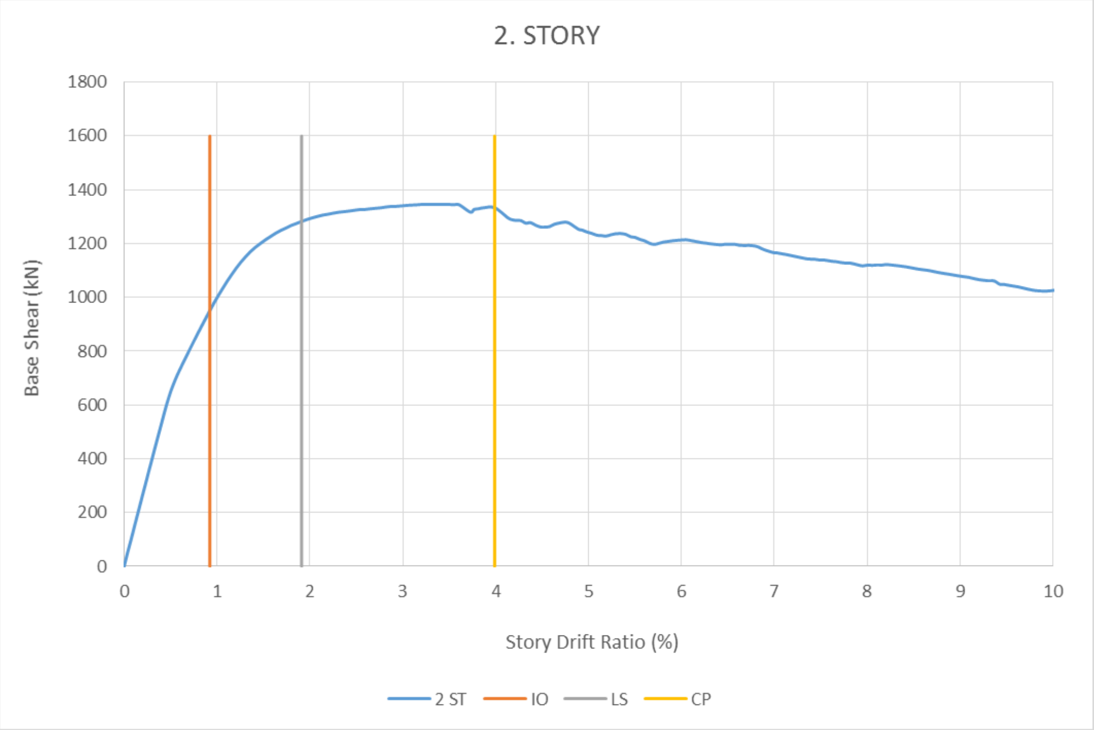

Figure 5.14 Base Shear vs. Story Drift Diagram of Triangular Load Distribution of 2nd Story, NWC

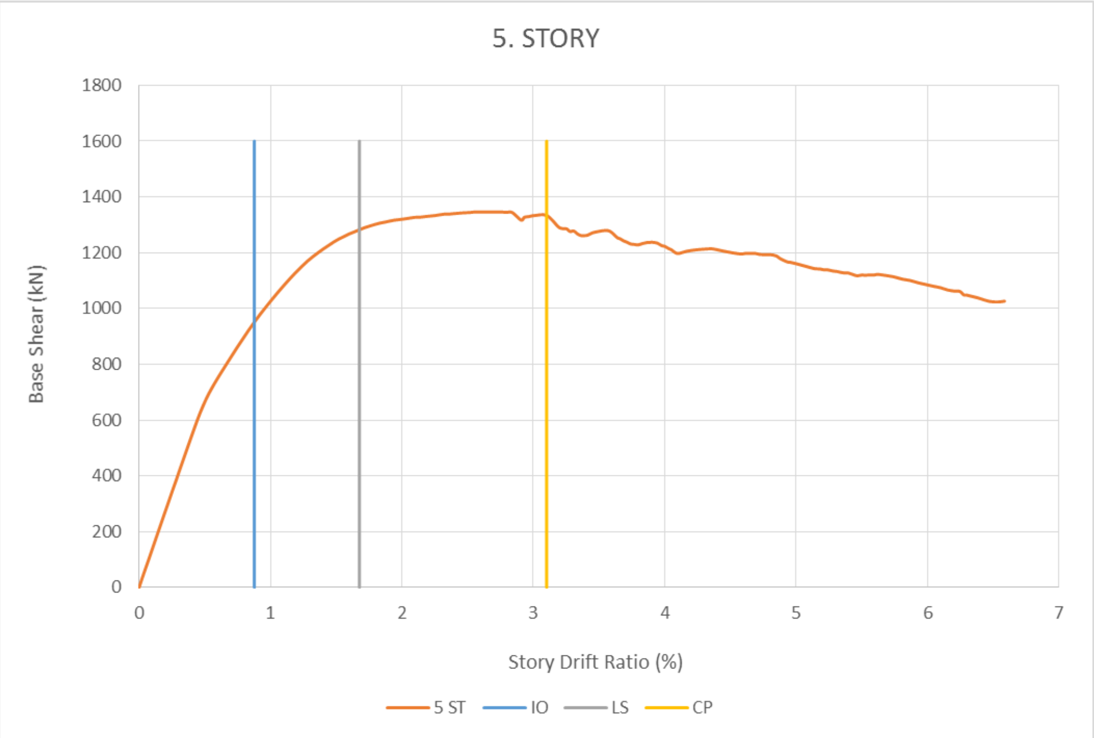

Figure 5.15 Base Shear vs. Story Drift Diagram of Triangular Load Distribution of 5th Story, NWC

In addition to general behavior of base shear vs. story drift ratios, first floor behaves in a more stable manner for the Immediate Occupancy and Life Safety Limit States. On the contrary to general idea of selecting roof node as control node, the 5th story has drifted even less than whole structure, especially for the Collapse Prevention Limit State. As seen in Figures 5.13, 5.14 and 5.15, the 5th story has performed a stable behavior.

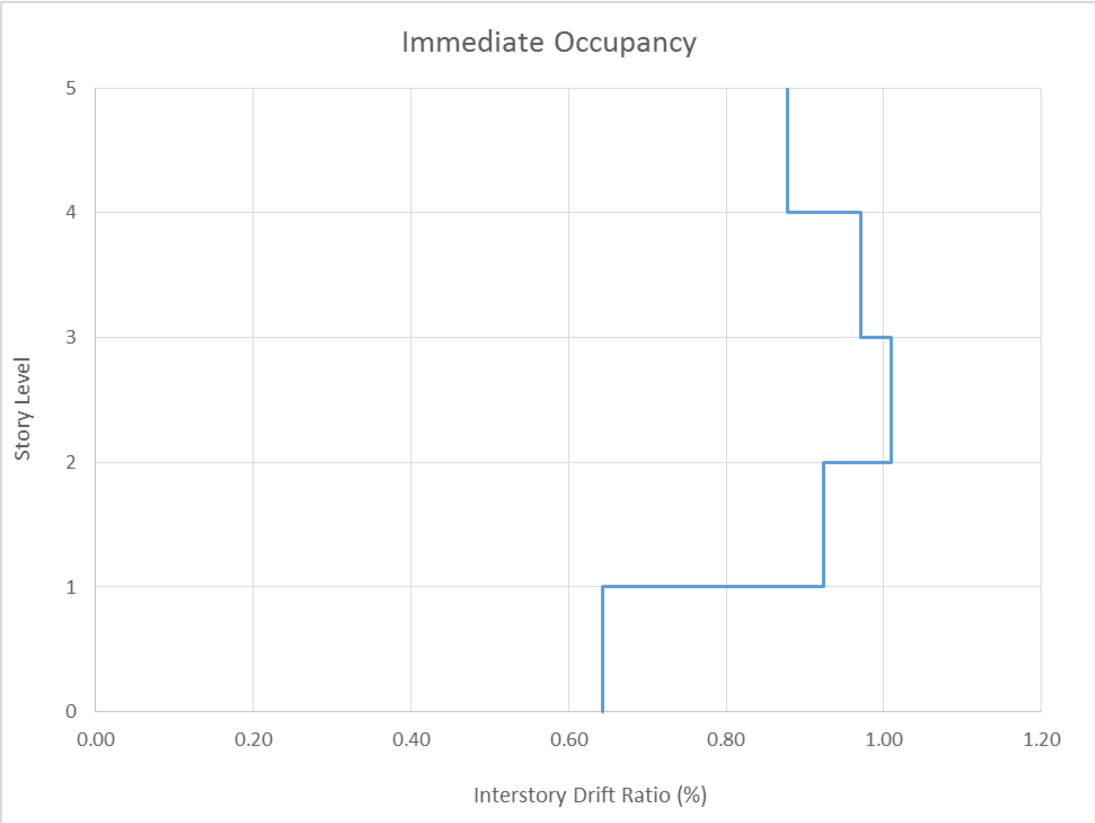

Figure 5.16 Story Level vs. Story Drift Diagram of Triangular Load Distribution, IO Limit State, NWC

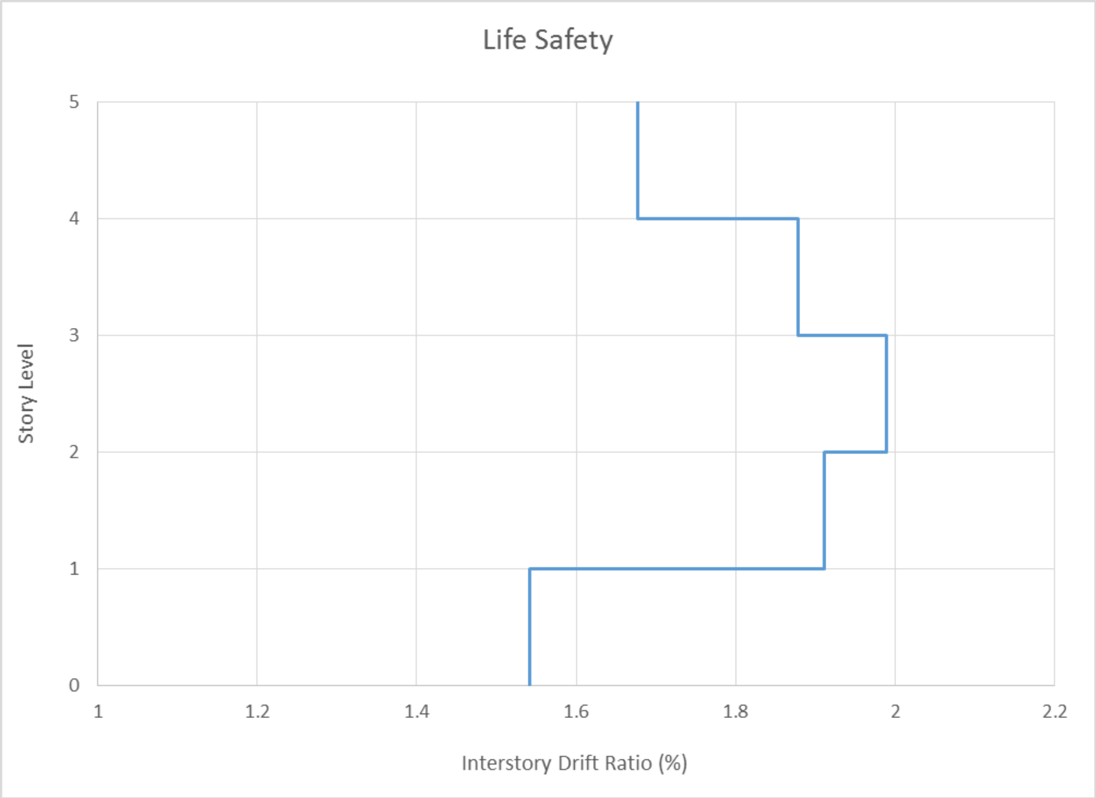

Figure 5.17 Story Level vs. Story Drift Diagram of Triangular Load Distribution, LS Limit State, NWC

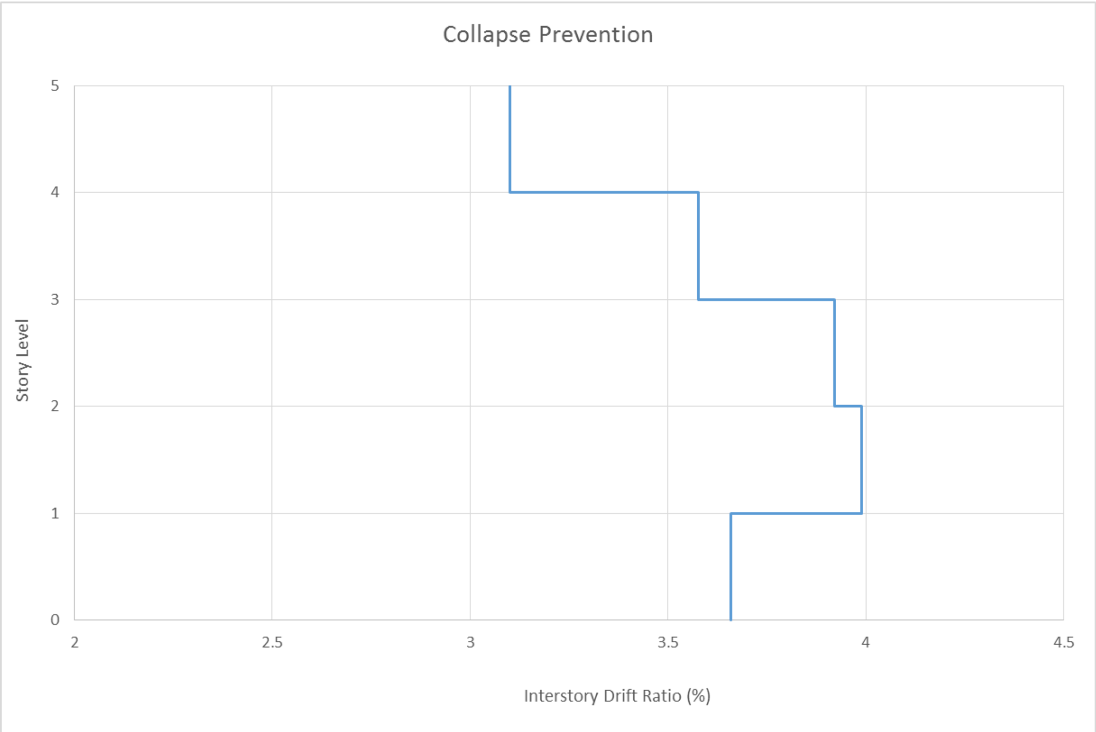

Figure 5.18 Story Level vs. Story Drift Diagram of Triangular Load Distribution, CP Limit State, NWC

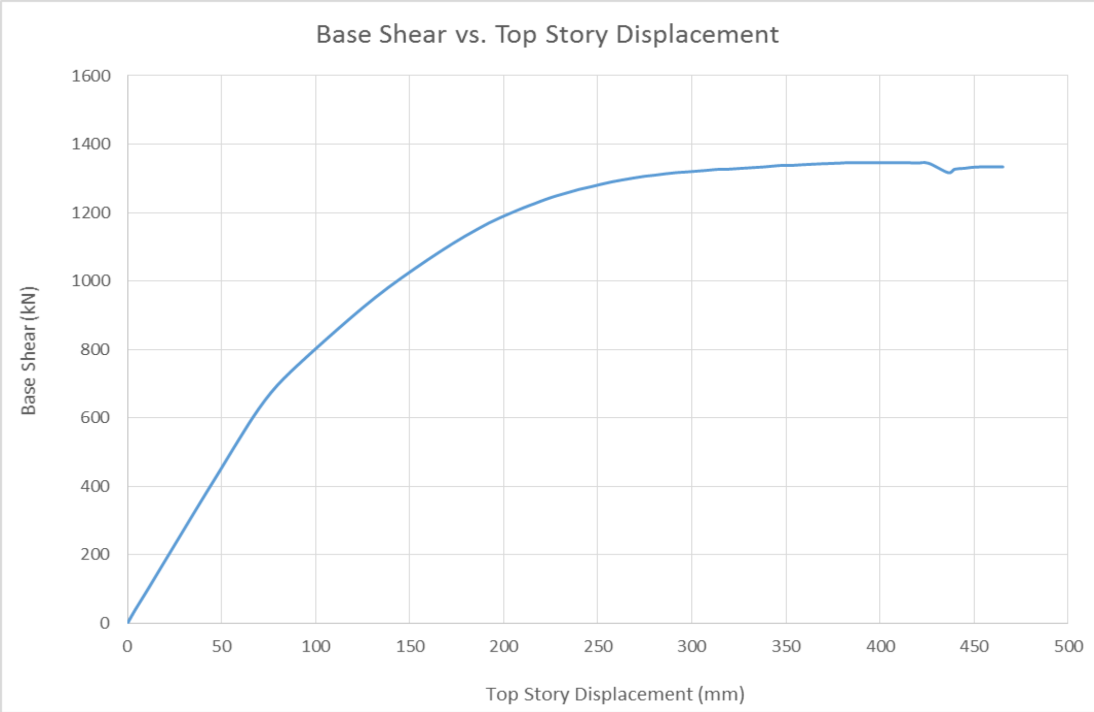

Figure 5.19 Base Shear vs. Top Story Displacement Curve of Triangular Load Distribution, NWC

According to the triangular load distribution, the structure is calculated to absorb 493,208 kN.mm amount of energy. The base shear related to this energy capacity is calculated as 1346 kN. In the calculation of energy absorption capacity, top story displacement of the structure has been taken into account whereas inter-story displacements are kept in the limits mentioned before. In Figure 5.19, overall behavior of the base shear versus top story displacement curve can be found.

In the uniform loading case results, 1^{st} and 2^{nd} story drifts are seen to be close to analysis limit of 10%. Similarly, Immediate Occupancy Limit, 1% is also reached by the 3^{rd} story and Life Safety Limit, 2% is reached by 2^{nd} story. Additionally, Collapse Prevention Limit, 4% is also reached by 2^{nd} story. Actually, the overall trends of two loading systems do not behave in a completely different manner. As seen in Figure 5.20, maximum drift ratios for a limit of 10% are also governed by 1^{st} and 2^{nd} stories. the On the other hand, inter-story drifts have been differed in some respects as presented in Figures 5.21, 5.22, 5.23.

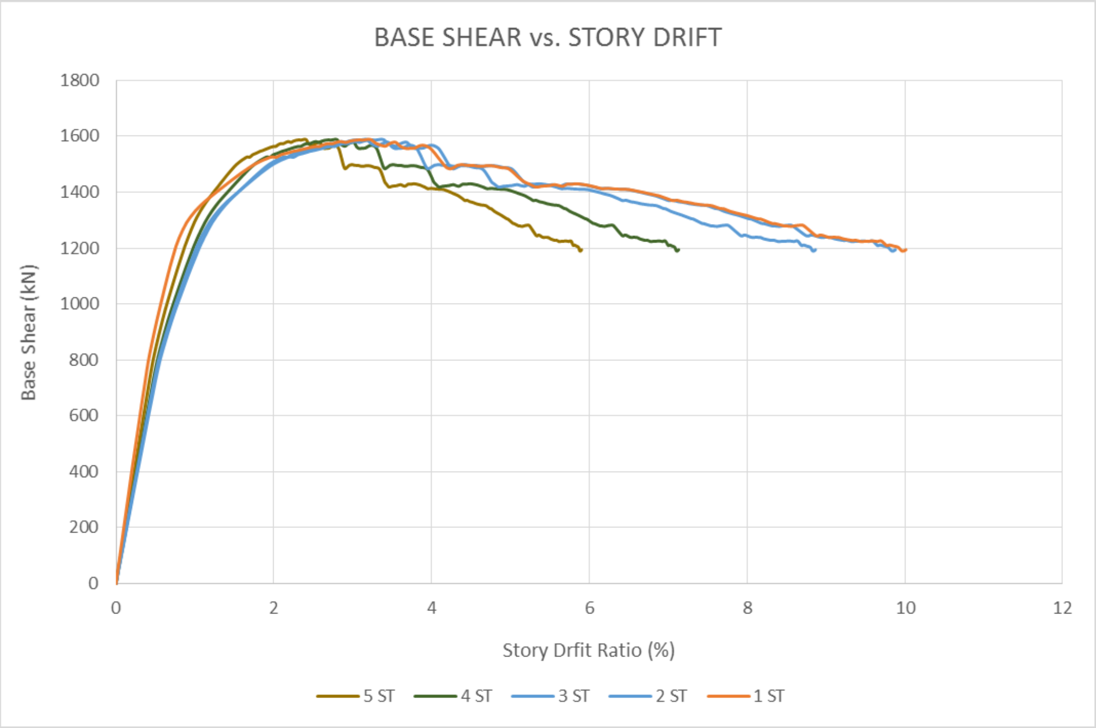

Figure 5.20 Base Shear vs. Story Drift Diagram of Uniform Load Distribution, NWC

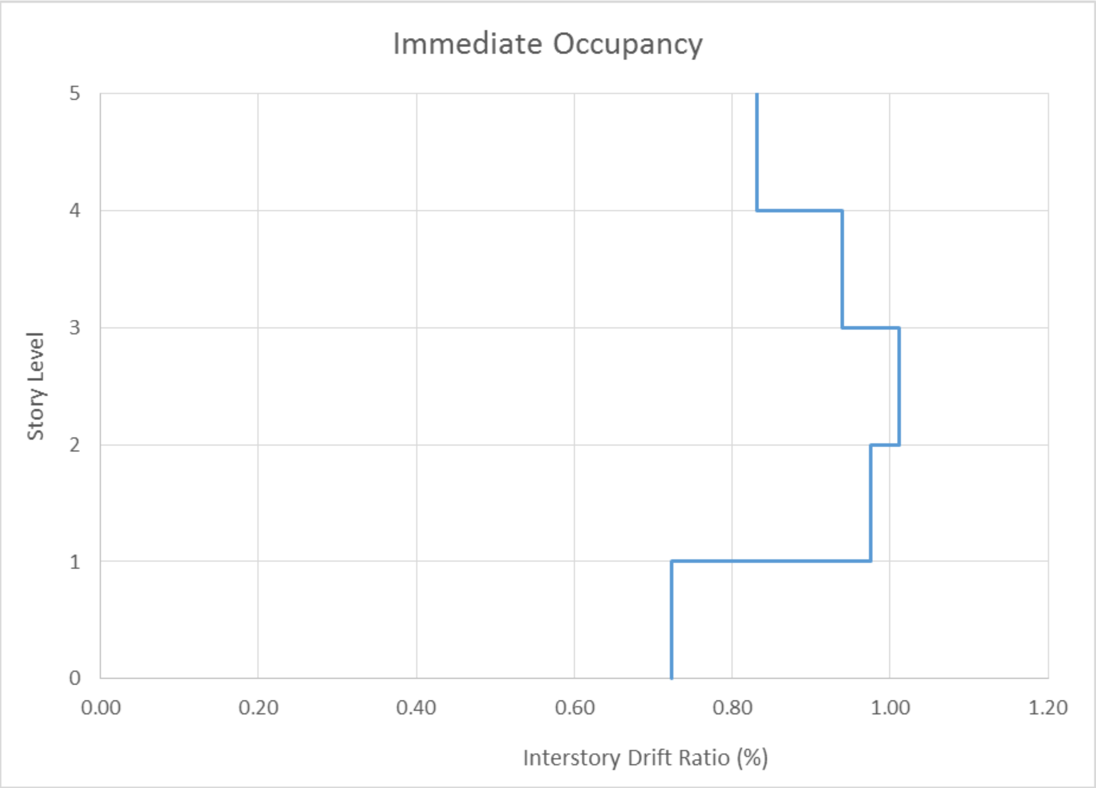

Figure 5.21 Story Level vs. Story Drift Diagram of Uniform Load Distribution, IO Limit State, NWC

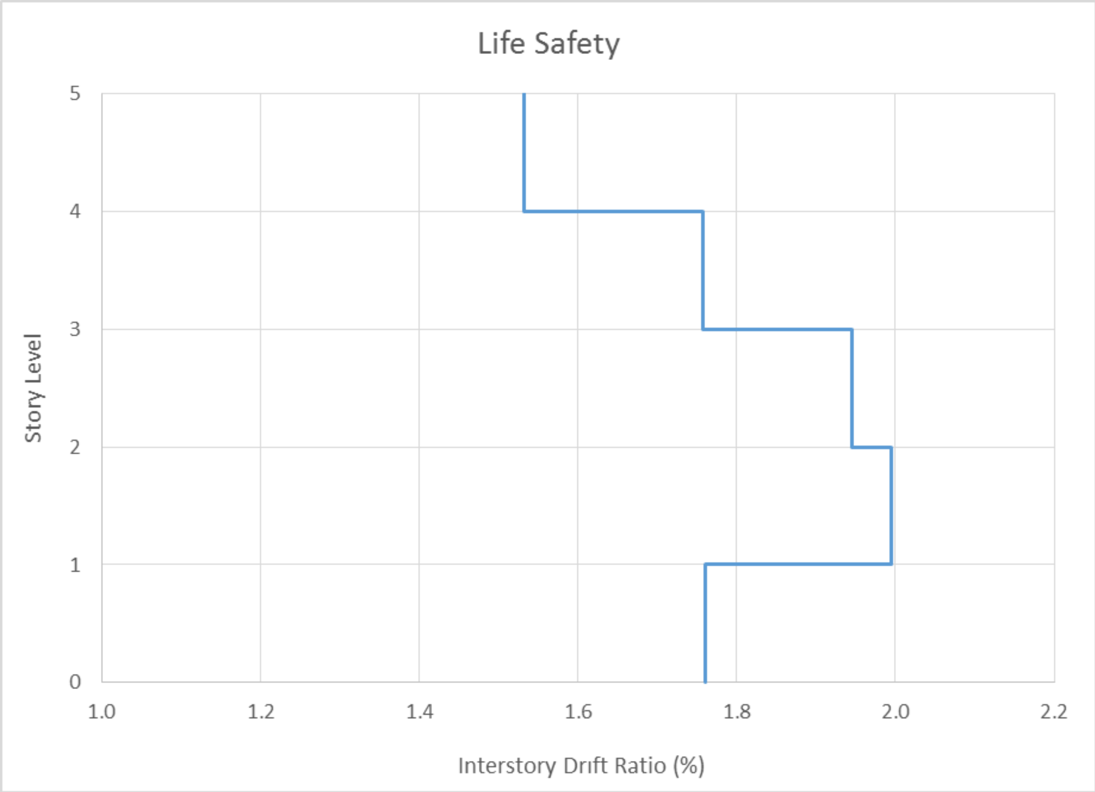

Figure 5.22 Story Level vs. Story Drift Diagram of Uniform Load Distribution, LS Limit State, NWC

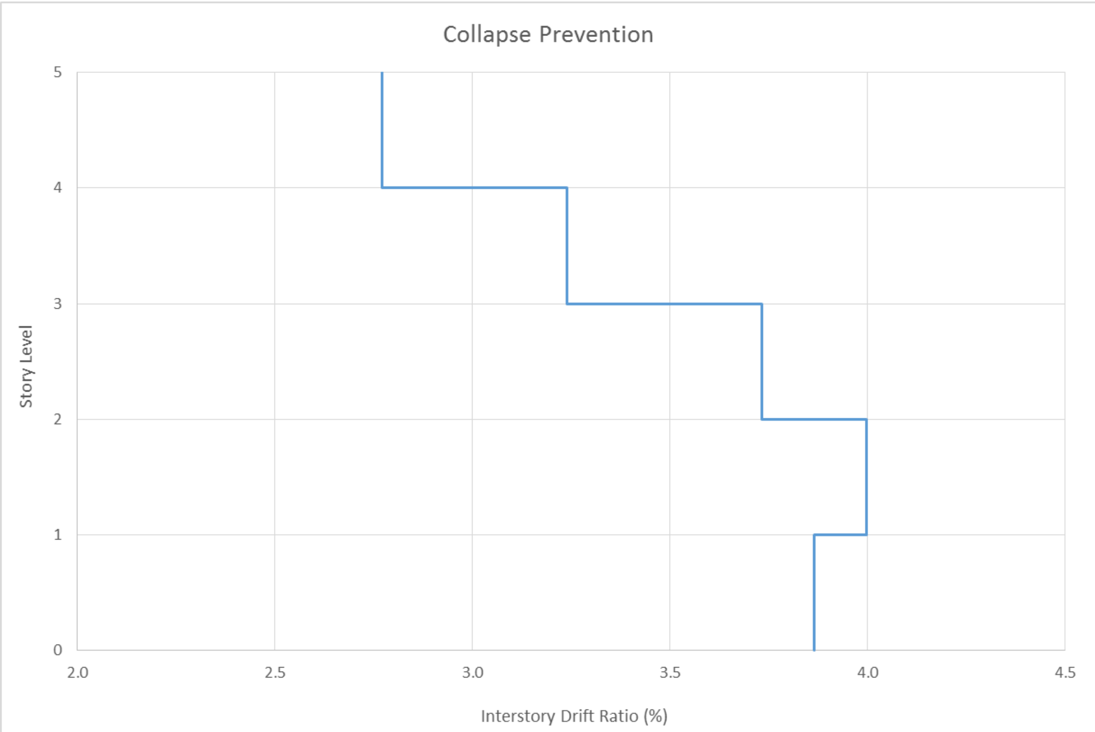

Figure 5.23 Story Level vs. Story Drift Diagram of Uniform Load Distribution, CP Limit State, NWC

Under uniform load distribution, the structure tends to absorb greater energy. The uniform load distribution analysis has resulted in an energy absorption capacity of 516,085 kN.mm with a base shear of 1589 kN. As used in the calculation of energy absorption capacity of triangular load distribution, top story displacement of the structure loaded with uniform loading, has been taken into account whereas inter-story displacements are kept in the limits mentioned before. The relation between base shear and top story displacement is presented in Figure 5.24.

In the light of analysis, uniform load distribution is proven to be more critical in order to evaluate and compare the structures. The greater base shear of uniform load distribution with comparatively smaller top story drifts could be thought to be important for the design of superstructure as well as substructure.

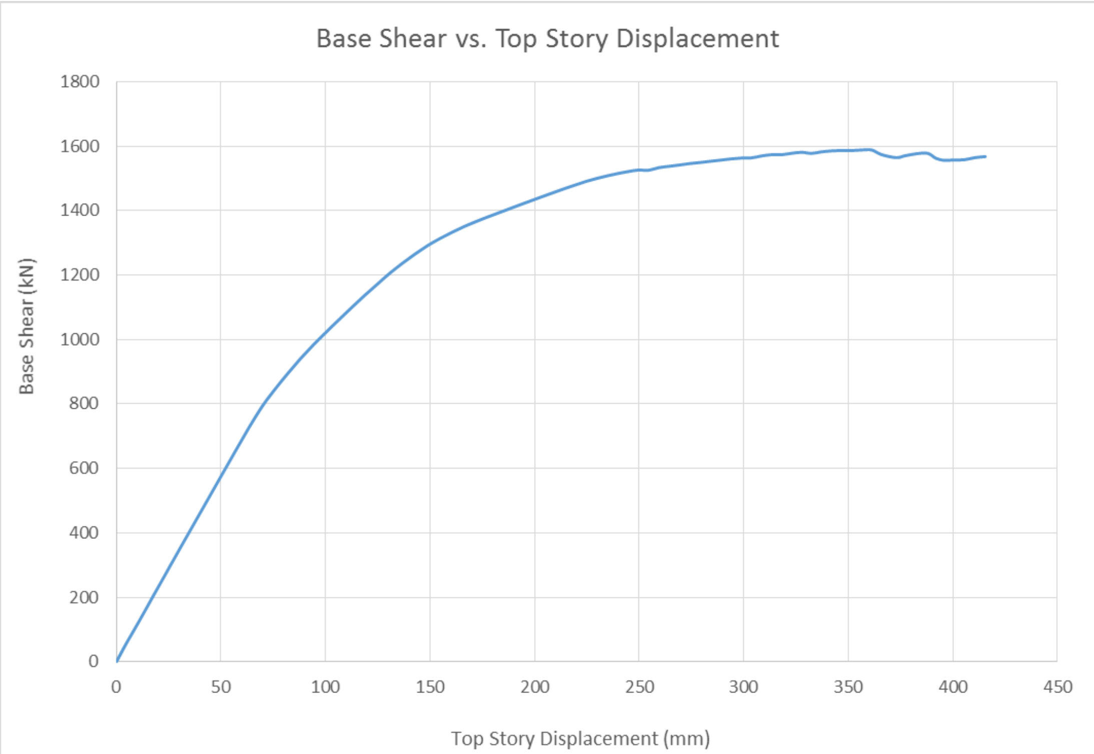

Figure 5.24 Base Shear vs. Top Story Displacement Curve of Uniform Load Distribution, NWC

In the analysis of lightweight concrete building, the uniform load distribution does also govern the results having 1493 kN base shear when compared the value of triangular load distribution of 1288 kN. The results of two different building systems are compared, namely normal weight concrete building and lightweight concrete building, base shear of lightweight concrete system is slightly smaller, 6%, than the normal weight concrete system.

In the case of triangular load distribution, the results are similar to the normal weight concrete system. In the Immediate Occupancy Limit State, 3rd story first reaches the limit state. Similarly, Life Safety and Collapse Prevention Limit States are reached by 3rd story. The overall behavior of 3rd story is shown in Figure 5.25. The suggested control node, 5th story reaches the limit states in 0.92%, 1.74% and 3.25% for Immediate Occupancy, Life Safety and Collapse Prevention Limit States respectively.

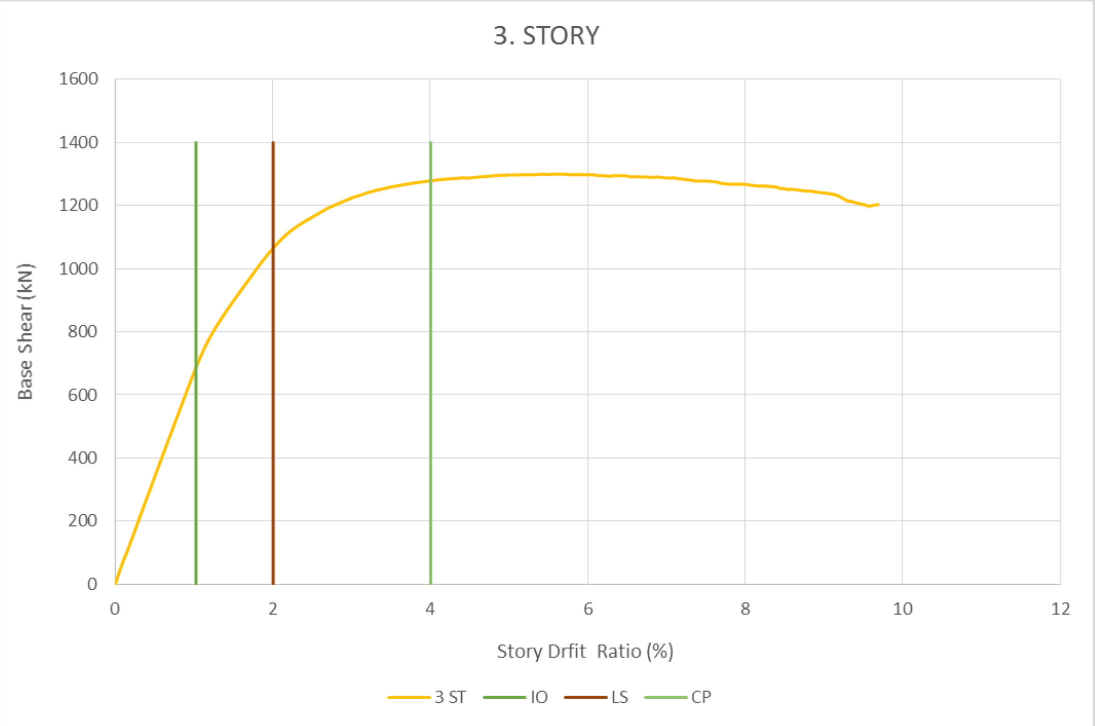

Figure 5.25 Base Shear vs. Story Drift Diagram of Triangular Load Distribution of 3rd Story, LWC

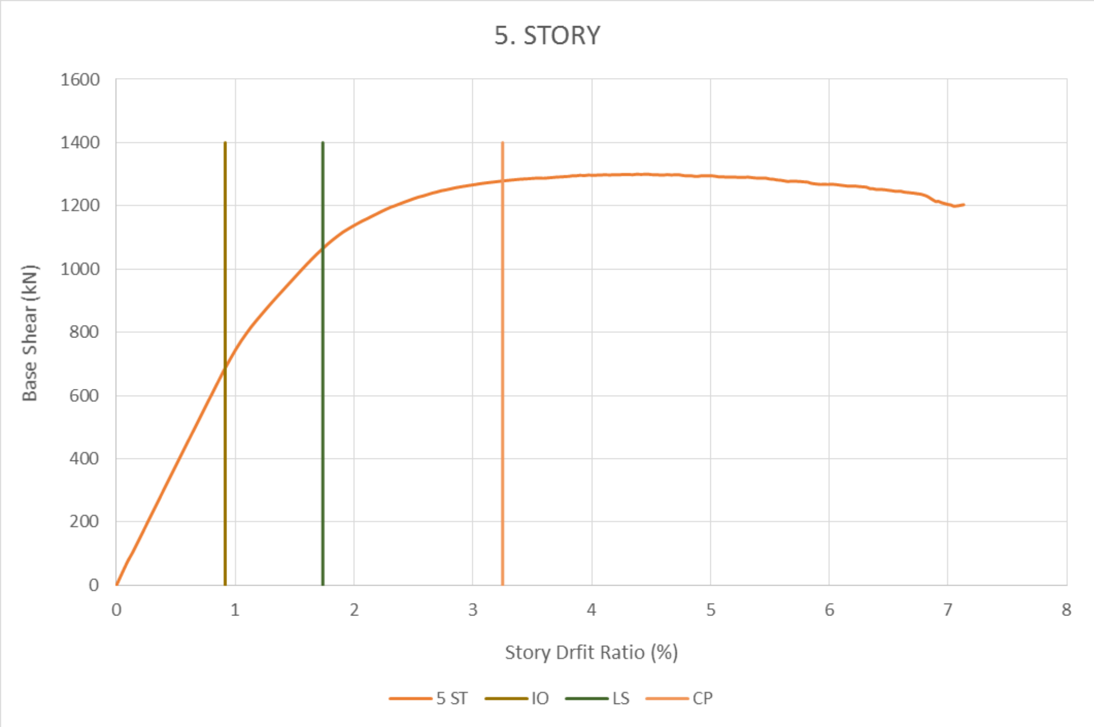

Figure 5.26 Base Shear vs. Story Drift Diagram of Triangular Load Distribution of 5th Story, LWC

The general trend in the case of normal weight concrete is sustained in the case of lightweight concrete. First floor behaves in a stable manner whereas the drift ratio of top level is kept below the maximum drift ratios and in no cases, top level govern the design. The relevant story level vs. inter-story drift ratios are shown in Figures 5.27, Figure 5.28 and Figure 5.29 for the limit states of Immediate Occupancy, Life Safety and Collapse Prevention respectively for the triangular load distribution. Similar to the triangular load distribution of normal weight concrete system, the governing story of the analysis is 3rd story for the Immediate Occupancy Limit State.

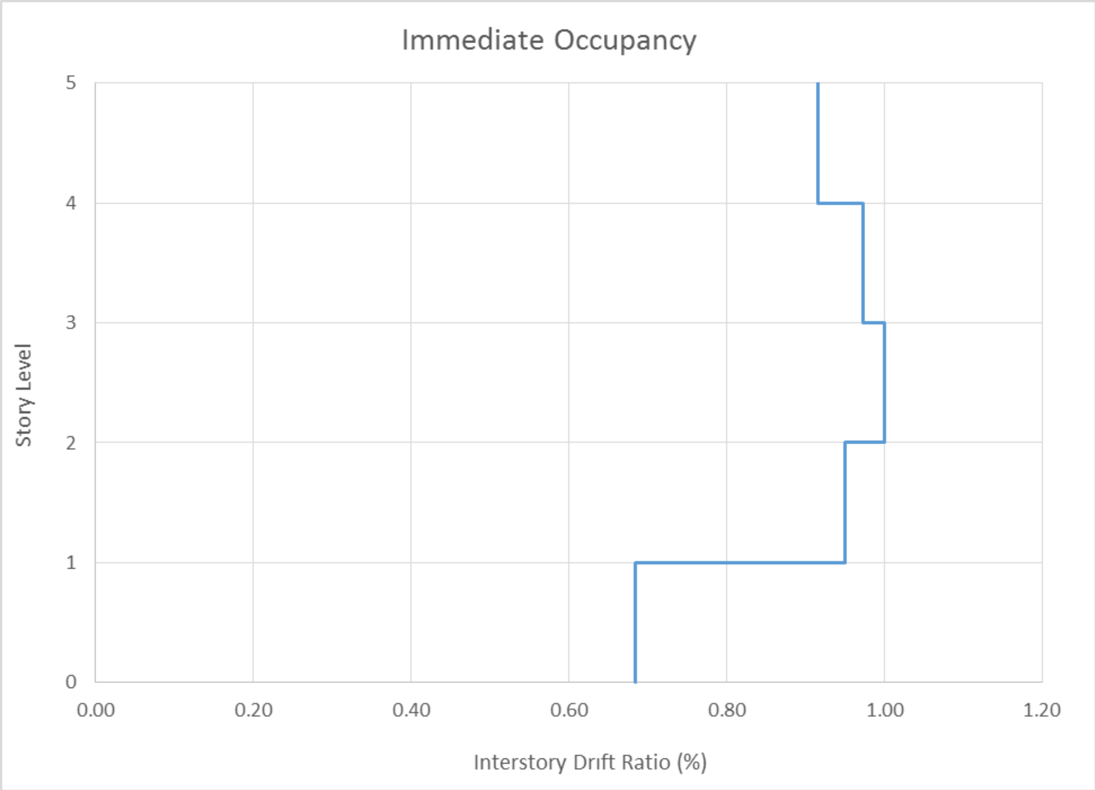

Figure 5.27 Story Level vs. Story Drift Diagram of Triangular Load Distribution, IO Limit State, LWC

On the other hand, 2nd floor drifts comparatively more than the normal weight case. The Life Safety Limit State is also concluded when the 3rd story reaches the limit drift ratio, whereas the second most drifted floor is 4th floor in this case. The energy absorption capacity of triangular load distribution is calculated as 431,690 kN.mm as presented in Figure 5.30. The calculated energy absorption capacity of the lightweight concrete is 13% lower than the normal concrete system for same loading system. The difference is mainly based on the greater base shear of normal weight concrete system and due to the difference in the initial stiffness. A more fair comparison will be presented in the lines below.

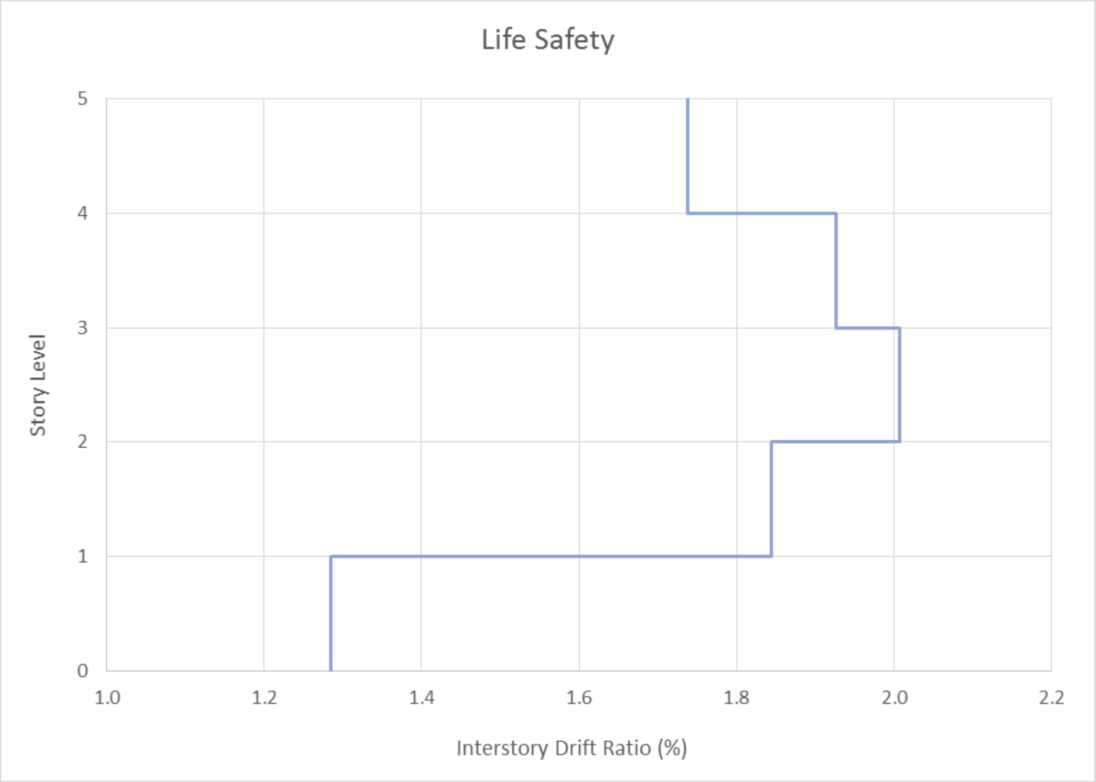

Figure 5.28 Story Level vs. Story Drift Diagram of Triangular Load Distribution, LS Limit State, LWC

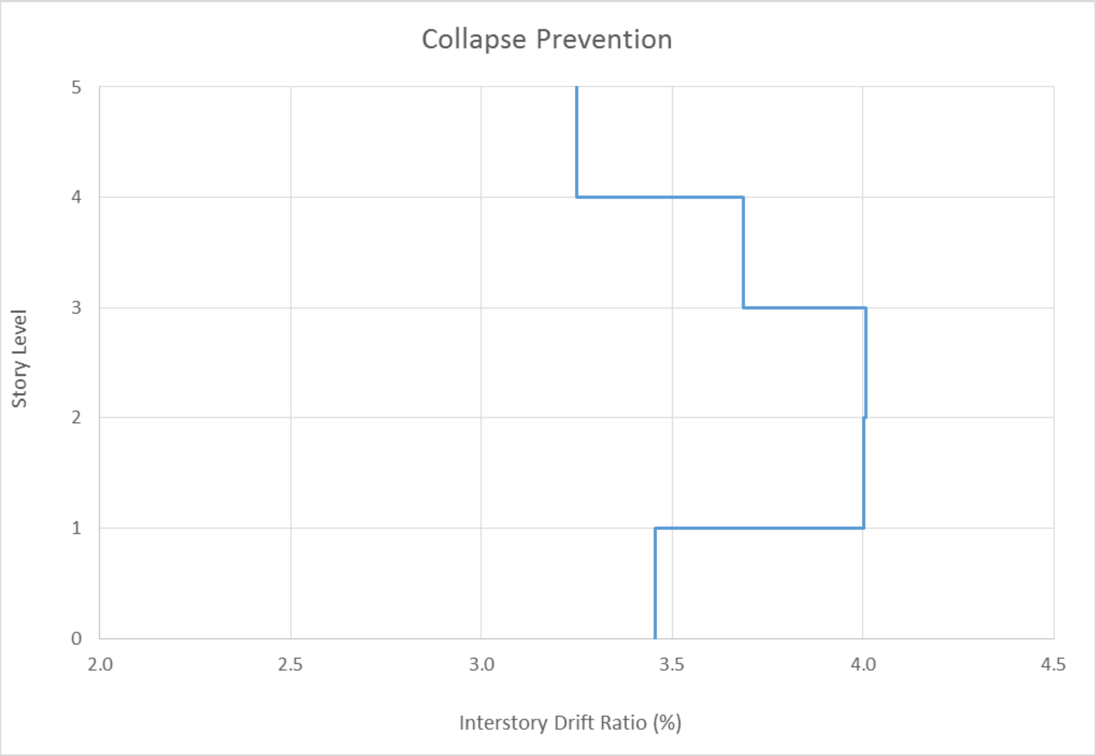

Figure 5.29 Story Level vs. Story Drift Diagram of Triangular Load Distribution, CP Limit State, LWC

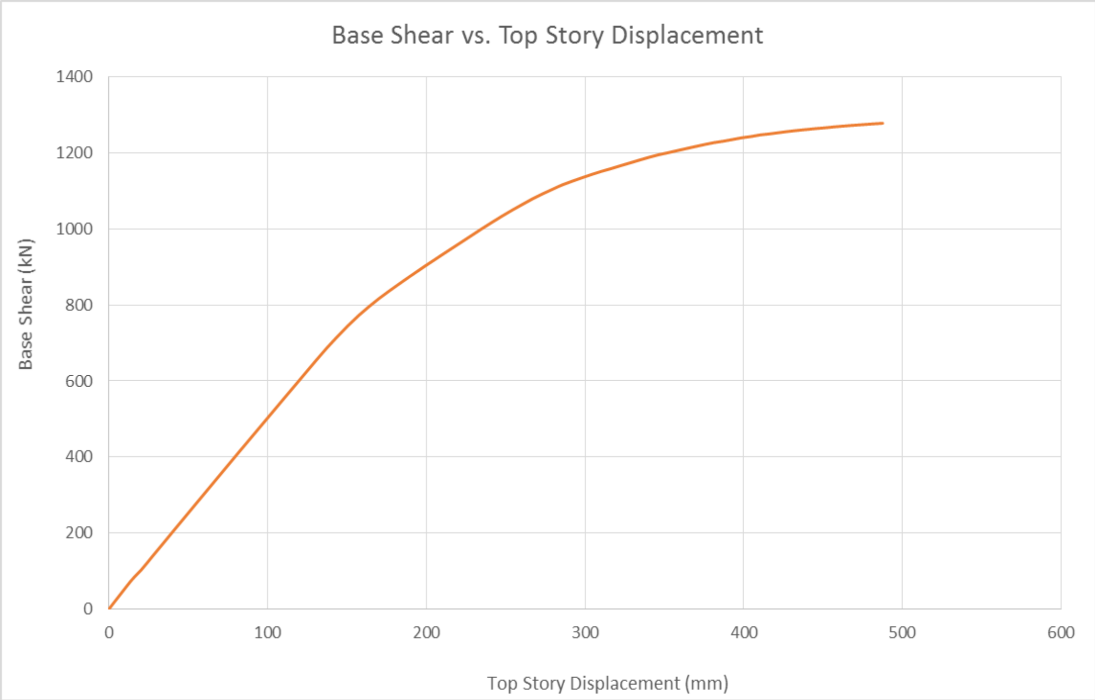

Figure 5.30 Base Shear vs. Top Story Displacement Curve of Triangular Load Distribution, LWC

In the uniform load distribution, the analysis is concluded with a base shear of 1493 kN. The calculated base shear is 6% smaller than the case of normal weight concrete, which is 1589 kN. In the analysis of distributed loading system in lightweight concrete, Immediate Occupancy Limit State does not differ from the same case of normal weight concrete. The governing drift ratio is controlled by 3rd floor in both cases as presented in Figure 5.31. Similarly, the second most drifted floor is 2nd floor in both cases (Figure 5.32)

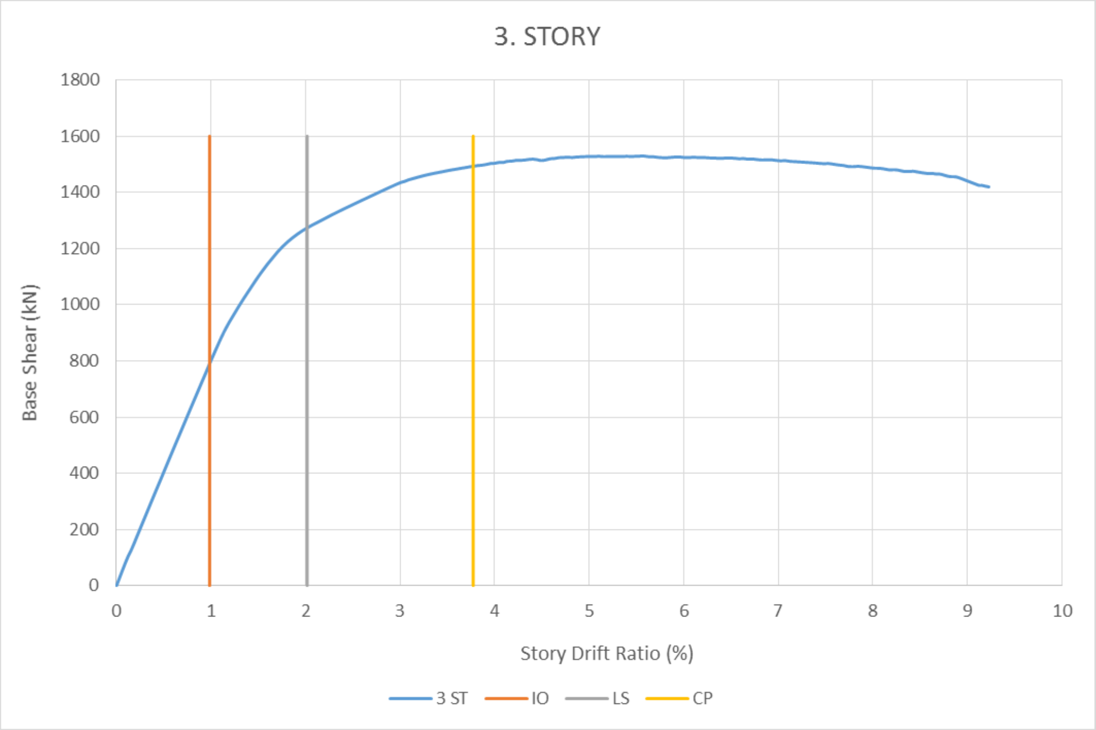

Figure 5.31 Base Shear vs. Story Drift Diagram of Uniform Load Distribution of 3rd Story, LWC

The suggested control node, 5th story similarly falls behind the limit stated as presented in Figure 5.28. The 5th story reaches the drift ratios of 0.83%, 1.64% and 2.88% for the Immediate Occupancy, Life Safety and Collapse Prevention Limit States respectively. The idea of controlling the all levels of structure is again to be more reliable for the design purposes.

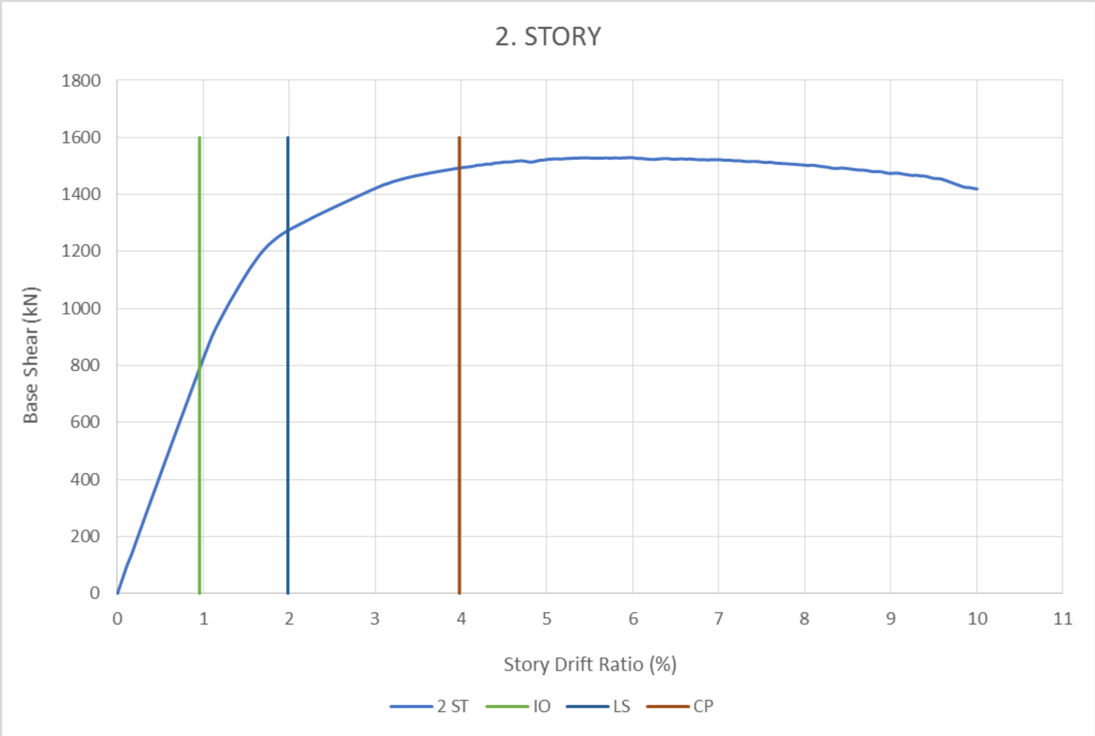

Figure 5.32 Base Shear vs. Story Drift Diagram of Uniform Load Distribution of 2nd Story, LWC

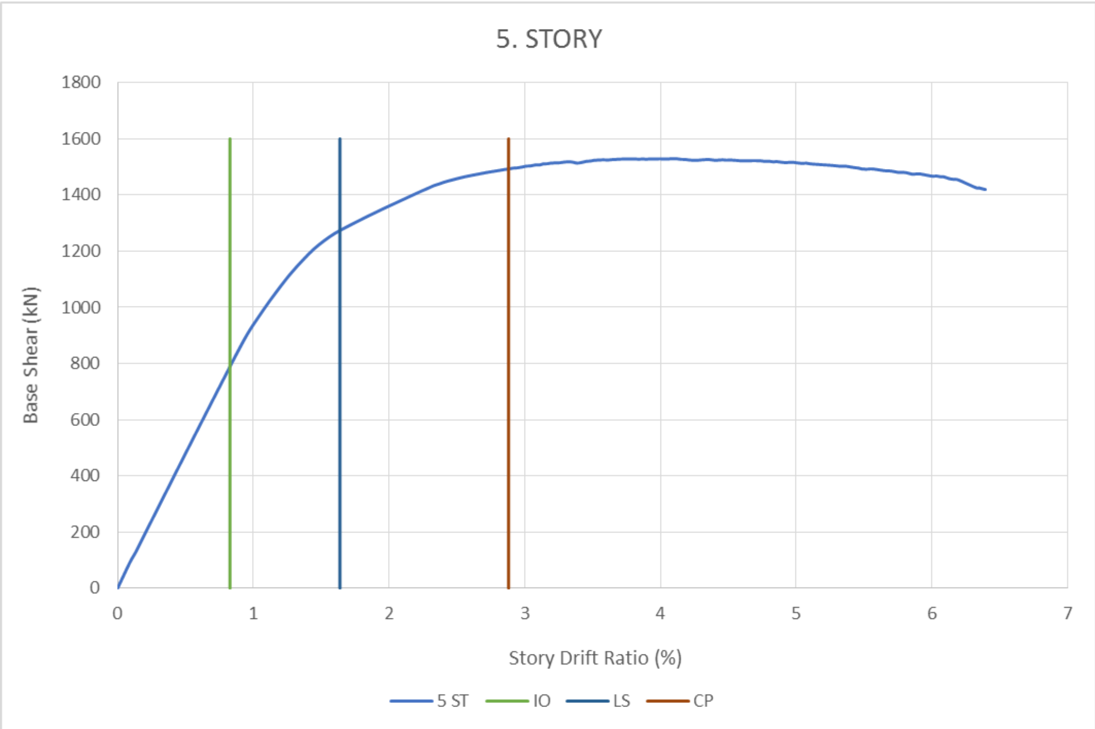

Figure 5.33 Base Shear vs. Story Drift Diagram of Uniform Load Distribution of 5th Story, LWC

In the uniform loading case of lightweight concrete building, the trend in Immediate Occupancy Limit State is kept as in the uniform load case of normal weight concrete (Figure 5.34). On the other hand, the trend is shifted for the Life Safety Limit State. As mentioned, 3rd floor is concluded to be the most drifted floor, followed by 2nd, 4th, 5th and 1st floors (Figure 5.35). Moreover, although the 2nd floor is the most drifted floor for the Collapse Prevention Limit State for both normal weight concrete and lightweight concrete in uniform loading, successors are differed from each other. In the Collapse Prevention Limit State of lightweight concrete for uniform loading, the second most drifted floor is the third floor, followed by 1st, 4th and 5th floors (Figure 5.36).

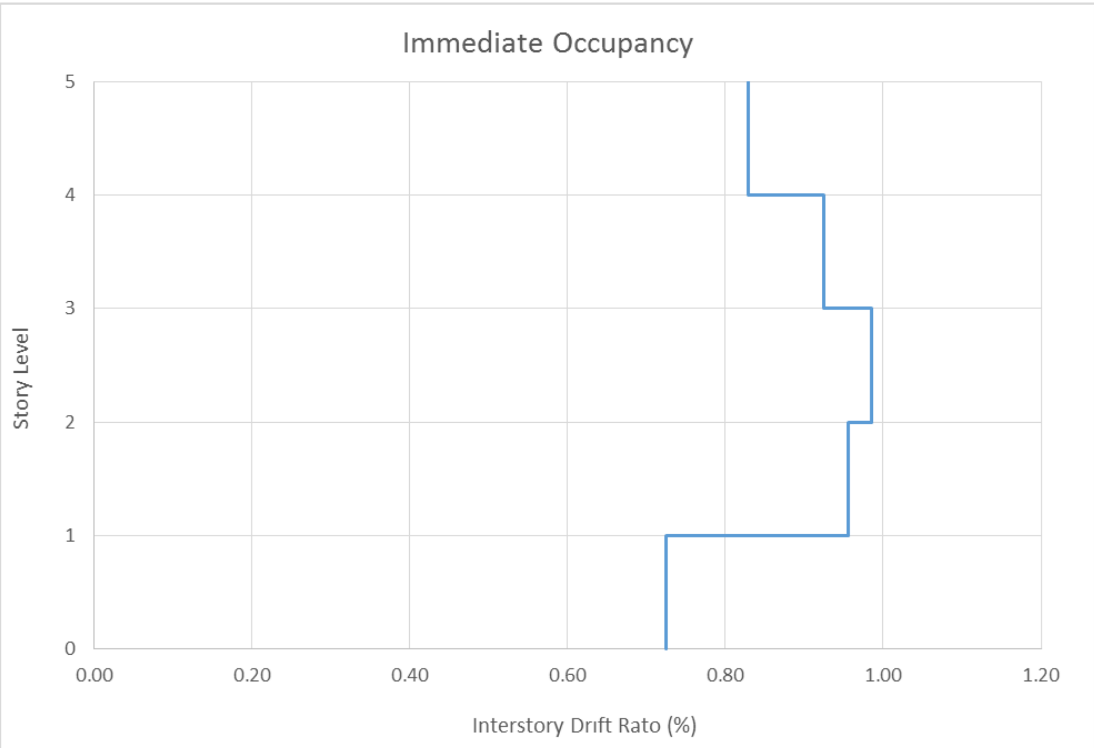

Figure 5.34 Story Level vs. Story Drift Diagram of Uniform Load Distribution, IO Limit State, LWC

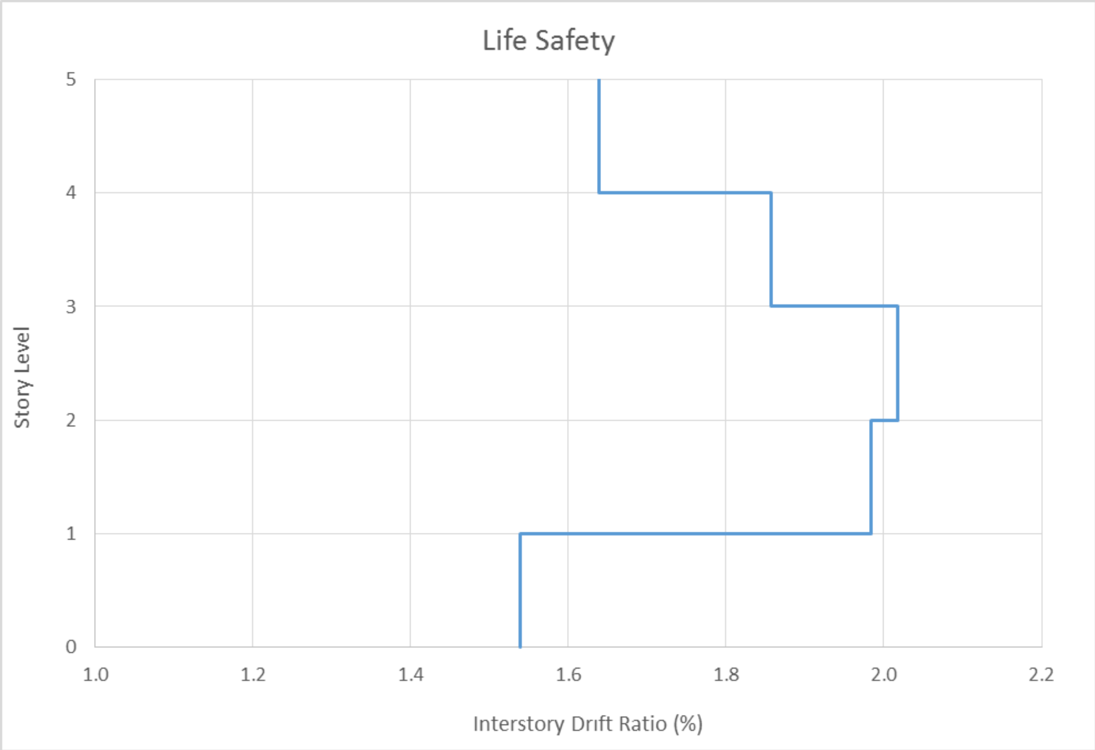

Figure 5.35 Story Level vs. Story Drift Diagram of Uniform Load Distribution, LS Limit State, LWC

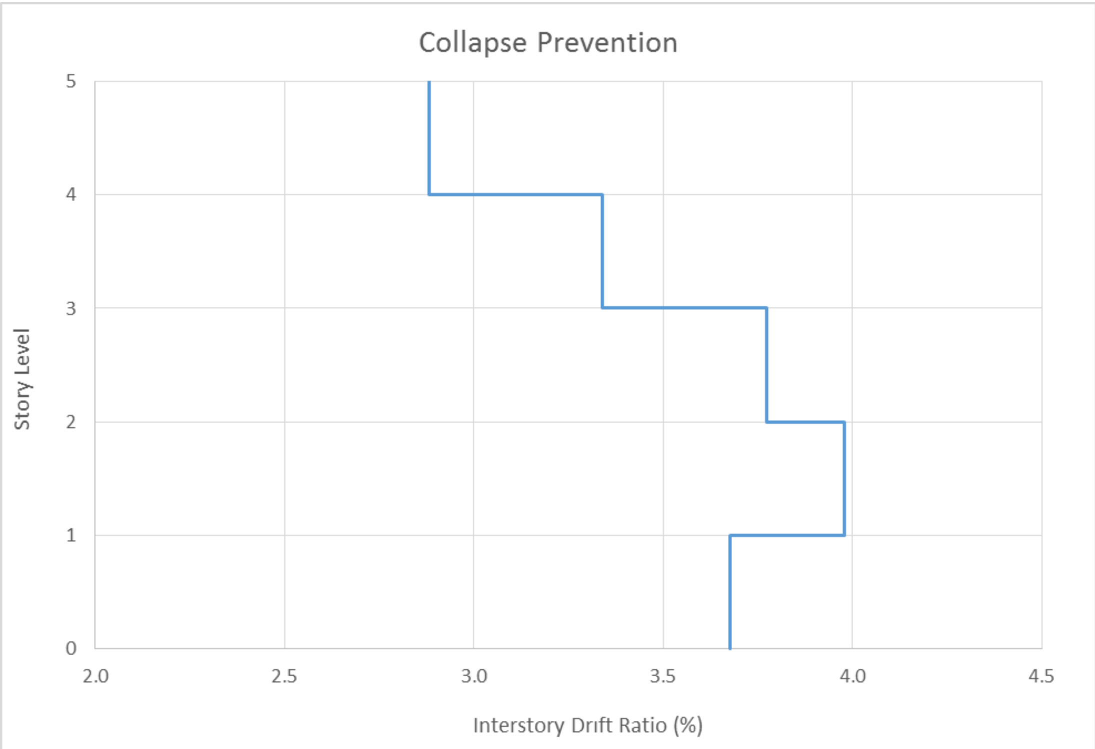

Figure 5.36 Story Level vs. Story Drift Diagram of Uniform Load Distribution, CP Limit State, LWC

The energy absorption capacity of uniform loading has resulted in greater results when compared with triangular loading case for normal weight concrete. Similarly, the uniform loading case in lightweight concrete has resulted in greater values when compared with triangular load distribution in lightweight concrete. The energy absorption capacity of uniform loading case in lightweight concrete has resulted in a value of 442,067 kN.mm. The results obtained in uniform loading for lightweight concrete is 14% smaller than the value from normal weight concrete building for the same loading condition. The overall behavior of the system is presented in Figure 5.37.

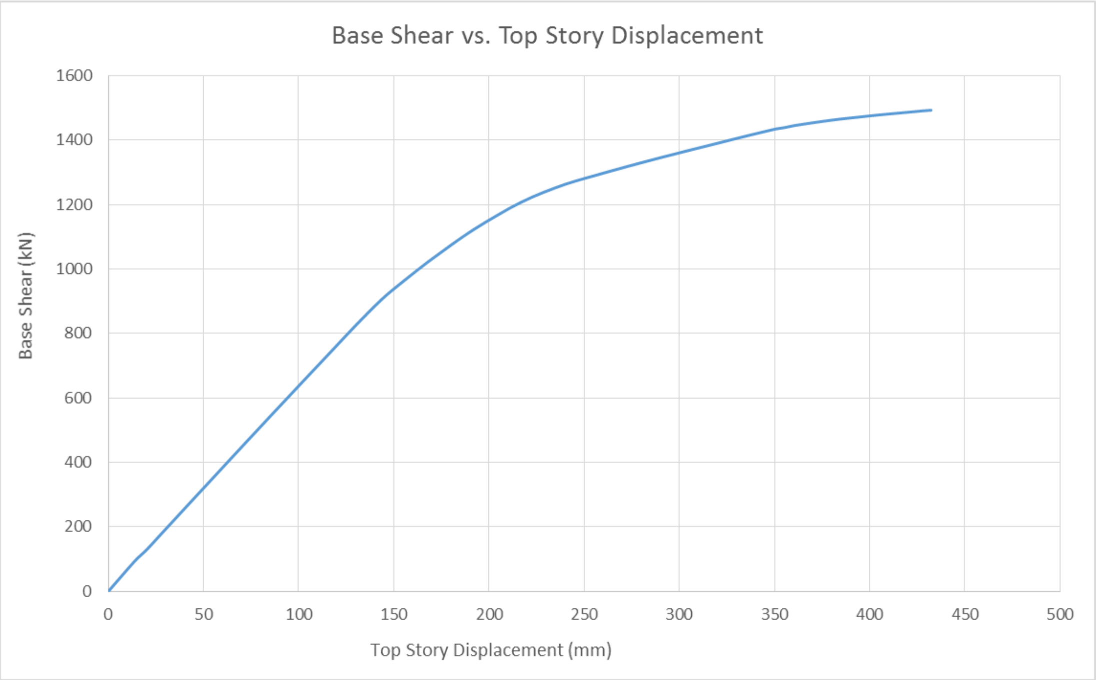

Figure 5.37 Base Shear vs. Top Story Displacement Curve of Uniform Load Distribution, LWC

5.5. Comparison of Results

In this section, results obtained from the analysis is compared, namely the 5 story buildings made of normal weight concrete and lightweight concrete. In the comparison, triangular load distribution is used since it is a good resemblance of first mode of the structure.

In the Figure 5.38, base shear versus top story displacement of two structures, under triangular load distribution is presented.

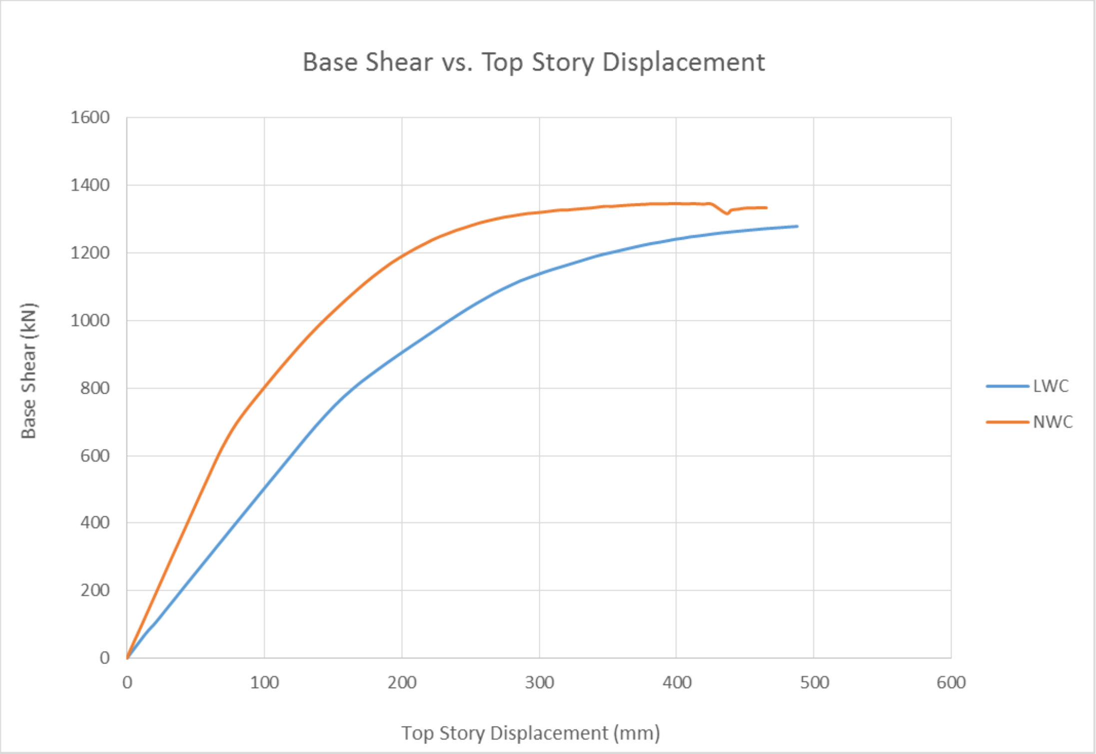

Figure 5.38 Base Shear vs. Top Story Displacement Curve of Triangular Load Distribution

In the case of LWC structure, it is easily seen that it keeps initial stiffness up to yielding for larger deformations when compared to the NWC structure. This behavior of structure leads to smaller energy absorption capacities than NWC structure for Collapse Prevention Limit State of 4% maximum inter-story drift in both buildings. On the other hand, NWC structure, due to its greater stiffness, experience initial yielding at lower deformations. The difference of energy absorption capacities is mainly caused of initial deformation level of the two structures.

As cited before, the structure made of normal weight concrete has an energy absorption capacity of 493,208 kN.mm at the collapse prevention limit state. The structure made of lightweight concrete has 431,690 kN.mm at the same limit state. Lightweight concrete structure has only 13% smaller energy absorption capacity. Although the LWC structure has smaller energy absorption capacity, it is remarkable that it has a more stable behavior for the lower rates of deformation.

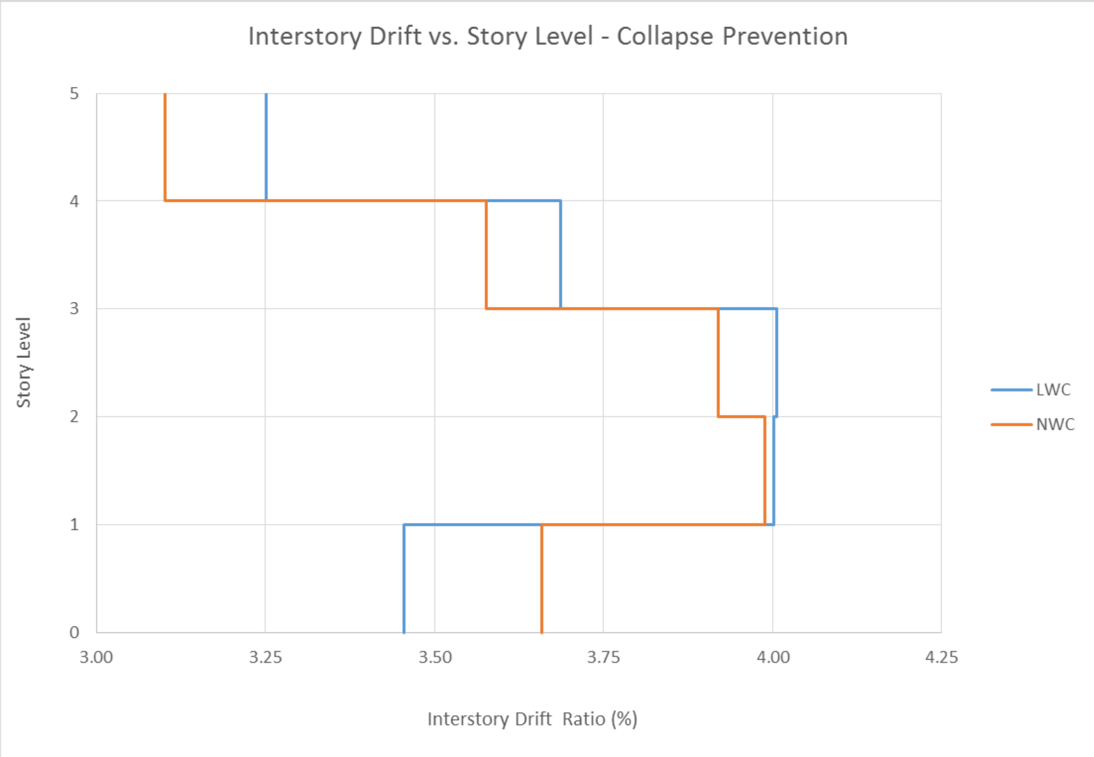

Figure 5.39 Story Level vs. Story Drift Diagram of Triangular Load Distribution, CP

As seen in the Figure 5.39, the overall behavior of both structures does not differ so much from each other. Although LWC structure has greater story drifts than NWC structures, it is in a reasonable limit. Namely, LWC structure has almost same properties and behavior of NWC structure.

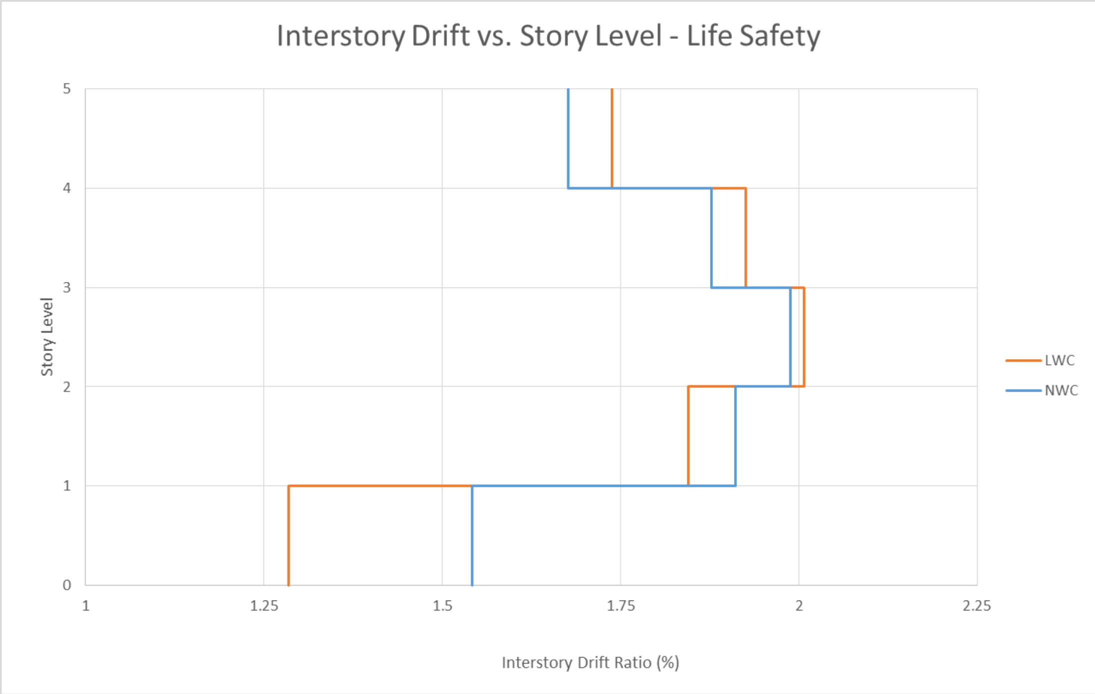

Figure 5.40 Story Level vs. Story Drift Diagram of Triangular Load Distribution, LS

Furthermore, the overall behavior observed from the Life Safety Limit State in Figure 5.40 has a similar trend as in the Collapse Prevention Limit State. The main difference may cited as the drift ratios for the first floors of both structures. The first floor of NWC structure has a drift ratio of 0.015 whereas the same floor of LWC has a 0.1285.

5.6. Evaluation of Results

In the evaluation of results, several parameters are considered in the light of previous studies and analytical studies performed by the author of this thesis. The results are compared in terms of base shear, energy absorption capacities Δ_U, Δ_Y and ductility index, where the calculation procedure of these parameters are presented in Figure 5.41 as suggested by FEMA 356 (2000). These parameters are presented in a tabular form in Table 5.2. In the calculation of Δ_U & Δ_Y, bilinearization method, is used.

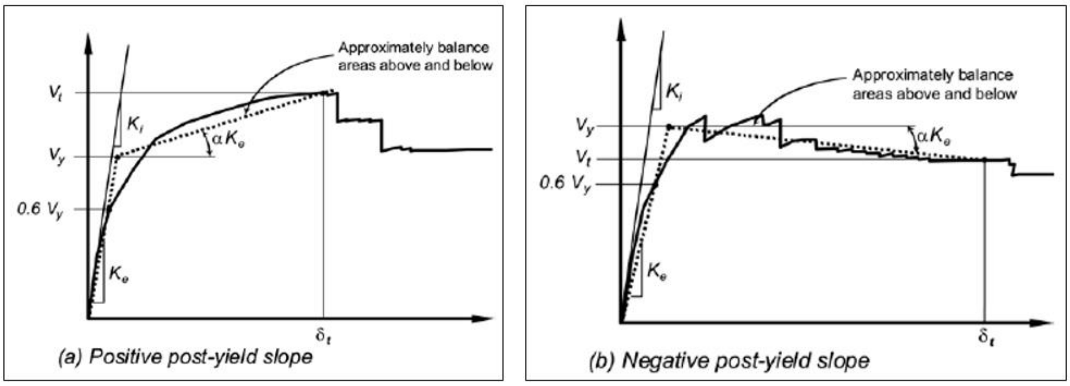

Figure 5.41 Idealized Force-Displacement Curves, FEMA 356 (2000)

The value of Δ_U stands for the deformation at the value of V_t whereas the Δ_Y stands for the deformation at the level of V_y. The base shear versus top story displacement curves, presented in Figure 5.38 is used in the determination of the values mentioned.

As seen in Table 5.2, response of lightweight concrete structure resulted in smaller base shear results. On the other hand, response of normal weight structure resulted in greater ductility indexes and energy absorption capacities for the same value of limit state, i.e. 4% maximum inter-story drift limit as specified as collapse prevention limit. Despite these facts, LWC structure has similar load-displacement and inter-story drift profiles with NWC structure. By the way, the current study considered the same cross-sectional dimensions for beams and columns for both NWC and LWC structures. By doing so, there is very small difference in the base shear carried by the structure by the use of LWC, however due to reduced weight it is obvious that LWC structure is advantageous since it is able to carry higher base shear compared to its dead weight, and furthermore the reduced dead weight is expected to results in smaller foundation dimensions. The current study can actually be extended to the match the stiffness's of both structures, and this will clearly eliminate the ductility deficiency of LWC structure. It can be overall concluded that the structures made of lightweight concrete may reach the performance of normal weight concrete structures easily.

Table 5.2 Evaluation of NWC and LWC Structures

BUILDING TYPE	UNIT	NWC		LWC	
LOADING CONDITION		TRI. LOADING	UNI. LOADING	TRI. LOADING	UNI. LOADING
BASE SHEAR	kN	1346	1589	1288	1493
ENERGY ABSORPTION CAPACITY	kN.mm	493,208	516,085	431,690	442,067
Δ_U	mm	465.25	415.51	487.66	432.26
Δ_Y	mm	99.52	125.47	216.47	210.09
$\mu=(\Delta_U/\Delta_Y)$		4.68	3.31	2.25	2.06

CHAPTER 6

CONCLUSION AND FUTURE RECCOMMENDATIONS

In the scope of this thesis, confinement effect of normal weight, lightweight and modified lightweight concrete is investigated. The effort is mainly focused on both experimental and analytical studies. Experimental studies are performed under a displacement-controlled machine with unconfined and confined concrete cylinder specimens with different spiral spacing values. The results obtained from the experimental studies are used for the verification of previous experimental studies and analytical study in order to compare the normal weight and lightweight moment resisting RC framed structures.

In the light of experimental studies on cylinder specimens, it is concluded that lightweight concrete and modified lightweight concrete have comparatively weaker performance in terms of ultimate strain and energy absorption capacities, but the presence of spiral reinforcement provides significant increase in absorbed energy for these materials. The performance of lightweight concrete as material cannot be disregarded in terms of its ultimate strength and strain values regarding this strength. Although use of lightweight concrete is prevented in Turkish building codes, through the experiments performed, it is obvious that lightweight concrete can reach the mechanical and physical properties easily. In this respects, limitations on the use of lightweight concrete does only prevent the advances in the area and does not attract the attention of both researchers and designers. Through the advances and studies in lightweight concrete, it will be easier to realize that lightweight concrete is a reliable construction material even for structural purposes as normal weight concrete does.

On the other hand, the analytical studies have concluded several results in line with the experimental studies. Although, the structures made of normal weight concrete tend to absorb more energy under lateral loads, the base shear of them are only seen to be slightly greater than the lightweight concrete structures when same cross-sectional dimensions are used for all structural members made of normal weight concrete structure and lightweight concrete structure. The decision of the use of normal weight concrete or lightweight concrete should be a design matter and the conditions and availability of the resources, and there should be no limitation towards the use of lightweight concrete in the construction of load carrying members of a structure.

In conclusion, the study performed in this thesis can be further improved for future studies. The comparison of normal weight concrete and lightweight concrete could be more effective by experimental studies performed on beams, columns and RC frames. Such tests will provide database for verification of numerical studies and more importantly will ensure a stable and reliable response of lightweight concrete structural members under both monotonic and cyclic loadings. Furthermore, parametric numerical studies on low-rise, mid-rise and high-rise RC framed lightweight concrete structures with and without the presence ıf shear walls can be evaluated under both nonlinear static and dynamic analysis in order to assess the performance of lightweight concrete structures under seismic loadings.

REFERENCES

Ahmad, S.H., Xie, Y., Yu, T., 1995, *Shear Ductility of Reinforced Lightweight Concrete Beams of Normal Strength and High Strength Concrete*, Cement and Concrete Composites, 17(2):147-159

Almousawi, A.N., 2011, *Flexural and Shear Performance of High Strength Lightweight Reinforced Concrete Beams*, PhD. Thesis, University of Illinois, Department of Civil Engineering, Chicago

American Concrete Institute (ACI), 1963, *Standard Building Code Requirements for Reinforced Concrete*, ACI 318-63

American Concrete Institute (ACI), 1983, *Standard Building Code Requirements for Reinforced Concrete*, ACI 318-63

American Concrete Institute (ACI), 1987, *Guide for Structural Lightweight Aggregate Concrete*, ACI 213R-87

American Concrete Institute (ACI), 2008, *Building Code Requirements for Structural Concrete*, ACI 318M-08

American Society of Civil Engineers (ASCE), 2005, *Minimum Design Loads for Buildings and Other Structures*, ASCE SEI/7-05.

American Society of Civil Engineers (ASCE), 2010, *Minimum Design Loads for Buildings and Other Structures,* ASCE SEI/7-10.

American Society for Testing and Materials (ASTM), 2014, *Standard Specification for Lightweight Aggregates for Structural Concrete*, ASTM C330/C330M-14

American Society for Testing and Materials (ASTM), 2014, *Standard Test Method for Static Modulus of Elasticity and Poisson's Ratio of Concrete in Compression*, ASTM C469/C469M-14

Aşık, M., 2006, *Structural Lightweight Concrete with Natural Perlite Aggregate and Perlite Powder*, MSc Thesis, Middle East Technical University, Department of Civil Engineering, Ankara.

ATC, 1996, *Seismic Evaluation and Retrofit of Concrete Buildings*, Vol. 1, ATC 40, Applied Technology Council, Redwood City, CA.

Chopra A.K. and Goel R.K., 2001, *A Modal Pushover Analysis Procedure to Estimating Seismic Demands for Buildings: Theory and Preliminary Evaluation*, PERR Report 2001/03, Pacific Earthquake Engineering Research Center, University of California, Berkeley.

Computers and Structures Inc. (CSI), 2006, *User Manual for PERFORM-3D v4.0*, Berkeley, California, USA, August 2006.

Ersoy, U., Özcebe, G., 2001, *Betonarme*, Evrim Yayınevi, İstanbul.

Expanded Shale, Clay and Slate Institute (ESCSI), 1971, *Lightweight Concrete; History, Applications, Economics*, ESCSI Document 7600.1

Eser, H., 2014, *High Performance Structural Lightweight Concrete Utilizing Natural Perlite Aggregate and Perlite Powder*, MSc Thesis, Middle East Technical University, Department of Civil Engineering, Ankara.

Federal Emergency Management Agency (FEMA), 2000, *Prestandard and Commentary for the Rehabilitation of Buildings*, FEMA 356.

Federal Emergency Management Agency (FEMA), 2009, *Quantification of Building Seismic Performance Factors*, FEMA P695.

Gupta B., Kunnath S.K., 2000, *Adaptive Spectra-Based Pushover Procedure for Seismic Evaluation of Structures*, Earthquake Spectra 2000;16(2):367–91.

Hlaing, M.M., Huan, W.T., Thangayah, T., 2010, *Response of Spiral-Reinforced Lightweight Concrete to Short-Term Compression*, Journal of Materials in Civil Engineering, ASCE, Vol. 22 Issue 12

Kalkan E., Kunnath S.K., 2007, *Assessment of Current Nonlinear Static Procedures for Seismic Evaluation of Buildings*, Engineering Structures, Vol. 29, No.3, pp. 305–316

Kent D.C. and Park R., 1971, *Flexural Members with Confined Concrete*, Journal the Structural Division, American Society of Civil Engineers, New York, Vol. 97, ST7.

Leung, H.Y. and Burgoyne, C.J., 2001, *Compressive Behaviour of Concrete Confined by Aramid Fibre Spirals*, The International Conference on Structural Engineering Mechanics and Computation, Cape Town, pp. 1357-1346.

Okuyucu, D., Turanlı, L., Uzal, B. and Tankut, T., 2011, *Some Characteristics of Fibre-reinforced Semi-lightweight Concrete with Unexpanded Perlite*, Magazine of Concrete Research, Vol. 63, No.11, pp. 837-846.

Zandi, Y., 2012, *Investigation of Behaviors of Monolithic and Prefabricated Structures Members Produced Using Lightweight Concrete*, PhD. Thesis, Karadeniz Technical University, Department of Civil Engineering, Trabzon